Stress minimization of artificial bone using Non Parametric Optimization

(ノンパラメトリック最適化を用いた人工関節の応力最小化)

MUSADDIQ ABDIL KHALIQ MALEH AL-ALI

Department of transportation and environmental systems

Graduate School of Engineering

Hiroshima University

Japan

2018

وربَّمَا أَوْجَبَ اسْتِقْصَاؤنَا
النَّظَر عُدُولاً عَنِ المشْهُورِ
والمتعَارَف فمَنْ قَرَعَ
سَمْعَهُ خِلاَفُ مَا عَهِدَهُ، فَلا
يُبَادِرْنَا بالإنْكَارِ، فَذَلِكَ
طَيْشٌ فرُبَّ شَنِعٍ حَقٌّ
ومَأْلُوفٍ مَحْمُودٍ كَاذِبٌ
والحقُّ حَقٌّ فى نَفْسِهِ، لاَ
لِقَوْلِ النَّاسِ لَهُ

ابن النفيس

Abstract

The enhancement of orthopedic mechanical and medical lifetime is a matter of intensive study for almost 4000 years. The most important aspect of orthopedics is the body rejection. The body rejection of orthopedics is cleared by phenomenon refer to as stress shielding. Stress shielding is simply prescribed as, the Osseointegration between the bone and the orthopedic start to deteriorate with time, such that the bone is dissolving exposing the orthopedic. The generated soft tissue and the mobility of orthopedic is a serious problem. The Osseointegration problem is addressed with wolfs law. In this work, long term Osseointegration is being addressed by two strategies i.e. the stiffness matching, and strain energy minimization of bone itself. In the first strategy, the orthopedic is designed and optimized to have a similar stiffness to the substituted bone for the designated loading and boundary conditions. The second strategy is to design the orthopedic with the constrained of minimizing the strain energy equivalent (Haigh stress) in the bone that produced by the force transfer from the orthopedic to the surrounding bone. In order do the orthopedic design, shape and topology optimization are investigated to have the optimal configuration and design scenarios. The suggested scenarios of topology optimization are divided into two categories. First category is the objective function investigation. The second category is the choice of shape optimization, topology optimization, or combination of both. Objective function been chosen are compliance, qp stress and pnorm stress, and fatigue life-based function. Finite element, and objective functions configurations are being studied. Topology and shape optimization were compared. Mesh morphing is being used as shape optimization method such that, it is used as medical based finite element modeling enhancement method, add to that the anticipated speed. Cascade method of topology optimization-shape optimization, and shape optimization-topology optimization models are being investigated. Due to the specifications of orthopedic designs requirements, and objectives, both mechanically and biomechanically, Topology optimization is being chased as the appropriate generalize methodology of design. Two medical examples are chosen to simulate and investigate. First model is the temporomandibular joint prosthesis. Treatment of bone tumors in the mandible often involves extensive excavation of affected bone, followed by mandibular reconstruction. Prosthetic implants that been investigated is needed to restore

jaw functionality. The challenges of making prosthetic bone implants include long term Osseointegration and extending the mechanical life of the implant is the main goal. Temporomandibular case studied the stiffness matching hypothesis. Topology optimization is perfumed of a computer generation of the missing bone. Occlusion mismatching is a challenging problem in maxillofacial surgery. By making the design domain match the exact bone topography, high precision machining can give an exact replica of the jaw part to achieve an accurate occlusion. Model is decided to non-design domain which is the aesthetic, and biomechanics compatibility. The design domain is the inner part of the prosthesis. A simulation of orthodox used orthopedic is performed. Pnorm with stiffness matching constraint, and the compliance maximization with stiffness matching constraint are been chosen as optimality criteria. Pnorm showed good anticipated fatigue life with stiffness of the design orthopedic, matches the missing bone. The material we used was titanium alloy (Ti-6Al-7Nb). Volume fraction of the orthodox implant was used (0.2872 for the studied case) as volume constraints. The volume constraint is being chosen such that the weight of the titanium alloy should not be heavier than the replaced bone for the best weight compatibility. Compliance of the bulk bone was set as a further constraint to match the stiffness of the bone with the designed structure. Results show a good life expectancy for the designed parts, with 12% higher life expectancy for stress-based topology optimization than for compliance-based topology optimization. Design using topology optimization gave a long-life expectancy in the simulation process. The compliance objective function achieves good results for fatigue life prediction, but stress-based topology optimization achieves better results. The Orthodox-based design has a shorter life expectancy than the new optimized designs. Compliance of the orthodox design is almost 210% differ from the original replaced bone. Therefore, stress shielding of orthodox designs is highly desirable. From the design time aspect, maximizing compliance can be considered to be a faster strategy. Anther medical case been chosen is the topology optimization of the orthodox femoral hip joint implant. The hypothesis of stain energy is being chosen to limit the stress shielding i.e. increase the Osseointegration strength. The minimization of pnorm of the Haigh stress of the surrounding bone was the objective function. Topology optimization of solid core orthopedics and conformal lattice structure-based scaffold were studied. Solid core orthopedics showed better minimization of Haigh stress in the

surrounding bone. An investigation of surface modification of simulated rapid prototyping structure is being performed. Electropolishing by precipitation is simulated. The simulation of loaded polished structure showed better limitation of the spots of singular stresses. In the scope of the results, algorithms are been introduced in order to efficient the design and manufacturing of fully custom orthopedics in shortest time as possible in the scope of the current software simulation and 3d metal printer capability.

Contents

List of Figures

List of Tables

Chapter 1 Engineering aspects of prosthesis design with topology optimization

1.1. Introduction

Bone considered the hard parts of the body which is responsible for protecting and support the body. It is a highly complex composite material with a lot of variance in component and composition within the body itself. The bone may suffer external stress causing fragmentation of bone, as motorcycle incidents, and so on; or physiological disorder, making normal stresses able to destroy the bone as a hip joint fracture in aged women. Designing artificial body parts to help to heal or replace permanently damage organs is a challenge for physician and engineers. The way of approaching the problem will vary, with the designer experience and way of thinking. Mostly there are two ways of thinking in the matter of orthopedic design; the strictly Engineering aspects, and medical aspect. These two ways of thinking are corporate and mutate to develop good orthopedic that satisfy the patient needs. Bone grafting [1-4] is used in some cases. Due to the limited resource regarding patient living bone, synthetics materials may use, however, the fatigue life and failure under static and dynamic load is a risk. Metal implants are one of the good choices in such matter. Such treatment traced to the ancient Egyptian 4000 years ago [5]. Recently, materials used for bone implant extended from metallic to advance ceramics and reinforced polymers. But still, metallic alloys considered as one of the important options.

1.2. The classical concept of stress

1.2.1. Mathematical representation of stress in space (elastic region)

Considering an arbitrary body in a state of equilibrium (shown in Figure.1). Forces, generally, may act upon the body outer boundaries (Surface forces) or generate internally driven by fields such as acceleration (gravity, centrifugal force) and magnetic forces. In case of static equilibrium, the body forces are in balance. Forces actions are

distributed through the body with what so-called internal forces. These internal forces are varying through the point of view within the domain. For example, taking the cut plane Z-Z. The internal forces inside the body appear on the cut surface. The intensity and direction of these forces at a point in a given plane, named as "Stress." Mathematically, Stress can be defined as the limit of the resultant forces for the chosen surface over the area. In case of taking (P) as a resultant, the normal stress (equation (1)) in the direction of (P) which is orthogonal to the surface is

$$\sigma_P = \lim_{dA \to 0} \frac{dP}{dA} \qquad \ldots (1)$$

For force resultant (T) per unit area which is parallel to the surface, the stress which is called "shear stress" is for the point (O) within the body as in equation (2).

$$\tau_T = \lim_{dA \to 0} \frac{dT}{dA} \qquad \ldots (2)$$

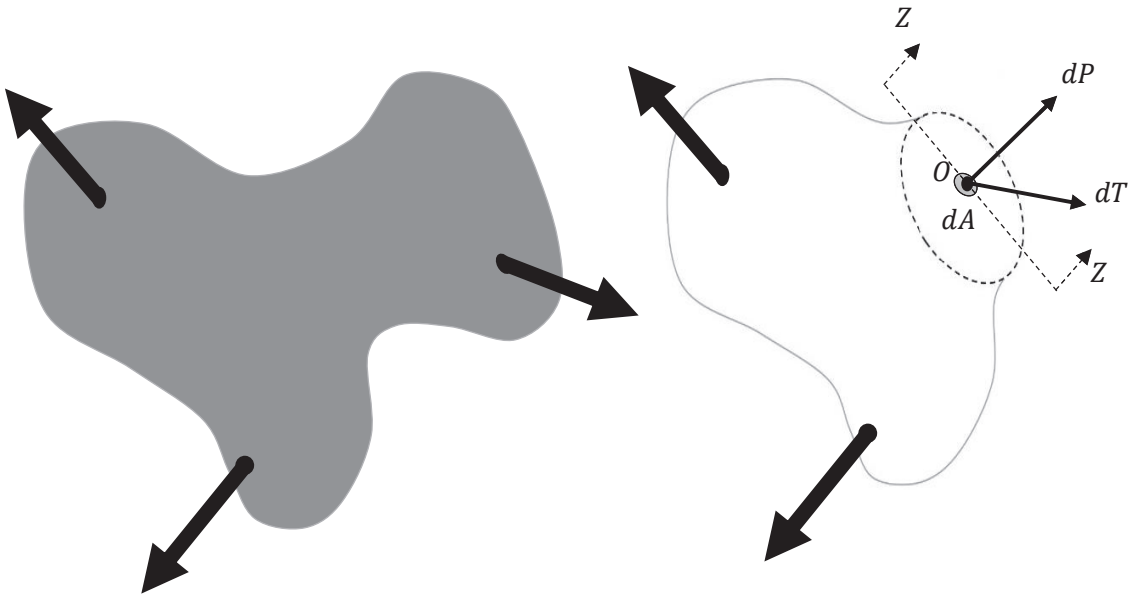

Figure 1. Free Body Diagram

There is an infinite number of possibilities to cut the surface. Each possibility has its own orientations, yielding to an infinite number of shear and normal stresses. According to that, to represent the case of stresses for a point in space, it needs generalizing the vector case to be described as a second-order tensor[6]. To derive the three-dimension representation of stress in space (referred to as Cauchy stresses) for the point (O) (Figure.2), let us consider the traction components and the force in static equilibrium as in equation (3)

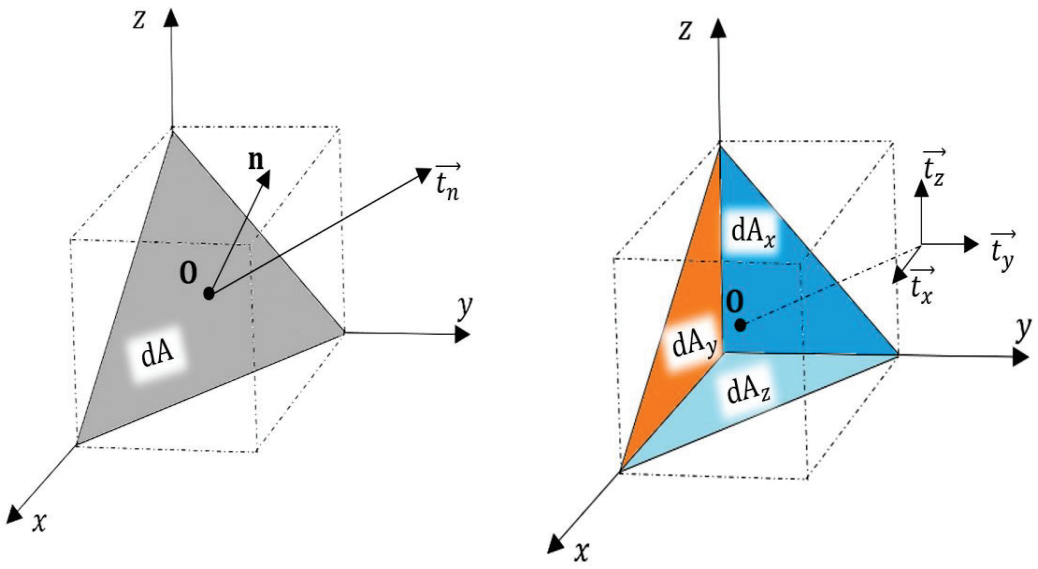

Figure 2. Traction components for a point in space

$$\vec{t}_x(dA) = \sigma_{xx}(dA.\cos\frac{n}{x}) + \sigma_{xy}(dA.\cos\frac{n}{y}) + \sigma_{xz}(dA.\cos\frac{n}{z})$$

$$\vec{t}_y(dA) = \sigma_{yx}(dA.\cos\frac{n}{x}) + \sigma_{yy}(dA.\cos\frac{n}{y}) + \sigma_{yz}(dA.\cos\frac{n}{z}) \quad \ldots (3)$$

$$\vec{t}_z(dA) = \sigma_{zx}(dA.\cos\frac{n}{x}) + \sigma_{zy}(dA.\cos\frac{n}{y}) + \sigma_{zz}(dA.\cos\frac{n}{z})$$

Generalizing the case for the other orthogonal components (shear stress) will give the general the tensor formation of the stress component in space (equation(4)) [7]

$$\begin{bmatrix} \sigma_{xx} & \tau_{xy} & \tau_{xz} \\ \tau_{yz} & \sigma_{yy} & \tau_{xz} \\ \tau_{zy} & \tau_{zy} & \sigma_{zz} \end{bmatrix} \quad \ldots (4)$$

For the same points, there is a plane at which only pure shear (equation (5)), or pure normal stresses (equation (6)), or hydrostatic stress (equation (7)) is acting as in.

$$\begin{bmatrix} 0 & \tau_{xy} & \tau_{xz} \\ \tau_{yz} & 0 & \tau_{xz} \\ \tau_{zy} & \tau_{zy} & 0 \end{bmatrix} \quad \ldots (5)$$

$$\begin{bmatrix} \sigma_1 & 0 & 0 \\ 0 & \sigma_2 & 0 \\ 0 & 0 & \sigma_3 \end{bmatrix} \quad \ldots (6)$$

$$\begin{bmatrix} \bar{\sigma} & 0 & 0 \\ 0 & \bar{\sigma} & 0 \\ 0 & 0 & \bar{\sigma} \end{bmatrix} \quad \ldots (7)$$

The stresses of a point in space are representing in what so-called Moher's circle.

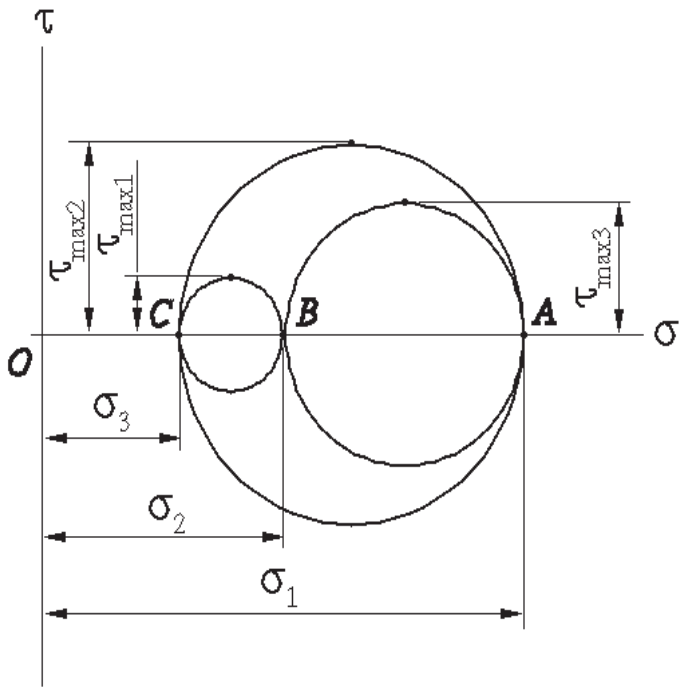

Figure 3. Three-Dimensional Moher's Circle

1.2.2. Singular stress

Stress is in simple approximating can be intuitively represented as a stream of forces crossing the body, confining by the cross-section. In case of a severe change in the spatial configuration, such as sharp edges, it will lead to increase the stress rapidly around the inclusion. Such inclusion called stress raisers. For example, a 2D infinite plate (Figure.4) of a circular hole in the middle shows stress increasing on the lateral poles of the hole. Such increase reaches 3 times the original applied stress. If the aspect ratio of the hole changes such as the length of the long diameter is twice the length of the shorter diameter. It shows a stress of 25 times the original stress. This phenomenon called "stress concentration."

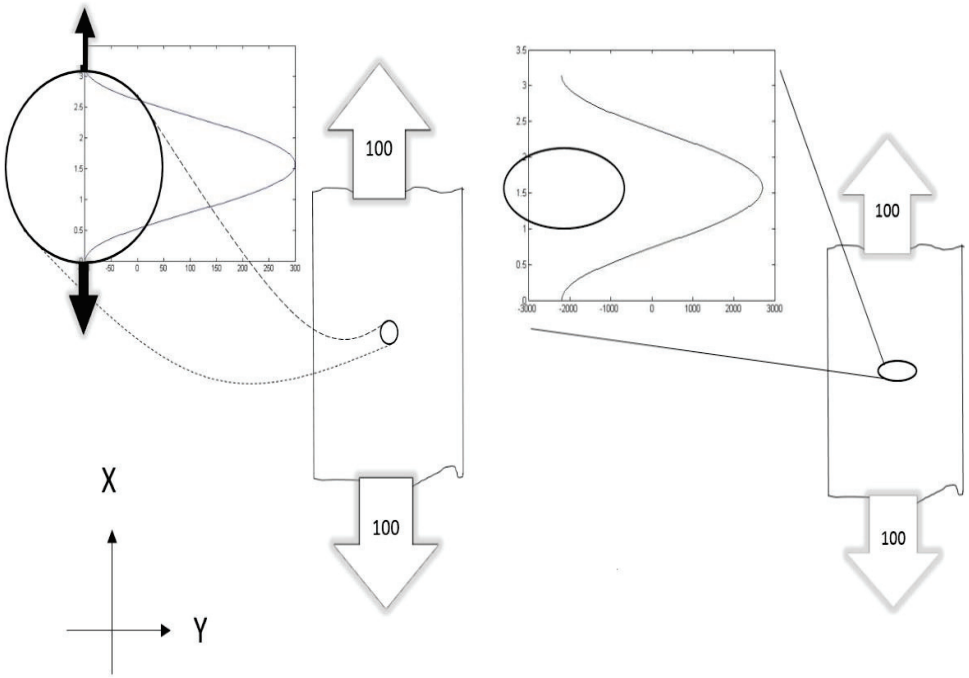

Figure 4. Stress concentration example.

1.2.3. Contact stresses

When two bodies contacting with each other under bearing loads. It will impose stresses reaching the maximum value under the contact area. The stresses are referring to as contact stresses. Stress distribution with the contacted region is mathematically changing with the geometry of the contacted surfaces. Heinrich Hertz in 1881 studied the

contact stresses for several shapes imposed on each other. His results were based on the assumption of the isotropy of the contacted area within the elastic limit. Contact stresses imposing high stresses underneath the surface. For example; in case of gear tooth contact, the tooth might be able to withstand the loading, however, the localized high stress in the contact region will lead to extract some part of the surface with what refer to as pitting phenomena.

1.2.4. The real elastic behavior of the material

Hooke's law as a keystone in mechanical engineering is considered to be limited (yet highly significant) in the real world. The range of deformation of Hook's Law is with the elastic range. Add to that the material itself, brittle materials, semi-brittle, ductile, and highly elastic materials have different ratios at which the linear Hooke's law is applied. Not to mention the temperature effect. Figure.5 shows some examples of engineering materials behavior. It shows the relation between the engineering stress and the engineering strain.

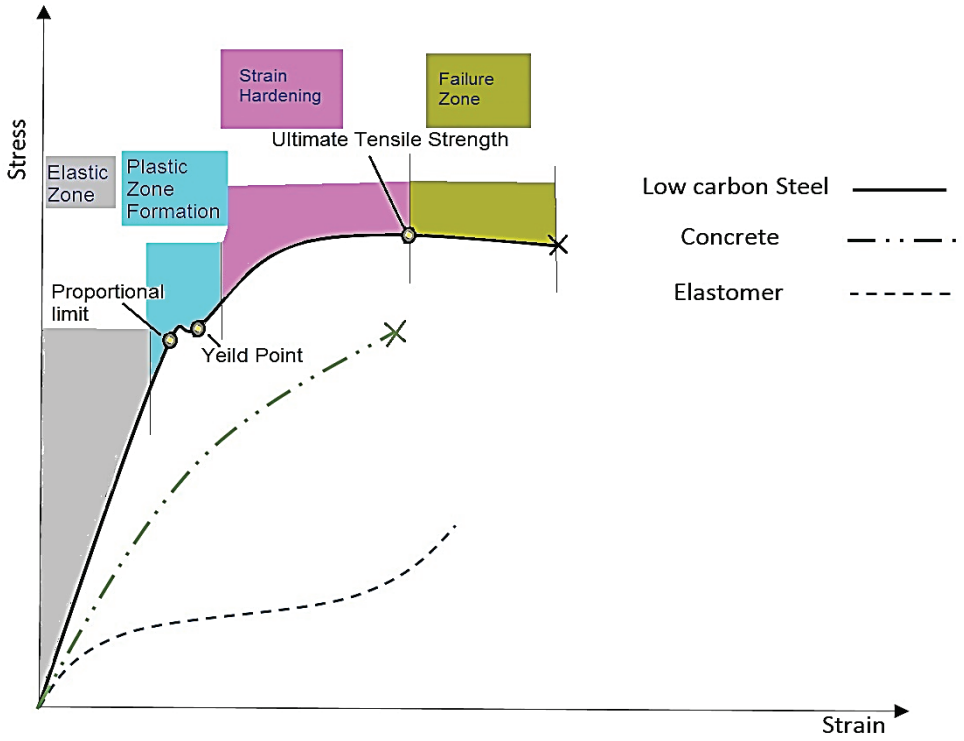

Figure 5. Engineering stress behavior for Engineering Materials

The definition of Young modulus of elasticity is extended to the nonlinear region by taking into consideration the plasticity and other related effects. In case of metallic alloys (that is been addressed in this work), when stressed beyond the elastic limit, it developed non-recoverable deformation called plastic deformation. If the loading making continues plastic deformation, this will lead to what so-called plastic flow[8]. Plastic deformation occurs by reaching the effective point at which the crystalline structure will be permanently defeated by slipping or twining. Slipping the driven by critical shear stress (τ_{cr})on planes of high molecular densities (Figure.7). The behavior of atoms versus distance plays a key role in this phenomenon. As shown in Figure.6. When atoms have big spacing within the limit of atoms mutual fields, they attract each other. The bond formation in metals is stronger than the attraction force, so the atoms in basic stay in crystalline formation. When atoms pressed into each other, this will cause repulsive force exponentially proportional to the atomic distance. This will rearrange the atomic movement to be parallel to the high-density plane. With increasing the stress to more higher level, this will lead to twining. Twining is the process by which the atoms will

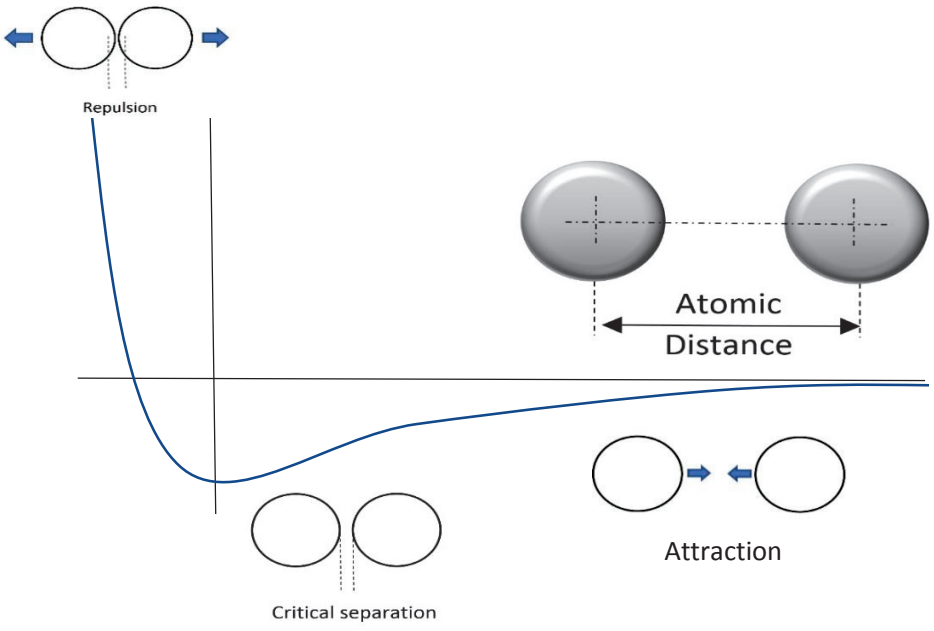

Figure 6 Atomic forces with distance

rearrange themselves to produce what looks like a mirror image of the surrounding crystals.

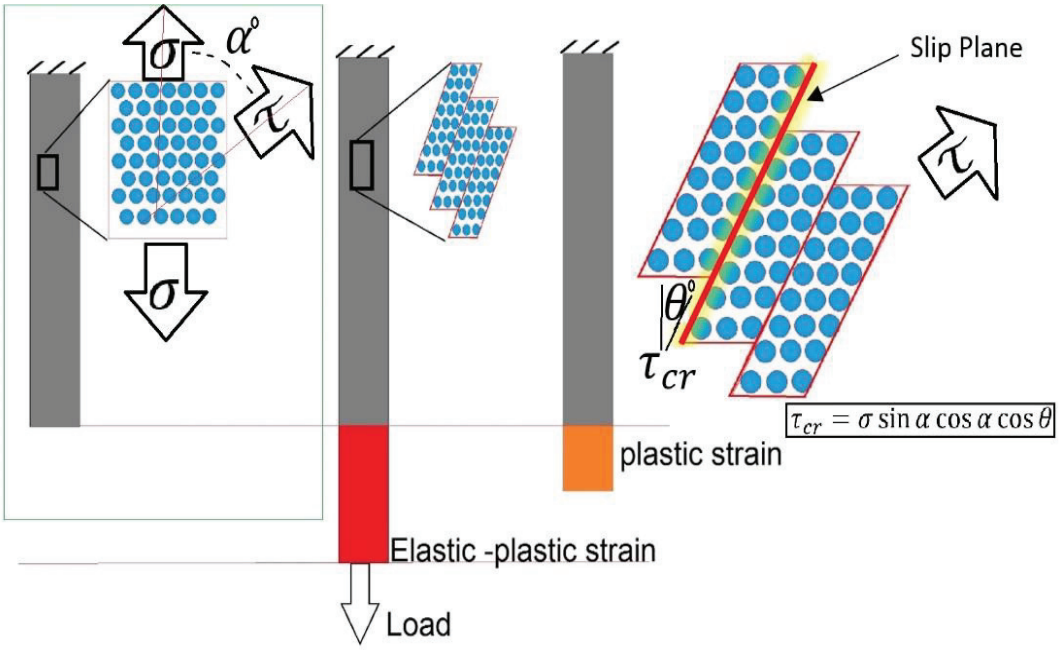

Figure 7 Slipping in Plastic deformation

1.2.5. Metallic surface

It is not enough to speak about the surface phenomenon of the metallic structure without pointing out the major aspects of the metal crystalline structure itself. Metals are crystalline stricture of rather free electrons vibrating in a sort of electronic cloud due to non-complete d-orbital. This what produce the metallic bond. This will lead to good metals conductivity in general. The metallic crystals are far from perfect, so it contains a lot of defects. Here the topographic defects will be addressed. There are three-man defects to be considered which are, chemical composition inhomogeneity, and dislocations, and voids. Chemical inhomogeneity is the describing several phenomena such as; an extrinsic atom, Schottky defect, and Frenkel defect. The extrinsic atoms that force itself in the system of main different atoms. The atomic size does not match (here, the corrosion is not addressed). The Schottky effect is the phenomena of introducing vacancy instead of atoms in the crystal. Frenkel defect is the unorthodox existence of atoms within

crystalline system making a heaver cluster than it is been anticipated. Dislocations or line defects [9] are areas of mismatch atomic distributions on a systematic mass scale. This may occur due to crystallization process. The examples of dislocations are the edge and the helical defects. Voids are the type of defects in which, lack of whole group atoms making a void.

1.2.6. Theories of elastic failures

The most vital inquiry about the mechanical structure is to identify the limit after which the failure will be highly expected. The young modulus of elasticity is the mechanical properties that reflect the elastic region of the materials that should not be exceeded. Most of the real-life cases have complicated loading, which led to complicated stresses. The stress value and behavior might change with changing the point of view for a single point within the structure, such that the stress is tensor. Taking this into account, many researchers investigate the limit at which the structure will be unsafe. All of these works address the stresses. Coulomb addresses the maximum shear stress as the one to consider his work was motivated by the deformation of tensile test of a ductile material. The evidence shows that the angle of flow coincides with the maximum shear stress generated inside the workpiece. Ranken proposed to address the maximum normal stress as the one should be under the yielding limit. The yielding according to Rankin is happened when the maximum stress exceeds the proportional yielding limit of the material. Haigh proposed to average the stress inside the material to obey the maximum normal strain energy (Equation (8).

$$\sigma_{U\max} = \frac{1}{\sqrt{2}}\sqrt{\sigma_1^2 + \sigma_2^2 + \sigma_3^2 - 2\upsilon(\sigma_1\sigma_2 + \sigma_2\sigma_3 + \sigma_3\sigma_1)} \quad \ldots (8)$$

In his work, a single stress can be obtained by equating its energy with the maximum normal strain energy of the stress tensor for a point. This lead to propose similar approached with one exception i.e. addressing the maximum distortion energy instead of normal strain energy (Equation (9)).

$$\sigma_{vms} = \frac{1}{2}\sqrt{(\sigma_x - \sigma_y)^2 + (\sigma_y - \sigma_z)^2 + (\sigma_z - \sigma_x)^2 + 6\,(\tau_{xy}^2 + \tau_{yz}^2 + \tau_{zx}^2)} \quad \ldots (9)$$

This equivalent stress usually been referring to as von Mises. Figure.8 shows the existing space of Haigh, and von Mises stresses. It is a matter of debate to identify the first who propose the maximum distortion energy theory. It has been mentioned that John Clark Maxwell is the first to propose. There are other yielding criteria are implemented such as the theory of internal friction, and Drucker-Prager yield surface[10]. It is worth to mention that, this methodology of addressing the failure is based on enveloping the safely designed stresses. The stress region outside the envelops is in non-existence.

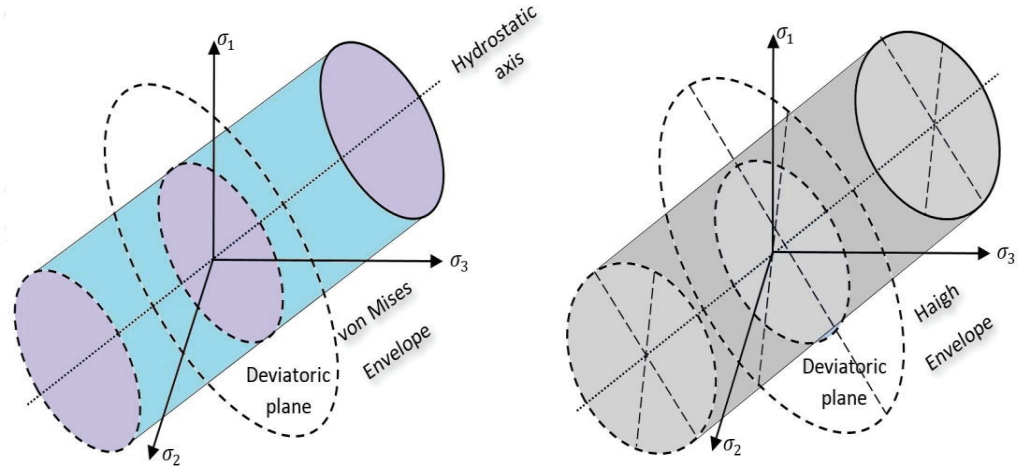

Figure 8 von Mises and Haigh Domains

1.2.7. Intuitive consideration of fatigue

Static consideration of stress-strain problem is the most common way of handling mechanical designs. However, dynamic loading tends to give a failure is not a predictable way (in the scope of previously mentioned static yielding criteria). The word “fatigue” used to describe the unexplained failure which done by reversed dynamic loading. With the development of steam engines, railroad axels, for example, are failed after the relatively short term of service. This made many scientific societies in Europe work independently to study this phenomenon. Especially after the disaster of Versailles rail accident in France. It is being registered that the first simulation apparatus of fatigue is been made by Albert in German Confederation (1829). Since 1841 the fatigue subject was studied intensively by Rankine in the United Kingdom followed by Wohler in

Germany. Wohler invented his testing apparatus with which he established the timeless prediction of fatigue, distinguishing the fatigue from creep. As been said, about science that it is not always where what the scientist wants it to be, Wohler established the following remarks for the first time.

1- The number of stress cycles is the fact of determining failure rather than test elapsed time.
2- Ferrous materials with stress loading below a certain limit (endurance limit) can withstand loading indefinitely

Simply fatigue failure has three stages, crack nucleation, crack propagation, and finally fracture. Crack propagation approach considered the logical approach since fatigue is a result of the crack in the first place. Moreover, it has been noticed that crack initiations period may cover most of fatigue life; especially in high cycle fatigue (HCF). As more detailed consideration of fatigue problem especially for metals, it states with localized plastic strain, cyclic hardening and softening, the followed by more visible failure i.e.

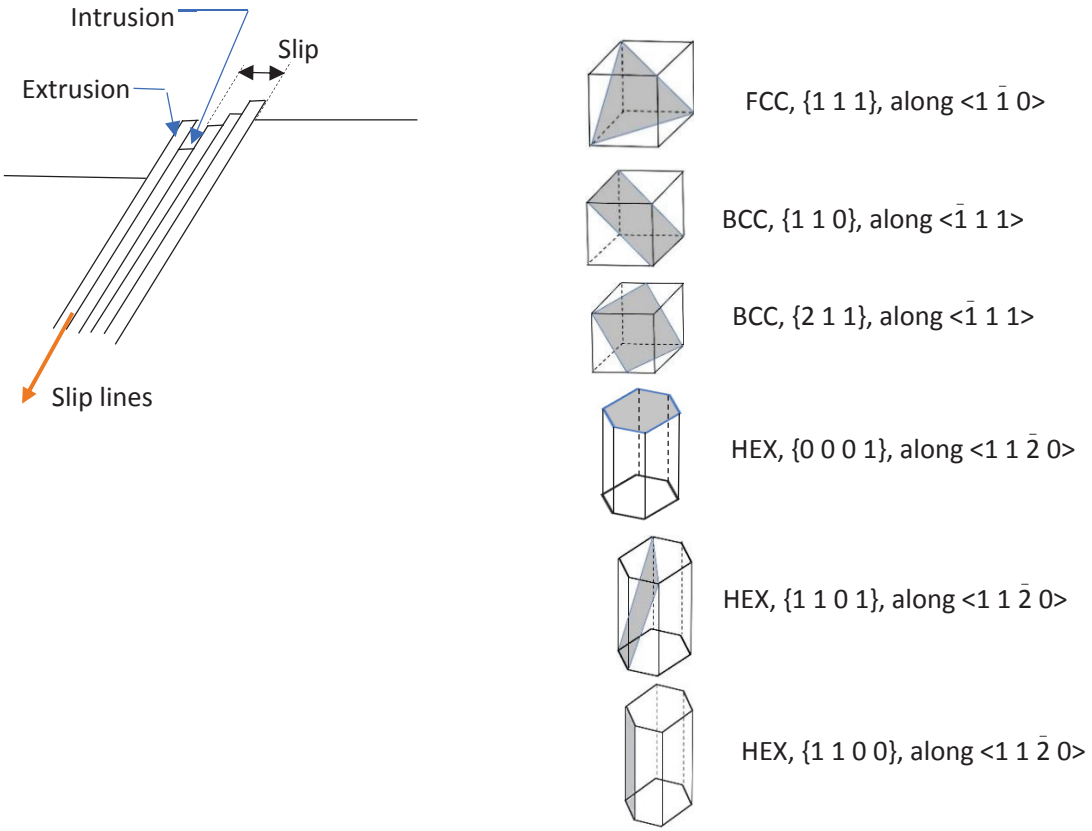

Figure 9 Slip planes of some crystalline structures

crack initiation and the repetition of the previously mentioned cycle which introduced the crack growth. Slip bands are done as an action representing the plastic strain. it has been noticed that slip behavior is intricately linked to the metal structure and strain conditions. So, slip anticipated to occur along the plane of the densest atoms (Figure.9). It is worth to mention that slip is not a straightforward process. Slip lines can be complicated, taking curvy lines or even cross slip. This is happening due to obstacles and crystal defects[11]. Generally, in one phase metals, slip bands are the main source of microcrack. The surface layer is the anticipated part to crack to happened. This is shown by many research and experiments including systematic surface polishing by ablation, surface oxidation, and surface hardening. Surface hardening can aggravate crack nucleation such that a severe transition region between the two phases of metal. The hardening process id depending on in general on making stronger phase and refining crystal dimension by extracting the solid solution energy to the ground state with shorting the time of transition to crystallization temperature by self-quenching in laser hardening as an example. The different phases cause stress resilience drops in the interface which promotes shear. Also, the difference of electronic intensity of the coexisting metal solution is not in the favor of chemical stability of the metal, so it is proportional to corrosion and aggression. Not all microcracks developed and propagate. Crack to propagate generally needs to pass the two stages. The first stage is extending itself in slip planes. Usually not deeper than few of crystals. This is mostly associated with maximum shear stress plane. In stage two, the crack grows macroscopically. Crack growth rate (crack length change per cycle($\frac{dl}{dN}$)is given in simple form as the relation between the crack length (l), stress (σ), and material properties associated with fatigue and crack withstanding ($Const.$) equation (10)

$$\frac{dl}{dN} = f(\sigma, l, Const.) \quad \dots (10)$$

Head at 1953 [12] in his model early model of crack growth rate, he considers the strain hardening around the crack tip to withstand the imperative of crack propagation until the stress is large enough to penetrate the plastic region creating another state of energy equilibrium (stating that with only purely elastic presumption). By dissecting the crack tip areas Figure.10, to the plastic region (A), Elastic region (B), and interchange region

(C). the interchange region is the region that transfers the stresses from the surrounding (elastic region) to the plastic region. If the stress is over certain limit $\sum_0$ the crack is propagating.

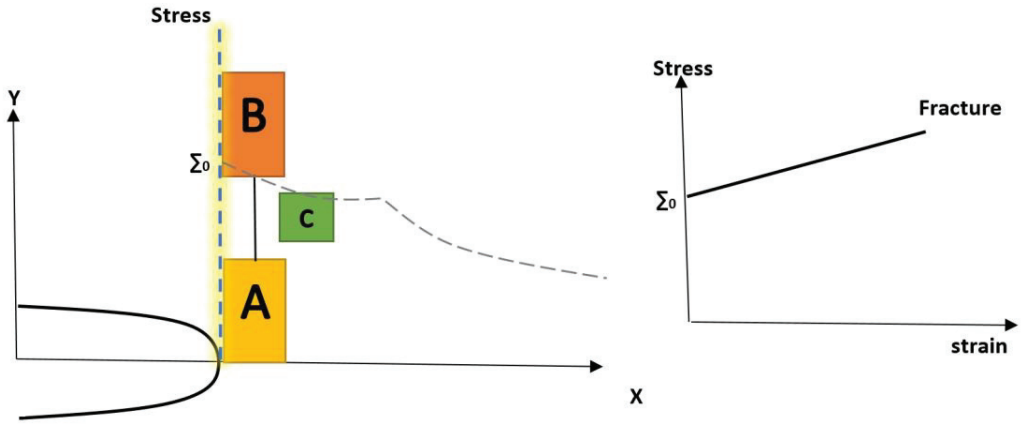

Figure 10 Head model of crack propagation

Paris and Erdogan [13], made more advanced model, from it, fatigue life can be predicted. Their relation work with critical boundaries of stress intensity factors interval, i.e. stage two.

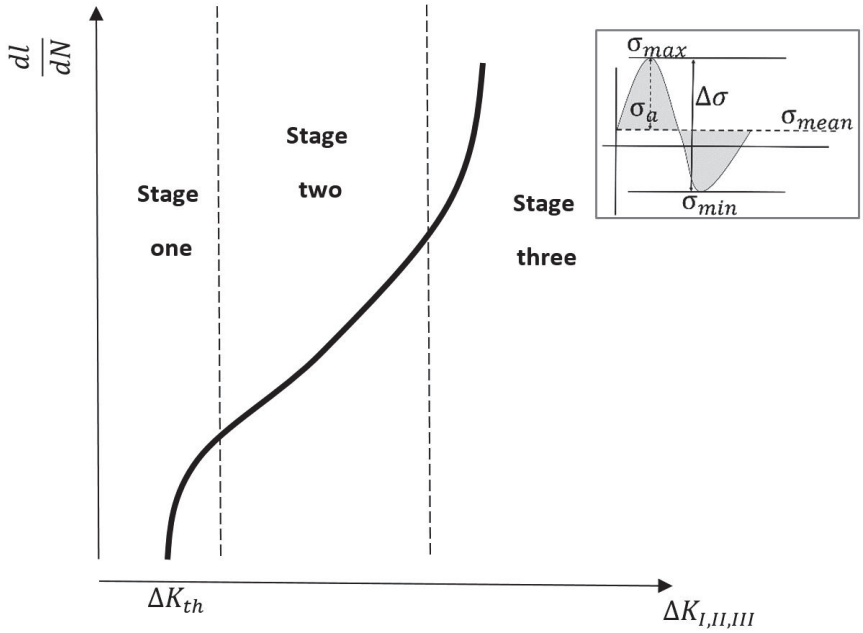

Figure 11 Paris Erdogan Model of Crack propagation

Figure.11 shows the relation between the change stress intensity factor ($K_{I,II,III}$) and crack propagation rate per cycle. Their model is presented in equation (11)

$$\frac{dl}{dN} = Const.(\Delta K_{I,II,III})^m \quad \ldots (11)$$

Here *Const.*, and *m* are material constants. $\Delta K_{I,II,III}$ can be calculating in the scope of linear elastic fracture mechanics (LEFM), considering approximating function describing crack problem $f(l, shape)$ as in equation (12).

$$\Delta K_{I,II,III} = f(l, shape).\Delta\sigma \quad \ldots (12)$$

The fatigue life expectancy (N_f) can be found by integration (Equation (13))

$$N_f = \int_{l}^{l_{th}} \frac{1}{Const.} \frac{dl}{(f(l, shape).\Delta\sigma)^m} \quad \ldots (13)$$

Paris-Erdogan model sensitivity toward stress ratio ($r = \sigma_{min}/\sigma_{max}$), [14]which pushed for more adaptive models, started with Walker[15] modification till Collipriest [16] completed the whole three stages in their model. Many models been introduced within crack propagation idea. And their kernel was Paris –Erdogan insight [17]. Paris-Erdogan was used to estimate fatigue life for human artificial organs replacements [18]. Stress life models as Wohler, Basquin, are the earliest models to formulate fatigue and predict number of the cycles (Figure.12)).

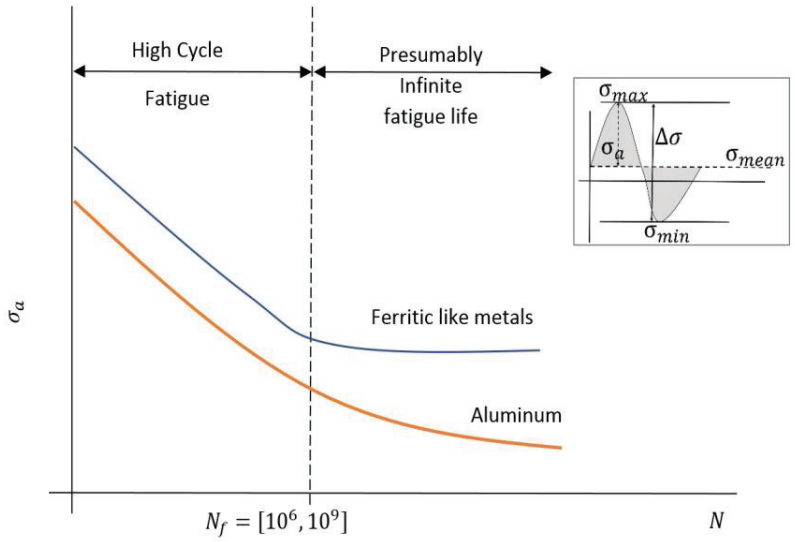

Figure 12 stress based fatuige life model

The correlation between amplitude stress σ_a and number of cycles N is taking the form

$$\sigma_a = \sigma'_f N^b \quad \ldots (14)$$

Here, $\acute{\sigma}_f$ and b are the curve constants. However, it is not recommended for life analysis of high loads, especially it lacks the strain hardening consideration. Cyclic deformation and strain life approach (ε-N) [19], is suitable for testing designs, and evaluate expected life, especially, cyclic hardening can consider.

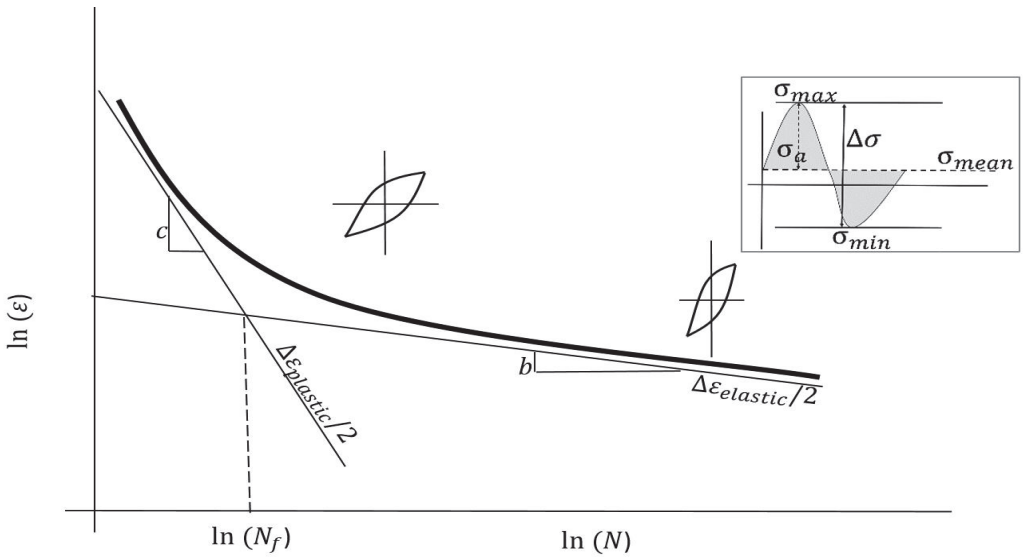

Figure 13 Strain life fatuige model

To find life generally, need to solve the correlation that is a combination of the change in elastic strain $\Delta\varepsilon_{elastic}$ (Figure.13) and change in plastic strain $\Delta\varepsilon_{plastic}$ (equation (15)).

$$\frac{\Delta\varepsilon}{2}=\frac{\Delta\varepsilon_{elastic}}{2}+\frac{\Delta\varepsilon_{plastic}}{2}\,|\,\Delta\varepsilon_{elastic}=\frac{\sigma'_f}{E}(2N)^b,\Delta\varepsilon_{plastic}=\varepsilon'_f(2N)^c \quad \ldots (15)$$

Here $\acute{\varepsilon}_f$, and c are curve constants, E is the Young modulus of elasticity. It is worth to mention that crack propagation is temperature dependent, so the crack for metal can change from ductile to brittle fracture with decreasing temperature[20]. Luckily in the case of implants, the living body keep the temperature in a level above 25-degree centigrade in order to maintain bio-organic reaction.

1.3. Static consideration of structural design

Structural Design is addressing the elastic envelope in the first step. Especially with the static of low loading. In the other hands and with fully reciprocal loading, the fatigue-based design should be considered. The design based on varying stress, (without considering intense stress hardening) is been studied many researchers such as Gerber (1874), Goodman (1899), Soderberg (1930), and Morrow (1960). The main design space (Figure. 14) is been chosen with respect to mean stress and stress amplitude. If the stress amplitude is zero, the design problem obeys the criteria of elastic failure as Higen (Maximum strain energy per unit volume), and Maxwell- Von mises-Hencky (maximum distortion energy per unit volume). The full reverse loading, the design process is addressed by fatigue criterion.

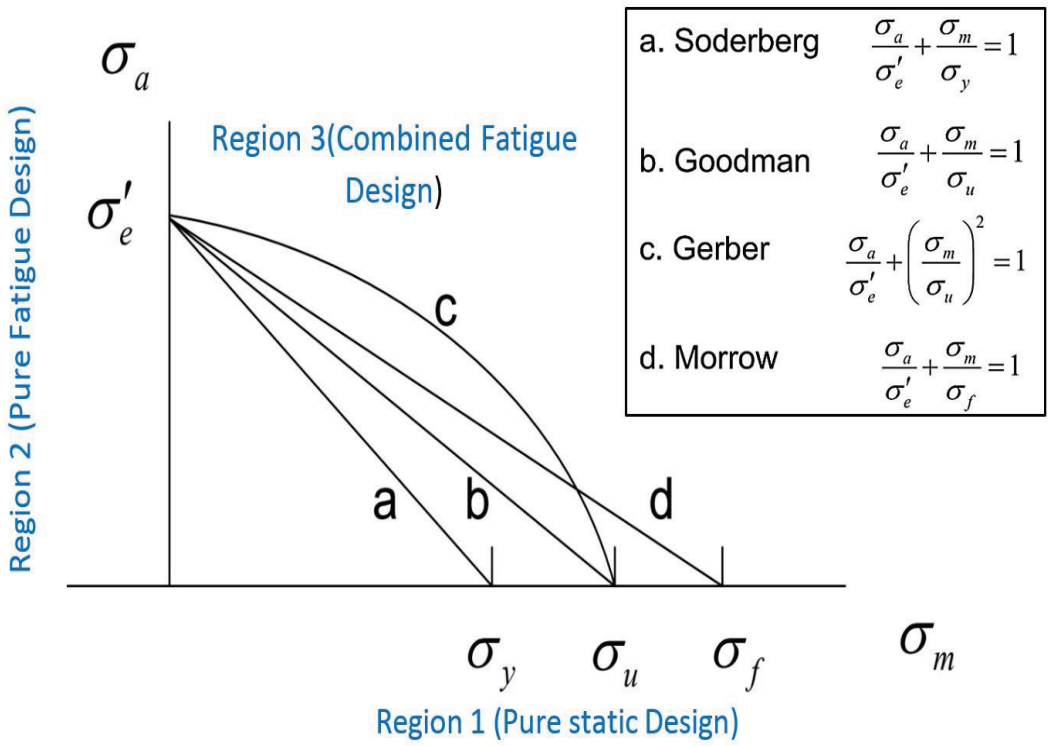

Figure 14 Static Design Consideration

The application is controlling the range of working characteristics. Stress is the desired characteristic to constrained designing process. Stress is the main quantity of which most failure criterion is used. Stress loading variance dictates the design criterion. First, let's consider the general loading (Figure.15).

$$\sigma_m = \frac{\sigma_{\max} + \sigma_{\min}}{2} \quad \ldots (16)$$

$$\sigma_a = \frac{\sigma_{\max} - \sigma_{\min}}{2} \quad \ldots (17)$$

$$r = \frac{\sigma_{\min}}{\sigma_{\max}} \quad \ldots (18)$$

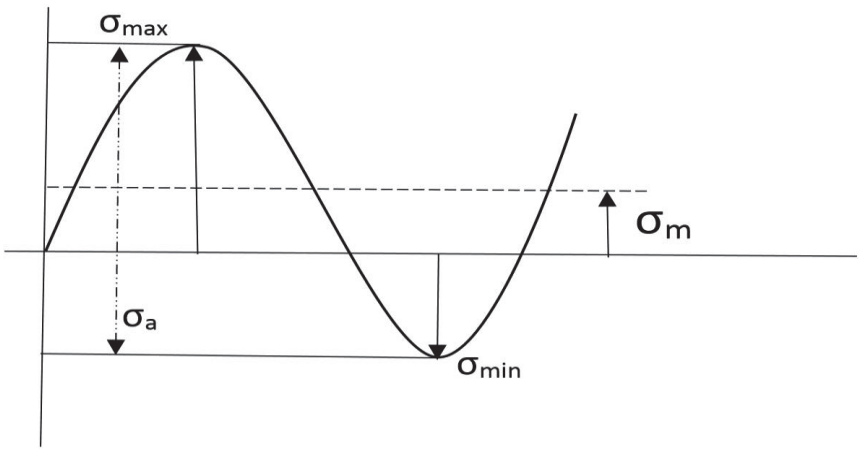

Figure 15 Fluctuation Stress avergingin

The problem of region 1of Figure.14 is restricted to elastic failure averaging based design. In general for most metallic structure, von Mises averaging is been used[21, 22]. The design process of structures concerning fatigue is actually turned to be statically approached by mechanical engineers[23-25]. Only the statistical representation of stress history is being taken into consideration i.e. mean, stress ratio, etc. and the order of various repetitive stress amplitudes. This is Justified by the Whole work and notes which is followed by intensive metallurgical experiments to study crack initiation and damage in various materials. The engineering models do not consider the time and its derivatives (velocity, and acceleration) into fatigue curves themselves. Creep is a terminology referring to the phenomenon of deformation considering time. The creep modeling is using the kinetic molecular energy approach using Boltzmann notations. This is spotting the difficulty of a direct time-dependent universal model of fatigue phenomenon. In complex modeling when stress flow is significant enough, such modeling (directly time-dependent) can be approached[26, 27]. In the case of Orthopedic design, the temperature and the loading are fixed to a range that such phenomenon can be omitted safely (In the scope of strictly mechanical Engineering, so the migration of ions to the live tissue, corrosion, and physical impact on the molecular compound in the living body are not the main concern of this work).

1.4. Optimization, a mathematical point of view

Optimization was defined by Snyman [28] as the set of scientific methodologies to find the best solution. Generally, optimization model consists of variables constraints (if any), and the objective function. Variables define the objective function shape, optimization methodology; even the constraints. Constraints if it been introduced to the optimization process, guide the solution to what so-called feasibility area of the solution. The objective function (presuming the smoothness through the design period) is the one that took the extremum process. The objective function is designed and, in some cases, rectify extensively according to the desired output. Objective function ideally should be convex. The stronger the convexity, the more global optimization solution could be found. Convexity can be described clearly by the following:

Consider the set which the distance of each two points in it as

$$\left\{\mathbf{x} \mid \mathbf{x} = x^a + \lambda(x^a - x^b),\ \lambda \in \mathbb{R}^n\right\} \quad \ldots (19)$$

The function f is convex if

$$f(\lambda + (1-\lambda)x^a) \leq \lambda f(x^b) + (1-\lambda) f(x^a) \quad \ldots (20)$$

This can be described graphically in Figure.16. in terms of minimization. Figure.16- A is a convex function. The global minimum is existing such that

$$f(\mathbf{x}) \geq f(\mathbf{x}^*)\ , \forall\, \mathbf{x} \in \mathbb{R}^n \quad \ldots (21)$$

For most practical engineering problems; strong convexity concept is not common for practical function characteristics within the chosen design set (smoothness, convexity, etc.) Satisfy the physical integrity and compatibility of the physical problem. However, averaging methods are used to describe the physical behavior in a systematic function

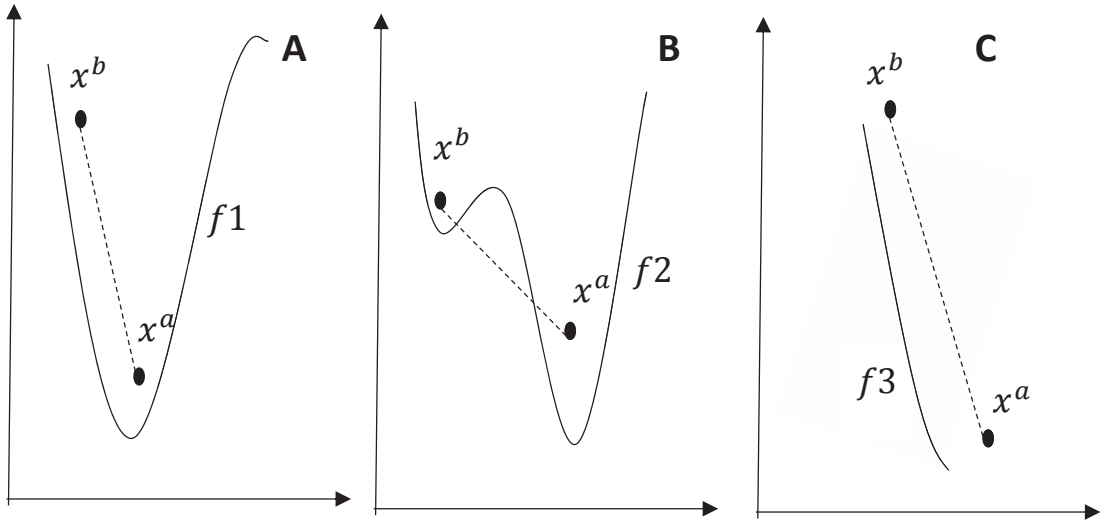

Figure 16. A. Strong Convex function. B. Weak Convex Function. C. Non Convex Function

with considerable good approximated smoothness. For example, random vibration ergodically traded by averaging the system statically in order to build a manageable function to use[29] and analyze[30]. In some cases, the mathematical modeling describes by the tangible approach. So, in the case of maintenances determinability of aircraft wings, the random vibration will be used as it is to be converted to equivalent stress loading and then transfer to fatigue state space.

1.4.1. Function behavior within optimization process

Smoothness is achieved by approximation of the problem to be confined within the smooth mathematical formulation. The approximation is extensively used for modeling of engineering problems. Getting global extremum can be a difficult task since the path of function test, usually confined by local extremum. For example, minimization problems are searching, seeking the global minima (equation (22)), so it highly probably hits the local minima (equation (23)) especially if the local minima are strong. Random multi-start application of local minimization process is a practical approximation to find

the global minimum. So, the minimum value obtained after several "sufficient "trails. A number of trails is proportional to the degree of convexity. Strong convexity needs only one trail.

$$f(\mathbf{x}) \geq f(\mathbf{x}^*) \,, \forall \mathbf{x} \in X \qquad \ldots (22)$$

$$f(\mathbf{x}) \geq f(\mathbf{x}^*) \,, \left\|\mathbf{x} - \mathbf{x}^*\right\| \leq \epsilon, \forall \mathbf{x} \in X \qquad \ldots (23)$$

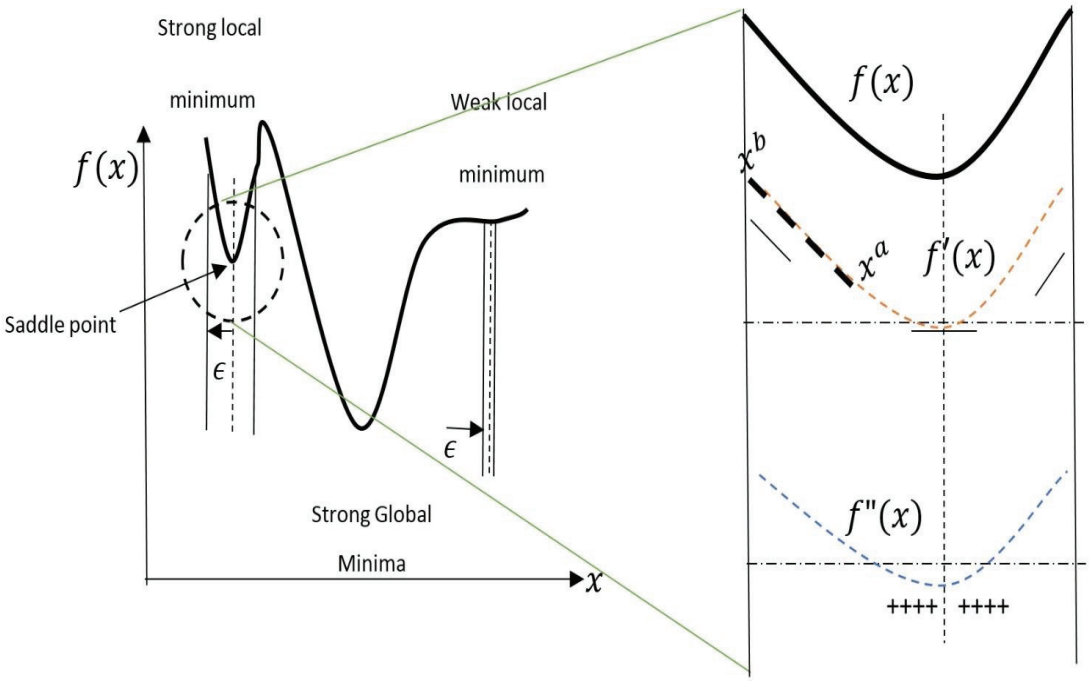

Figure 17 Mathematical Optimization concepts

Saddlepoint (Figure.17) exists for extremum points. With the presumption of smoothness in second-order differentiation ($f(x) \in C^2$), the single variable function ($F(\lambda)$) along the line ($\overline{x^a x^b} = \mathbf{x}(\lambda) = \mathbf{x}' + \lambda \mathbf{u}$) be

$$F(\lambda) = f(\mathbf{x}(\lambda)) = f(\mathbf{x}' + \lambda \mathbf{u}) \qquad \ldots (24)$$

The first order derivative is

$$\frac{dF(\lambda)}{d\lambda} = \frac{df(\mathbf{x}(\lambda))}{d\lambda}\bigg|_u = \nabla^T f(\mathbf{x}(\lambda)) u \qquad \ldots (25)$$

The second order derivative is

$$\frac{d^2F(\lambda)}{d\lambda^2} = \nabla^T(\nabla^T f(\mathbf{x}(\lambda))\mathbf{u})\mathbf{u} = \mathbf{u}^T\mathbf{H}(\mathbf{x}(\lambda))\mathbf{u} \quad \dots (26)$$

$\mathbf{H}(\mathbf{x}(\lambda))$ is widely known as Hessian matrix. If the Hessian matrix is positive definitive for all the points within the chosen set ($\forall \mathbf{x} \in X$) and the tangent of the function is zero, then the point is strong minimum.

1.4.2. Unconstraint extremum

In order to extremum function, generally, a direct search algorithm is commonly used. The algorithm is summarized as following[31]:

Start from a starting point of estimated strong convexity. The general extremum optimality criterion takes the form

$$\begin{aligned} &Extremum\ F(\lambda) = f(\mathbf{x}^{i-1} + \lambda\,\mathbf{u}^i) \\ &\left\|\mathbf{x}^i - \mathbf{x}^{i-1}\right\| &&< \epsilon_1 \\ &\left\|\nabla f(\mathbf{x}^i)\right\| &&< \epsilon_2 \\ &\left\|f(\mathbf{x}^i) - f(\mathbf{x}^{i-1})\right\| &&< \epsilon_3 \end{aligned} \quad \dots (27)$$

$\epsilon_{1\to 3}$ are larger than zero

Getting the gradient of the function can be a complex task. The numerical approximation may be adopted such as finite difference. An indirect method such as Newton's method is used as optimization method, by searching for the points of zero slop angle (stationary points). Expanding the first gradient of the stationary points, using Taylor series, under the assumption of the stationary point is a local extremum $(\mathbf{x})$ with associated error (δ), it gives the equation (28)

$$\nabla f(x) = 0 = \nabla f(\mathbf{x}^i + \delta) = \nabla f(\mathbf{x}^i) + \mathbf{H}(\mathbf{x}^i)\delta + High\ order\ terms.. \quad \dots (28)$$

The high order terms can be ignored by presuming the infinitesimally of the error. Onley the first two terms are needed to be solved. The iterative scheme be

$$\mathbf{x}^{i+1} = \mathbf{x}^i - \mathbf{H}^{-1}(\mathbf{x}^i)\nabla f(\mathbf{x}^i) \,|\, \lim_{i\to\infty} \mathbf{x}^i = \mathbf{x}^* \quad \dots (29)$$

1.4.3. Constraint extremum

Extremizing function with the special condition will lead to feasibility consideration of the designed problem. The constraint is the mathematical terminology for the special conditions. Constraint extremum can be transformed substitute unconstraint optimization by introducing penalty function formulation. Penalty function.

$$\left.\begin{matrix} Extremum \quad f(\mathbf{x}) \\ s.t. \quad g(\mathbf{x}) \end{matrix}\right\} \rightarrow Extremum\, P(\mathbf{x}) = f(\mathbf{x}) + \sum \beta g^2(\mathbf{x}) \qquad \ldots (30)$$

Where (β) is the penalty parameters. Choosing penalty parameters is crucial for the optimization problem. The lagrangian function is another method which is successfully applied for solving the constraint problem. This is done by introducing Lagrange multipliers (ℓ).

$$\left.\begin{matrix} Extremum \quad f(\mathbf{x}) \\ s.t. \quad Cond = \begin{cases} g(\mathbf{x}) = 0 \\ h(\mathbf{x}) = 0 \end{cases} \end{matrix}\right\} \rightarrow Extremum\, P(\mathbf{x}, \ell) = f(\mathbf{x}) + \sum \ell Cond \qquad \ldots (31)$$

Constraints type plays an important role in solving the problem. In general, the constraints classified as: equality constraints ($g(\mathbf{x}) = 0$), and non-equality constraints ($g(\mathbf{x}) < 0$). The optimality conditions based on the linear Lagrangian theory, in general, is earthier necessary, or sufficient. Necessary is referring to the number of conditions that it must be obtained to solve the system. Optimality might have reached a false target, such as local extremum, or even be in case of the non-convergence state. Here, the term Sufficient conditions are introduced, referring to the number of conditions that guarantee the extremum process. Matter of extremum is a complicated process, and it is based on the function valid optimization problem conditions that previously mentioned. If the condition function and the target function are convex, the necessity and sufficiency of the conditions are existing together. In term of Lagrangian optimization approach, necessary conditions referring to the rank constrains (m) which is necessary to identify the unique extremum of the function (m). Let ($\mathbf{x}^*$) is the extremum point of the function (f). The function is constrained to function (g). Assuming that ($\mathbf{x}^*$) is a regular point for both

target and constraint functions (∂f and ∂g are analytical at $\mathbf{x}^*$); there is unique ($\bar{\ell} \in \mathbb{R}^m$) at which, the Lagrangian function derivative is satisfying the following:

$$\frac{\partial P(\mathbf{x}^*, \bar{\ell})}{\partial \mathbf{x}_j} = 0 \ , \ j = 0,1,...,n$$
$$\frac{\partial P(\mathbf{x}^*, \bar{\ell})}{\partial \bar{\ell}_j} = 0 \ , \ i = 0,1,...,m \qquad \ldots (32)$$

In general, the necessary conditions are not sufficient to imply constrained extremum for $\mathbf{x}^*$. to find the sufficient rank of the constraints, we need to introduce complementary extremum indication. The most desire induction is the second order derivative, which is translated in a set of equations as the Hessian matrix. So, let $\mathbf{x}^*$satisfy the regularity principle mentioned before. If Hessian of the target and constraint functions ($\mathbf{H}_{f,g}$) is positive, definitive, for the constraint rank, then the rank is sufficient.

$$\mathbf{H}_{f,g} = J(\nabla f(\mathbf{x}^*) + \sum_{i=1}^{m} \lambda_i J(\nabla g_i(\mathbf{x}^*)) \qquad \ldots (33)$$

Here J refers to the Jacobian operator.

1.4.4. Inequality constraints optimization, Karush-Kuhn-Tucker (KKT) approach

In order to optimize inequality constraint using Lagrangian, Karush (1939), Kuhn, and Tucker (1951), independently driven the necessary conditions. For extremum problem with equality ($g_{i=1..m}$), and inequality conditions($h_{k=1..p}$). Assuming the Regularity of the conditions (Active inequality and equality conditions are linearly independent), the necessary conditions should satisfy the following:

Gradient conditions as

$$\nabla f(\mathbf{x}^*) + \sum_{i=1}^{m} \bar{\ell} \nabla g_i(\mathbf{x}^*) + \sum_{k=1}^{p} \bar{\bar{\ell}} \nabla h_k(\mathbf{x}^*) = 0 \qquad \ldots (34)$$

Constraints (primal feasibility)

$$g_i(\mathbf{x}^*) = 0$$
$$h_k(\mathbf{x}^*) \geq 0 \quad \ldots (35)$$

Complementary slackness

$$h_k(\mathbf{x}^*) = 0 \quad \ldots (36)$$

Active constraint means that, the constraint is zero at the point of interest.

1.5. Structural optimization

Originally, structural optimization is a matter of a determinably functional analysis based on the noticeable physical model. With increasing of adopting mathematical modeling in real-world application associated with the advancement of mathematics (understanding and technique), the variational methods are introduced to include the previously Underdetermined problems. Virtual work concept expanded the scope of solving the real-world cases[32]. Structure optimization tends to be known as parametric and non-parametric optimization. Parameters usually taking the aspects of topographical representation domain in terms of well approximated mathematical model related to the constraints and the optimality criteria. Heuristic and metaheuristic methodologies are used effectively for the parametric optimization. Sizing optimization is an example of parametric optimization, such that cross-section, size of desired material, and/or holes could directly have linked to stress minimization problem. Finding the optimal material representation in space for best structural design is not an easily represented in the scope of the known quantities that represent the problem such as masses, loads, reactions, etc. The meaning of the easiness here is to link the topology design directly to the known values (constraints) and make universal parametric objective for it. This lead to the other optimization methodology which is non-parametric optimization. Examples of such method are topology optimization (layout and shape optimization).

1.6. Finite element method

Modern physical problems have become complex, making continuous mathematical models are not quite practical to be used. The numerical solution is used to simplify the modeling. Finite difference method (FDM) and finite elements method

(FEM) (as shown in figure.18) are examples of special discretization of the physical problems which are successfully used.

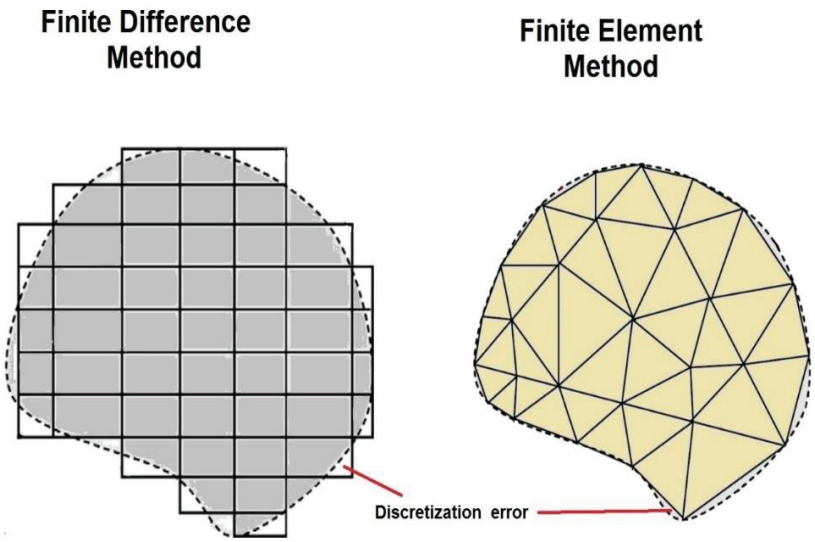

Figure 18 Finite element versus Finite Difference error

The beginning of Finite element method (FEM) is tracked to Richard Courant[33]. In his work, He used liner approximation to prescribe the functional minimization over subdomains. He divided a square hollow box to points joined as meshes of elements to solve the Saint Venant stress induced by torsion. FEM according to J. N Reddy[34], the most powerful numerical discretization method ever used for analyzing engineering problems. The finite element modeling is widely used in commercial mechanical engineering software's, so it gives continuum mechanics, with accurate mathematical modeling, numerical analysis for getting the algorithmic solution, and computer libraries which can apply for large-scale classical problems. FEM modeling has the three general features, first, approximating the design domain into the collection of pre-chosen collective subdomain called elements. The choice of the elements is the second aspect. Element represents the approximation of the variables. It consists of the combination of algebraic polynomials and undetermined parameters. The parameters and polynomial design should be satisfying the presumed governing equations. Nodes as unknown parameters are geometrically identified at the beginning of the solution. The collective algebraic relation associated with known nodes and elements is the third step. The

collective algebraic equation of elements will form matrix formation. Weighted residues method is used to convert the physical problem into finite element numerical set. Let's consider the generalized physical form in operator form

$$L[f(x)] = g(x) \quad \ldots (37)$$

Here, L is the operator, $f(x)$ is the unknown function and $g(x)$is the solution set function. In order to solve the problem, the unknown function $f(x)$ can be represented by a set of sub simple functions $V_n(x)$. These functions are tuned with arbitrary constants a_n. The aim of the use of such approach is that the subfunction will be chosen as easy to calculate and solve set. The weights will aid in minimizing the number of the subfunction is needed to describe the unknown function.

$$L[\sum_n a_n V_n(x)] = g(x) \quad \ldots (38)$$

By taking the constants outside the operators it gives us the final form as

$$\sum_n a_n L[V_n(x)] = g(x) \quad \ldots (39)$$

In order to measure the arbitrary functions $f(x)$ and $g(x)$, a set of another weighted functions $W_m(x)$. This will be as in equation (40)

$$\left\langle W_m(x), \sum_n a_n L[V_n(x)] \right\rangle = \langle W_m(x), g(x) \rangle \quad \ldots (40)$$

Which as similar as been done for equation (41)

$$\sum_n a_n \langle W_m(x), L[V_n(x)] \rangle = \langle W_m(x), g(x) \rangle \quad \ldots (41)$$

The equation (41) can be easily written in matrix form as

$$\begin{bmatrix} \langle W_1(x), L[V_1(x)] \rangle & & \\ & \ddots & \\ & & \langle W_m(x), L[V_n(x)] \rangle \end{bmatrix} \begin{Bmatrix} a_1 \\ \vdots \\ a_n \end{Bmatrix} = \begin{Bmatrix} \langle W_1(x), g(x) \rangle \\ \vdots \\ \langle W_m, g \rangle \end{Bmatrix} \quad \ldots (42)$$

The most popular method of constructing finite element is Galerkin method (named after Boris Grigoryevich Galerkin). He proposed to choose the sub simple functions as weighted function $W_m = V_n(x)$. Finite element method discretizing the domain into small regions set and driven and set as libraries. These elements are classified into two main categories: nodal elements, and edge elements. Historically, nodal elements are the first to be driven and implemented. The field values are being calculated for the nods only. Any other point needs interpolation. Nodal elements approach suffers from spurious (extraneous) solutions and vector parasites. This is noticeable in Vibration problem[35], so the resonant frequencies are dependent on the element size, and distribution. In order to eliminate the non-valid solution, edge element was suggested. In the edge elements, the boundaries are the part to be considered regarding field calculations. However, Mur [36](1994) showed that there is no guarantee of spurious free solution for edge element. In this work only, the nodal element is used. Shape function that is chosen to describe the problem is divided generally into two types. First one is the Lagrangian interpolation function for which an inner node is introduced for high order elements. The second one is the serendipity elements, for which only boundary nodes are exists for high order elements. Figure. 19 shows some of the used nodal elements

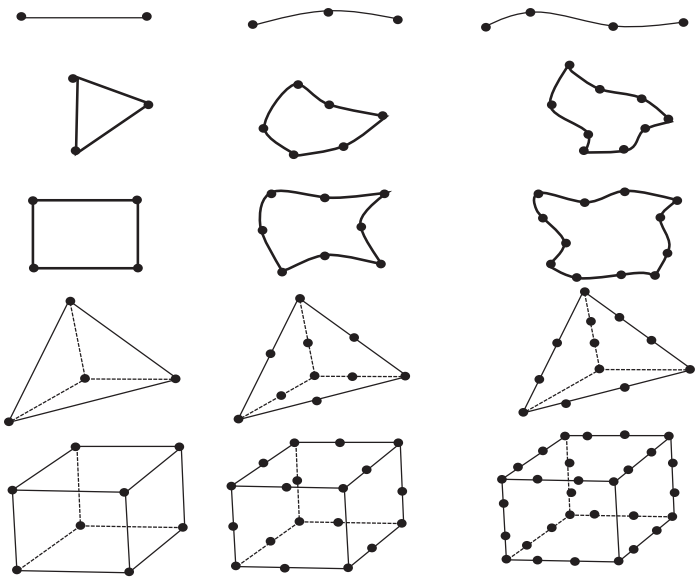

Figure 19 Examples of Finite elemnts

In basics; elements should not overlap and should not be a gap between them. In other words, elements should have conformed perfectly.

1.6.1. Triangular nodes element derivation

The 3 nodes element take the form of a triangle. It has six degrees of freedom, two for each node. The element is connected to the neighbored one with the shared nodes. To derive the finite element formation, First the consideration the coordinate transformation is needed. the coordinates transformation is the link between the local coordinates for the element as an individual system and the globalization of the linked elements in order to build the spars system that represents the physical problem. The plane stress problem in the 2D case is the final goal. Local parameters of the triangle are taking the form of ξ_1, ξ_2 , and ξ_3. The summation of these parameters equal to unity.

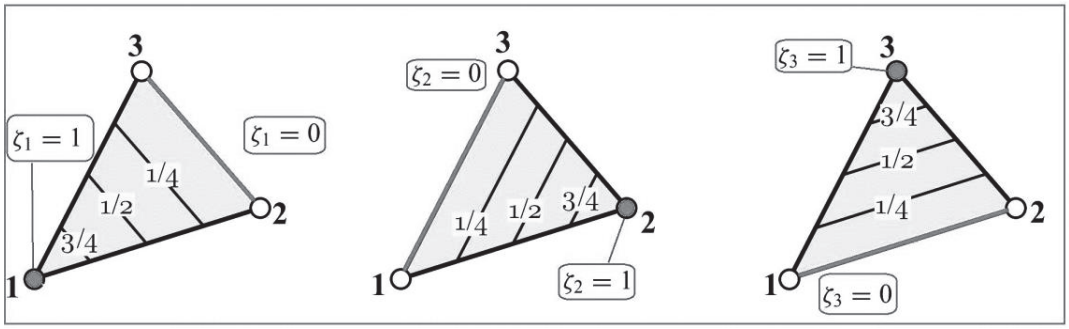

Figure 20 Triangular Coordinates

Taking the Cartesian coordinate as the system of global domain. The link between the Cartesian and local coordinate is presented in equation (43)

$$\begin{Bmatrix} 1 \\ x \\ y \end{Bmatrix} = \begin{bmatrix} 1 & 1 & 1 \\ x1 & x2 & x3 \\ y1 & y2 & y3 \end{bmatrix} \begin{Bmatrix} \xi_1 \\ \xi_2 \\ \xi_3 \end{Bmatrix} \quad \dots (43)$$

The displacement of the element center (of the triangular parameters ξ_1, ξ_2 and ξ_3) is taking the form (equation (43))

$$\begin{Bmatrix} u_x \\ u_y \end{Bmatrix} = \begin{bmatrix} \xi_1 & 0 & \xi_2 & 0 & \xi_3 & 0 \\ 0 & \xi_1 & 0 & \xi_2 & 0 & \xi_3 \end{bmatrix} \begin{Bmatrix} u_{x1} \\ u_{y1} \\ u_{x2} \\ u_{y2} \\ u_{x3} \\ u_{y3} \end{Bmatrix} = \mathbf{Nu} \quad \dots (44)$$

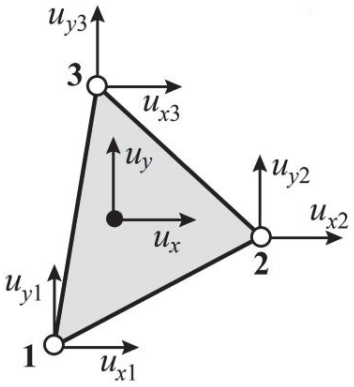

Figure 21 Displacement Interpolation over the 3 nodes element

The elements shape function (N) are found from equation (45).

$$\begin{Bmatrix} \xi_1 \\ \xi_2 \\ \xi_3 \end{Bmatrix} = \frac{1}{A} \begin{bmatrix} x2y3 - x3y2 & y2 - y3 & x3 - x2 \\ x3y1 - x1y3 & y3 - y1 & x1 - x3 \\ x1y2 - x2y1 & y1 - y1 & x2 - x1 \end{bmatrix} \begin{Bmatrix} 1 \\ x \\ y \end{Bmatrix} \quad \dots (45)$$

Where (A) is the determinant of the core matrix of equation (43). The strain of the element can be found by the differentiation of the displacement fields

$$\varepsilon = \begin{bmatrix} \frac{\partial u_x}{\partial x} & \frac{\partial u_y}{\partial y} & \frac{\partial u_x}{\partial y} + \frac{\partial u_y}{\partial x} \end{bmatrix} = \mathbf{Bu} \quad \dots (46)$$

Where B matrix is the strain-displacement matrix. Stress can be formed by the multiplication of the material constant and the strain ($\boldsymbol{\sigma} = \mathbf{E}\boldsymbol{\varepsilon}$). The variation of the total potential energy for the element which is composed of the internal strain energy($\frac{1}{2}\boldsymbol{\varepsilon}^{\mathbf{T}}\mathbf{E}\boldsymbol{\varepsilon} = \frac{1}{2}\mathbf{u}^{\mathbf{T}} \int_V \mathbf{B}^{\mathbf{T}}\mathbf{E}\mathbf{B}dV\mathbf{u}$), and the traction forces energy. By implementing the principle of minimum potential energy[37], this will give the spar system in terms of the traction and displacement as in equation (47).

$$\int_V \mathbf{B}^T \mathbf{E}\mathbf{B} dV \mathbf{u} = \mathbf{K}\mathbf{u} = \mathbf{F} \quad \ldots (47)$$

Here **K** is the stiffness matrix

1.6.2. High order two-dimensional element derivation

Starting from the same steps of the previously mentioned element (section 1.6.1), a suitable shape function is chosen to represent the relation of local and global coordinates of the element. The Shape functions of the linear and the quadratic element are listed in the set (48), and (49). The same steps of section 1.6.1, may be taken to derive the final stiffness form.

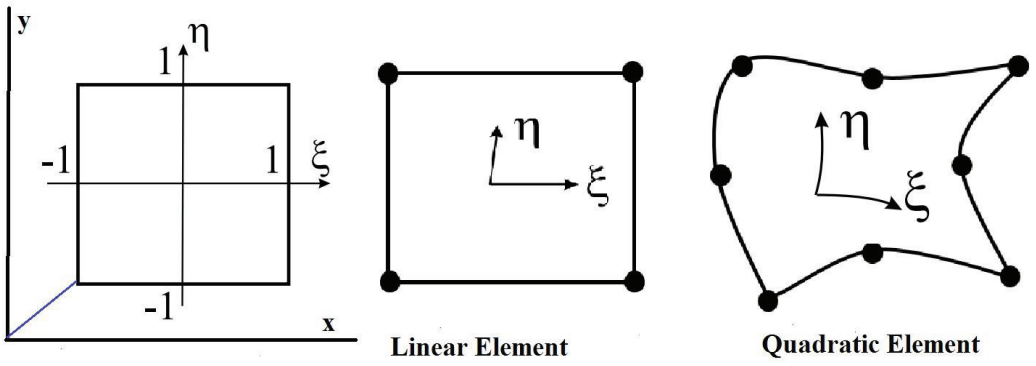

Figure 22 Linear and quadratic element

$$N_{4nodes} = \begin{Bmatrix} \frac{1}{4}(1-\xi)(1-\eta) \\ \frac{1}{4}(1+\xi)(1-\eta) \\ \frac{1}{4}(1+\xi)(1+\eta) \\ \frac{1}{4}(1-\xi)(1+\eta) \end{Bmatrix} \quad \ldots (48)$$

$$N_{8\ nodes} = \begin{Bmatrix} \frac{-1}{4}(1-\eta)(1-\xi)(1+\xi+\eta) \\ \frac{-1}{4}(1-\eta)(1+\xi)(1-\xi+\eta) \\ \frac{-1}{4}(1+\eta)(1+\xi)(1-\xi-\eta) \\ \frac{-1}{4}(1+\eta)(1-\xi)(1+\xi-\eta) \\ \frac{1}{2}(1-\eta)(1-\xi)(1+\xi) \\ \frac{1}{2}(1+\xi)(1-\eta)(1+\eta) \\ \frac{1}{2}(1+\eta)(1-\xi)(1+\xi) \\ \frac{1}{2}(1-\xi)(1-\eta)(1+\eta) \end{Bmatrix} \quad \dots (49)$$

The equation 49 will be substituted into equation (46) to obtain the stiffness matrix.

1.6.3. Example of FEM challenges

Modeling of the physical problems is a trail to simulate the researcher prospective (weather its genuine intuitive or a common scientific doctrine). Using finite element for simulation is not a preparation of any kinds mesh and nodes. Modeling requires that the physical entity of the problem to be understood and well represented. Appropriate kind of elements system, and mesh size is one step. The mathematical representation of the fields within the design domain is impacted by the series that is created inside the problem that represented by the stiffness matrix. The series is the translation of elements shape and size. Bad shape element and not appropriate size are the first step to be taken into consideration, but only if the problem is well experienced and tested with finite element analysis. The mathematical derivative of the mesh element itself impacting the process of solution, such that, the element is been driven with certain level of assumption (simplicity) for range of problems.

1.6.3.1. Stress concentration sensitivity (shape induced divergence).

For confined regions with expected high-stress concentration factor, FEM faces the challenge of accurate stress measurement. By design, classical FEM lacks the ability

to give accurate stress prediction with a minimum number of nodes. The jump of the special configuration of the nodes and the field in it cause under or overestimate stresses values. For example, to show the underestimation in stress measurement; the problem shown In Figure.23. Finite element convergence test was performed by increasing the number of elements and measuring maximum von Mises stress. von Mises stress reading kept rising with increasing element number.

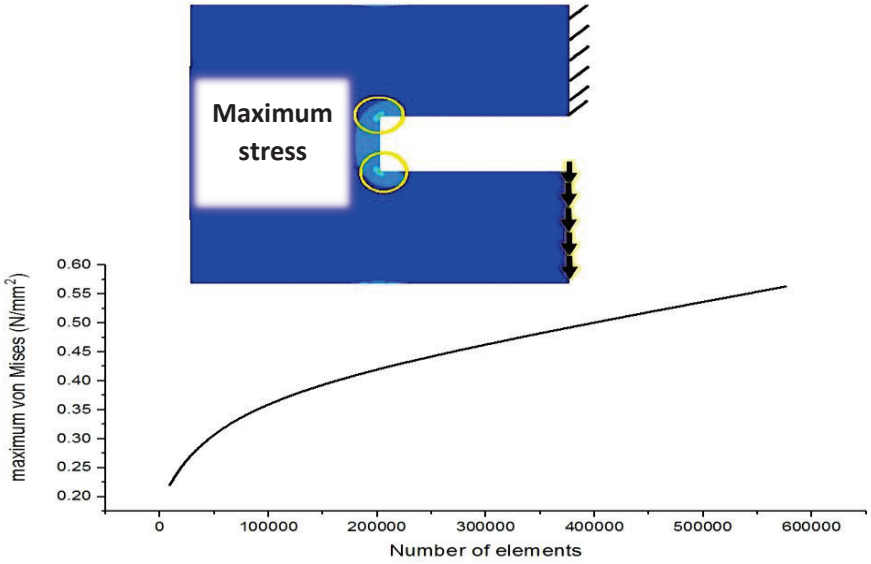

Figure 23 Stress non convergence for singular stress areas

1.6.3.2. Localized stress with local load

Figure.24 shows the overestimation of stress measuring in FEM. Due to the concentration of load in one node, the stress is been maximized to be singular stress.

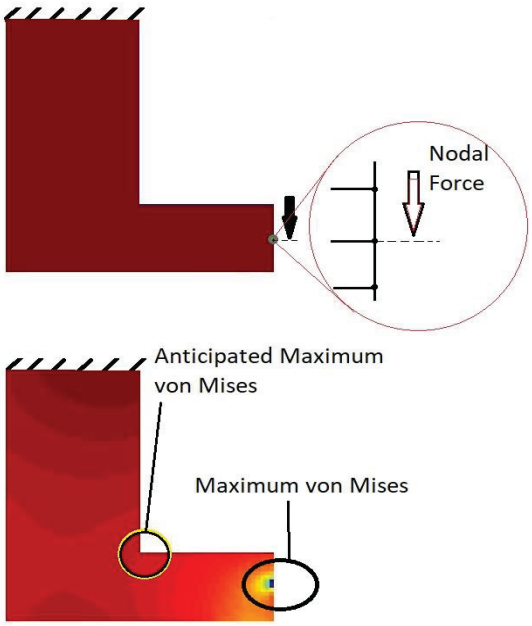

Figure 24 localization of stress around the local nodal load

1.6.3.3. Multiphysics problem; Arbitrary Lagrangian-Eulerian method

This methodology is first introducing for simulating the structure fluid interaction. It is a combination of Lagrangian and Eulerian algorithms. In Lagrangian algorithms[38], the node is associated with material particle permanently in motion. The free surface of the structure can be successful tracked, but with moderate displacement, so in case of large displacement, the method is not successfully. Eulerian algorithm[39] is used in fluid mechanics, and it describes large distortion in relative ease. However, the interface definition and the resolution are poorly defined. Here, the Arbitrary Lagrangian Eulerian (ALE)[40] is been presented to compline the strength of the two methods in one successful- free computational method.

1.7. Topology optimization development

Topology optimization has been developed rapidly in last decades, and still a considerable attractive topic to be addressed due to free computer design. It based on the based auto design in order to find the optimal shape of the designed part based on updating the status of subdomain within the design domain, such that the subdomain will take the optimal spatial configuration to construct the final optimal domain. Topology

optimization [41] generally divided into: of layout optimization and generalized shape optimization. The discretization of the domain into finite pates with distinctive relation of the parts based on spatial configuration (as finite difference, boxes, element, and volumes). Topology optimization started as a layout problem. The fundamentals of layout optimization is doing the design of specific region (design domain), with fixed traction and support in a point belong to that design space [42]. Maxwell in 1869[43] studied in detail the traction effect in frame structure in several papers. Deriving virtual energy formulation to evaluate displacement and applied forces for deterministic and non-deterministic problems, He gave a bound which is the difference of compressive and tensile stress within frame members. Michell[44] used Maxwell lemma, and did exact analysis formulation and optimization. Feasible optimal design can be achieved due to conditioning based optimization. Hegemier et al[45] review Michell's structure problem for optimal stiffness, creep resistance and natural frequency. Drucker et al [46] applied constant dissipation per unit volume as their study to stress-strain fields and strain energy. Chan [47] study the optimization of static stability of truss structure by developing a technique to determine topographic based strain filed. Dorn et introduced numerical discretization in layout optimization. Bartel[48] in his report, minimized structure weight using sequential unconstrained minimization and Constrained Steepest Descent techniques. Charrett and Rozvany [49] adopted Prager – shield implementation in order to find optimal design criterion considering rigid-perfectly plastic systems under multiple loading. Rozvany and Prager [50]studied optimal design of grillage like continua. Their approach was spatial distribution within confined grillage units. Rossow and Taylor[51] used finite element method as a numerical solution to find the optimum thickness of variable thickness sheets. Potential energy for the elastic sheet in-plane stress assumption was addressed. By introducing holes into plate structure, this work founded shape optimization. Cheng and Olhoff[18] implement finite element method as a numerical solution to optimize the thickness of annual plate with stiffened like approach. Homogenization as averaging method was being adopted in topology optimization a target of the discretized continuous optimality criterion (DCOC) by Bendson et al [52]. This work led to adopt the concept of fictitious material by Bendsoe [53] which then

derived the famous Solid Isotropic Material with Penalization method (SIMP). Figure 25 is showing the algorithm of topology optimization.

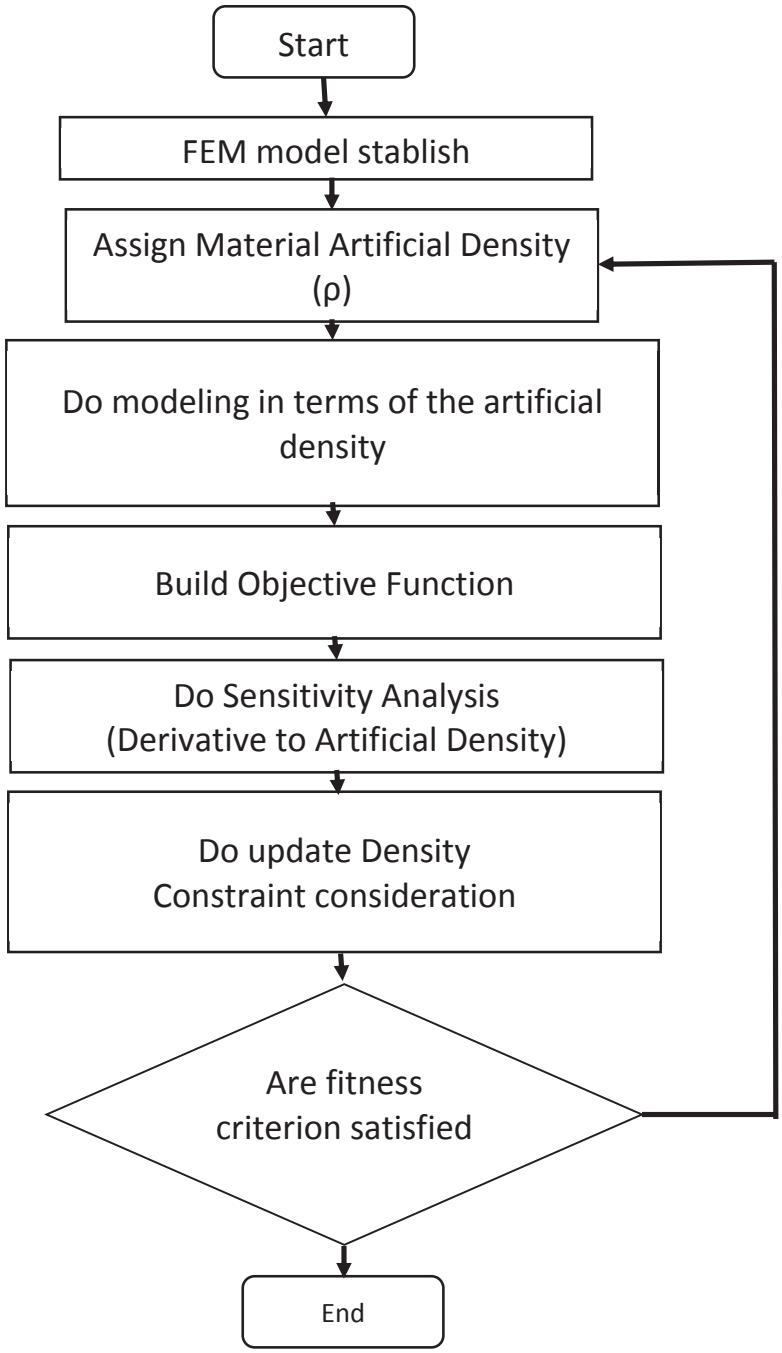

Figure 25 Topology optimization algorithm

1.7.1. Solid isotropic material with penalization

Solid Isotropic Material with Penalization (SIMP) is a scheme apply for discretized design domain to find smooth optimal structure (Figure.26). SIMP method is a direct derivative of homogenization theory [54]so it is stating that the material is consisting of isotropic segments. The results forced the function or the what so-called artificial density to be penalized. SIMP penalization was used for almost a decade and a half till it been proven to be mathematically acceptable[55]

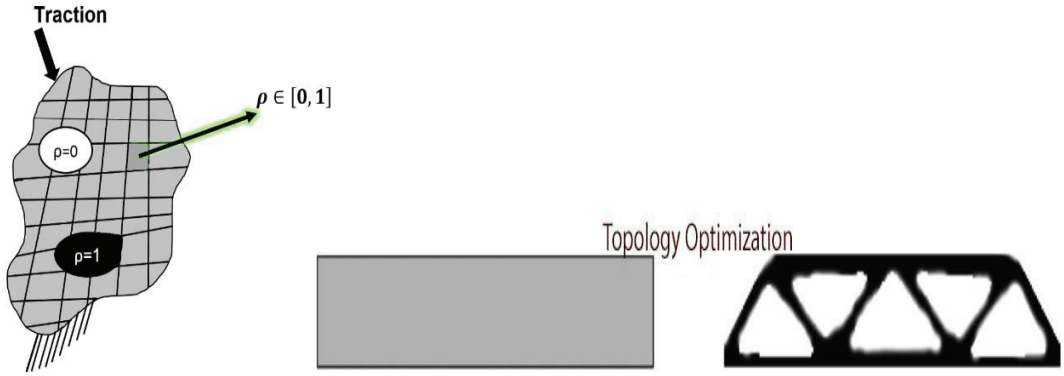

Figure 26 Topology optimization scheme of SIMP Method

In which, material properties set to be constant for the discretized domain, however, the existence of building block which is set in what so-called density function composed of the material existence of conditioned power multiply by mechanical properties.

$$\begin{aligned} &Extremum\, f(\rho) \mid \rho^{p} \\ &s.t.\ \rho \in \{0,1\} \\ &\quad Constraints\, if\ any \end{aligned} \qquad \ldots (50)$$

Where $f(\rho)$ is an objective function, ρ ,is represents the penalized (to power p) non-parametric representation of the problem in term of numerical discretization, which is in this case is the artificial isotropic density (the design variable). The solution in the scope of current scheme face some challenges as checkerboards and Nonexistence. The latter is Mesh dependency problem, so Nonexistence tends to introduce nonexistence element,

severely, to satisfy solution with decreasing value of objective function. To solve it, relaxation principal is introduced, modifying density function with what so-called gray region [56] $(0 < \rho < 1)$. As well as grey area, heuristic searching with sufficient constraint, will be a remedy. Checkerboards is also a byproduct of discretization (Figure. 27).

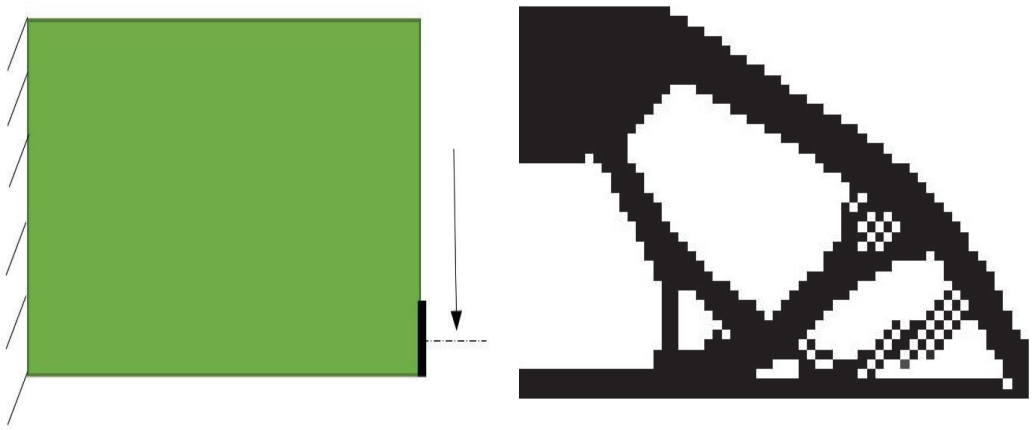

Figure 27 . Checkerboard Problem example with 4 nodes element (60x40 elements)

By the advancement of the search for the best solution, the elements are either be diminished (multiply by zero) or exist (multiply by 1). When the i^{th} element existence is change, it will change the numerical value of an objective function of the overall structure. Because of the discretization by finite element, the sensitivity numbers become discontinues across the elements. This problem appears especially with low order elements. Increasing the number of nodes for the element may seem to be a solution.

Figure 28 Checkbording limitation using 8 nodes element (60x40 elements)

However, it will impact the computational time severely. Increasing the resolution of the problem is another strategy may use. By increasing the number of elements, the check boring region decreases in size significantly.

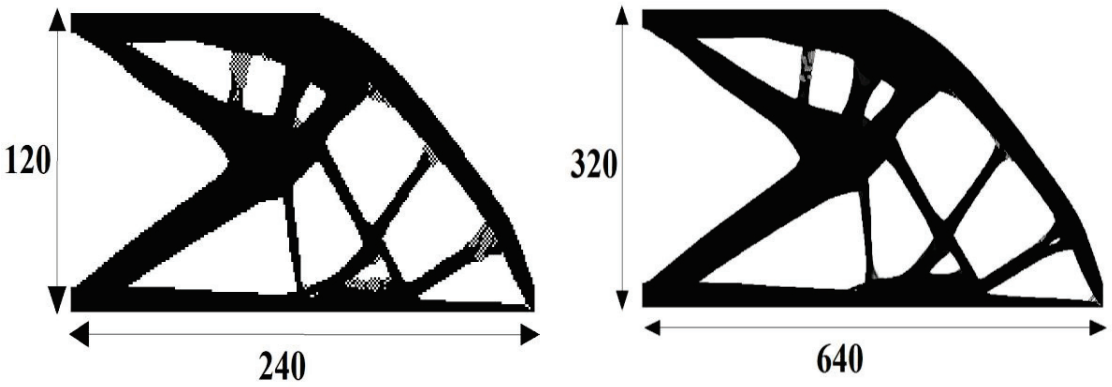

Figure 29 Increasing number of linear elements and checkboard problem

Another solution is by averaging the elements sensitivity which is connecting to the i^{th} node. The modified sensitivity is taking the form (equation (51)) [57-59]

$$\frac{\partial \widehat{f}(\rho)}{\partial x_e} = \frac{1}{x_e \sum_{n=1}^{N} (r_{\min} - dist.(e,n))} \sum_{n=1}^{N} (r_{\min} - dist.(e,n)) x_n \frac{\partial f(\rho)}{\partial x_n} \quad \ldots (51)$$

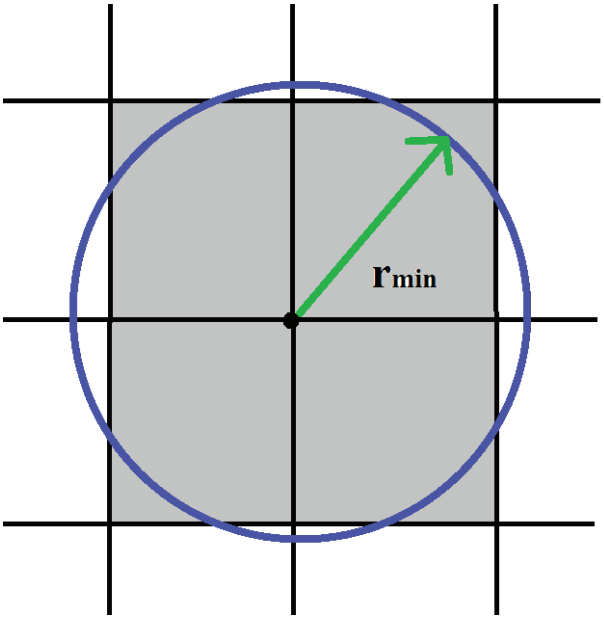

Figure 30 Mesh independency filter

Where $dist.(e,n)$ is distance between central element x_e and each neighbor elements $x_{n=1\to N}$. The produced modified sensitivity will update the designated Optimally criteria.

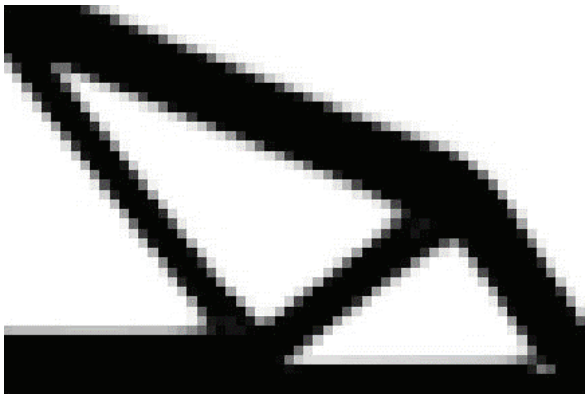

Figure 31 Checkboard limitation using 4 nodes element (60x40 elements)

1.7.2. Topology optimization merits and challenges

Topology optimization promoted as the methodology of new possibilities, with the purity of mathematical logic. The aspects of the design are based on the mathematical optimization of a known state space, or higher order set of objective criteria. Such design should obey only the necessity of satisfying the optimizing process which give theoretically the best feasible (solution bounded by designed period), optimal solution

can be unique and highly adaptive. The same points of promotion are actually pointing a serious point to be careful at. For example, deriving sensitivity for gradient-based optimization is not easy task specially with complicated and cascade functions. Numerical sensitivity may ab an option. However, numerical sensitivity consumes a lot of time and computational power. The good results also need high resolution to get so high consumed power is inevitable. Not to mention the discretization as well as the simplification (which is needed and highly accepted) will not give the full picture of the physical phenomena, and the accurate solution for it. In the other hand, mathematical chaos which is highly anticipated in complex model can leads to failure in the whole computation operation. All of this can be categorized as the mathematical challenge of the topology optimization. Objective function design is a challenge has been mentioned in mathematical optimization section. Well-designed objective function may give strange optimal results which is by the original mathematical model of the problem is highly suspicious solution. For example, the topology optimization of heat conduction which produce the famous tree-like model[13](Figure. 32). According to the propagation of heat in solid, the wavefront should be moving in an even distribution. The tree model seems even in distribution, yet mas is not distributed evenly in all directions to satisfy the anticipated best distribution. Yan et al [60] presented another model showing the validity of these suspicions. Another example is the topology optimization of discretized Maxwell equation. Despite the fact that, the discretization itself is limited for the advanced problem which such non-parametric i.e. layout and shape optimization (Topology optimization) are needed; the suggested criteria are also affect seriously on producing at least 80% accurate design which satisfy the physics of electromagnetic phenomena. For example, the optimization of magnetic circuitry[61]. The design been produced are mathematically challenging, yet the real application is predicted to finds them unsatisfying. This is the Human factor of the topology optimization challenges. Another aspect of topology optimization challenge is the discretization itself. In the produced design, areas on non-feasible design may occurs[62] as shown in Figure.34-A). It been noted that the compliance objective function tends to produce sprout members through the design procedure, especially with non-benchmark problem (Figure. 34-B). This behavior is used by Martinez et al [63] to produce natural like designs. This is varying with using high

order degree of freedom (Figure. 35). To solve this problem, extra filtering usually been used. The filtering in relying on the designer experience and better Judgment. Topology optimization is a methodology uses the full potential of the advancement in computation power and methodologies. This will lead to the possibility of fully autonomous design. For example, non-man mission can do design or repair itself based on such methodology, aided with advanced computer vision and rapid prototyping. Topology optimization may be the only way in certain application such as the inner design of custom orthopedic cause it is based on geometrically complex system. It is hard enough to perform accurate analysis considering the real physical model of the organ. This will leave only topology optimization as the main method for revolutionary and satisfying design because it is as been mentioned before; it is relying on the pure logic of mathematics.

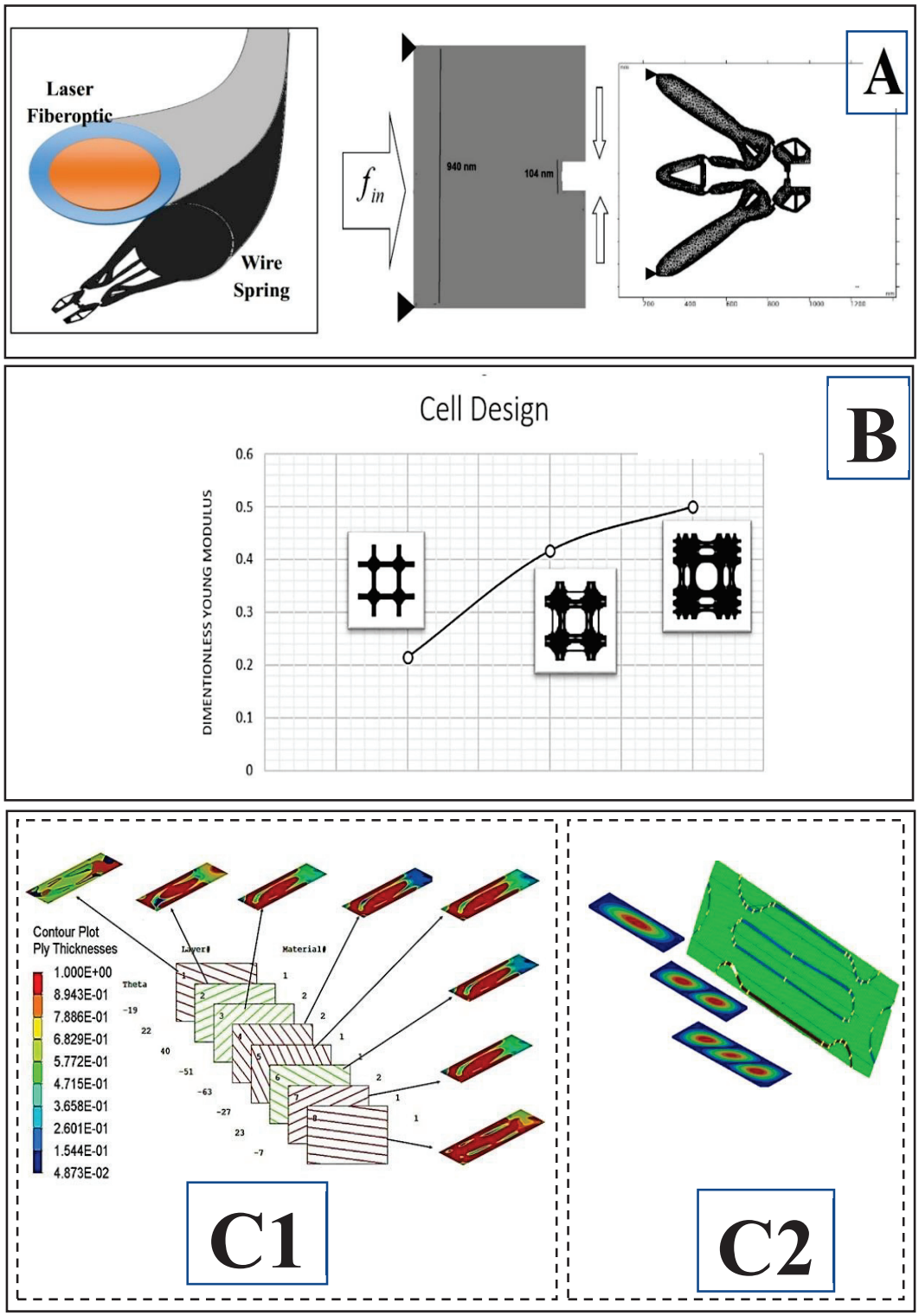

Figure 32 Novel Designes Examples of Topology Optimization: (A) Photodynamic therapry aiding pizoelectric nanogripper.(B) Inverse homogenization periodic structure design for selective modulus of elasticity (C1) Lmina shape optimization of hybrid composite plate for modal control in hilicopters (C2) Stiffner design for case (C1) for selective modal analysis.

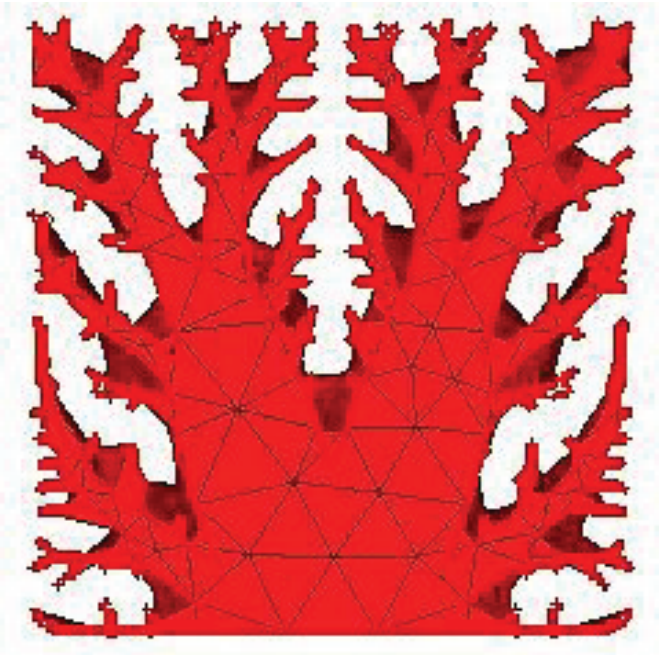

Figure 33 Topology optimization design- tree like model for electronic devices passive heat sink

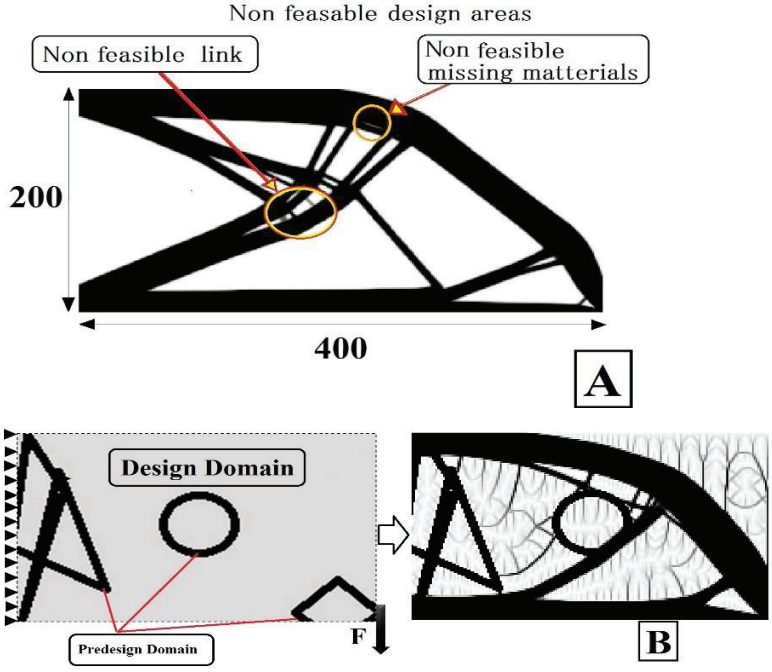

Figure 34 Objective function noise

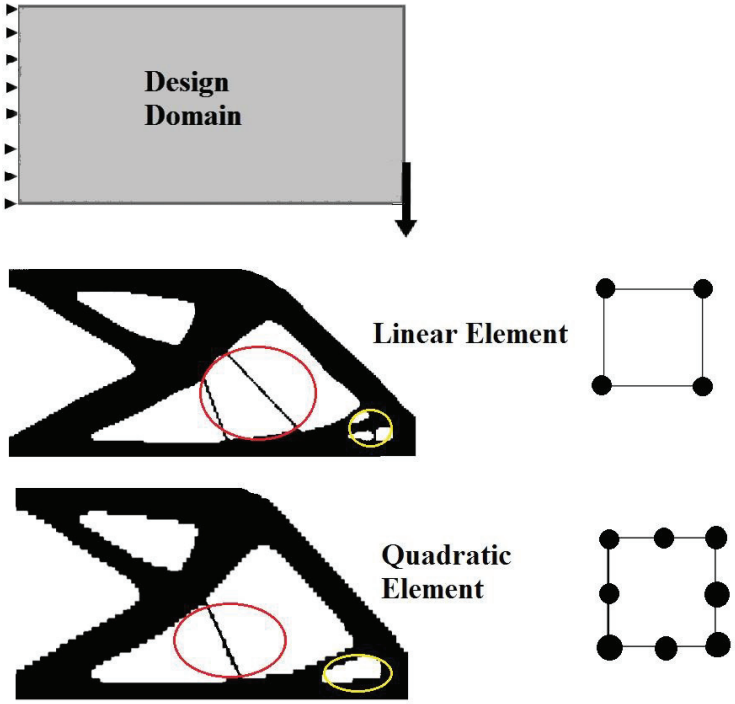

Figure 35 Design feasibility for the used element

1.7.3. Shape optimization

Shape optimization is the part of structural optimization which deals with extremum structural boundaries. The shape is the term of the outline of the structure, Mathematically the limit of the function by the first order gradient. In shape optimization, besides the objective function, shape representative is being chosen to address boundaries growth.

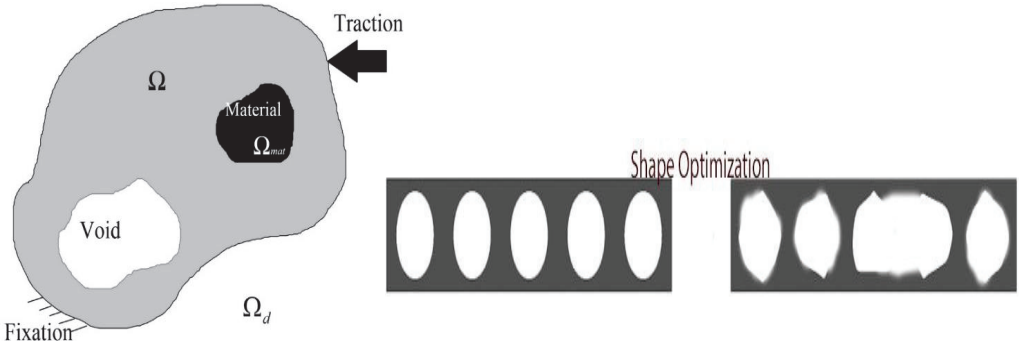

Figure 36 Shape optimization

Level set method[64, 65], is an example of shape optimization(Figure.37). Mesh morphing on the other hand can be adopted for shape optimization[66].

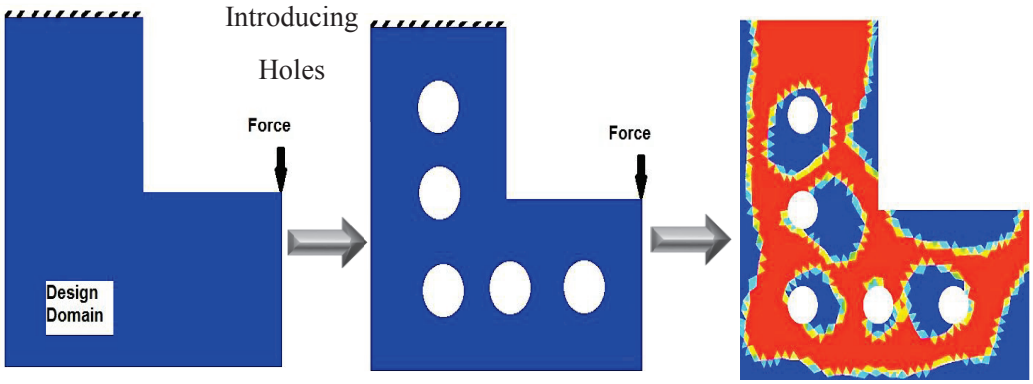

Figure 37 Shape optimization with level set method

Phase field is another example of shape optimization [67-69]. The shape optimization in terms of the previously mentioned methods is bounded to the discretization design domain. In order to get the best design, the design domain should be rich in size, so the deletion process will not eliminate the better design due to limited spatial period. Some solutions is done to mend this draw back such as different resolution mesh[70], different discretization methodology, one for calculation and one for update, such as FEM and FDM[71] and the extended to use XFEM for extra resolution adaptability[72]. Still the design domain evolution is limited by the fixed discretization methodology. The need of methodologies of extending the discretization beyond the fixed domain are necessity. Mesh morphing is a potential candidate for such task. Morphing in finite element terminology refers to mapping set of nodes of what so-called source elements. The process is widely used in transportation systems [73]and medical simulations[74, 75]. Morphine in this work is done by picking up nodes on the finite element model, to be moved within the spatial period (in this case upper and lower coordinates). These nodes will be referred to as handlers. Handler (Figure.38) are set to move, forcing the design domain to extend or shrink by extruding the elements. Mesh morphing has a drawback such as Mesh quality problem. During the mesh morphing, nodes are moved to the transformed final geometry. It is possible that some elements may get distorted beyond

an acceptable limit. This will lead to a negative Jacobean problem within FEM analysis. In order to solve that, mesh size should be chosen to be big enough to not distorted badly by the morphing process. Decreasing mesh resolution will affect analysis quality, such as stress. Another solution is to adopt hybrid mesh. in such case, boundary mesh will be added associated with the higher special-order mesh. i.e. 1d mesh at the boundaries associated with 2D mesh for the design domain. this will increase the resolution of the solution, yet it is not quite enough, especially in the case of stress singularity. Another solution is by increasing the degree of freedom of the system with maintaining, same special representation. This is done by adopting higher order element types. In the case of the need to increase the mesh resolution, the upper and lower limits of the morphing optimization process should be chosen, in a way to not distorting the element badly (as getting negative Jacobian).

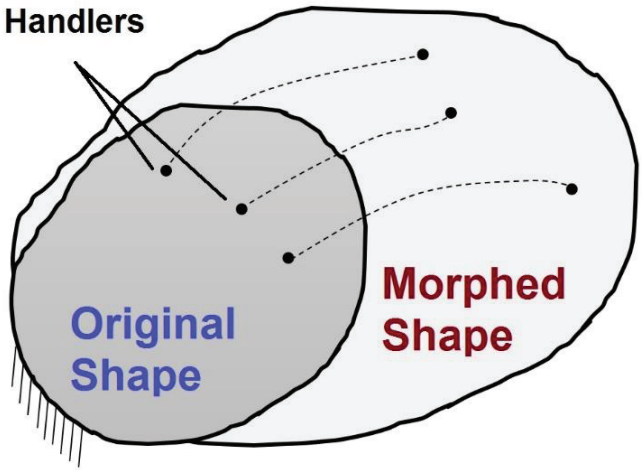

Figure 38 Mesh morphing overview

Chapter 2: The bio-mechanical interaction principal

2.1. Introduction

Before going into bone fracture and orthopedic details it is imperative to have brief understanding of the human body and cell generation. Human body is consisting of group of cells. the origin of all cells is the fertilized egg, which is simply a single cell. Through mitosis cycles [76] the central part of the cell divided to two parts then the cell split to be two attached cells. the cells started to mutate at each mitosis cycle and specialized as tissues. Human tissues are classified as according to the functionality representation. There are four types of tissues, Epithelial tissue, Connective tissue, Muscle tissue, and Nerval tissue. Connective tissues support the body. Bone is considered as a connective tissue. Bone is considered as typical composite materials. As a complex composite system, it consists of cells, fibers, and ground substance all supported by extracellular matrix. The matrix aids the major mechanical response for the external and internal fields. About 70% of matrix is inorganic matter. Mostly hydroxyapatite ($Ca_{10}(PO_4)_6(OH)_2$) and Calcium Carbonate ($CaCO_3$). As composite, bone density will vary around 1.7 gm/cm^3. Brittle is the propitiate description of mechanical response of such materials [77]. Cellularly, bone majorly made of building blocks called “Osteon”, consists of concentric rings structure, in which blood vessels and nerves penetrate periosteum through horizontal openings called perforating (Volkmann’s) canals. The major role of bone channels is to support the vascular and nervous systems of bone. The vascular and nerval systems are playing a vital role in bone healing and regeneration. Bones are different in shape and sizes (Figure.39). Bone can be classified according to the shape as: Long bone which are Cylinder-like shape, longer than it is wide (femur, tibia, fibula), Short bones which are Cube-like shape, approximately equal in length, width, and thickness (carpals, tarsals, patella), Flat bones which are thin and curved (e.g., parietal bone, scapula, sternum), Irregular bones which are Complex shape (e.g., vertebrae, hip bones). The different between bone shapes reflect the inner construction of bone structure. Bone injuries are majorly caused by vehicle and sport accident. Mandibular fracture is frequently needed to be consider for patient

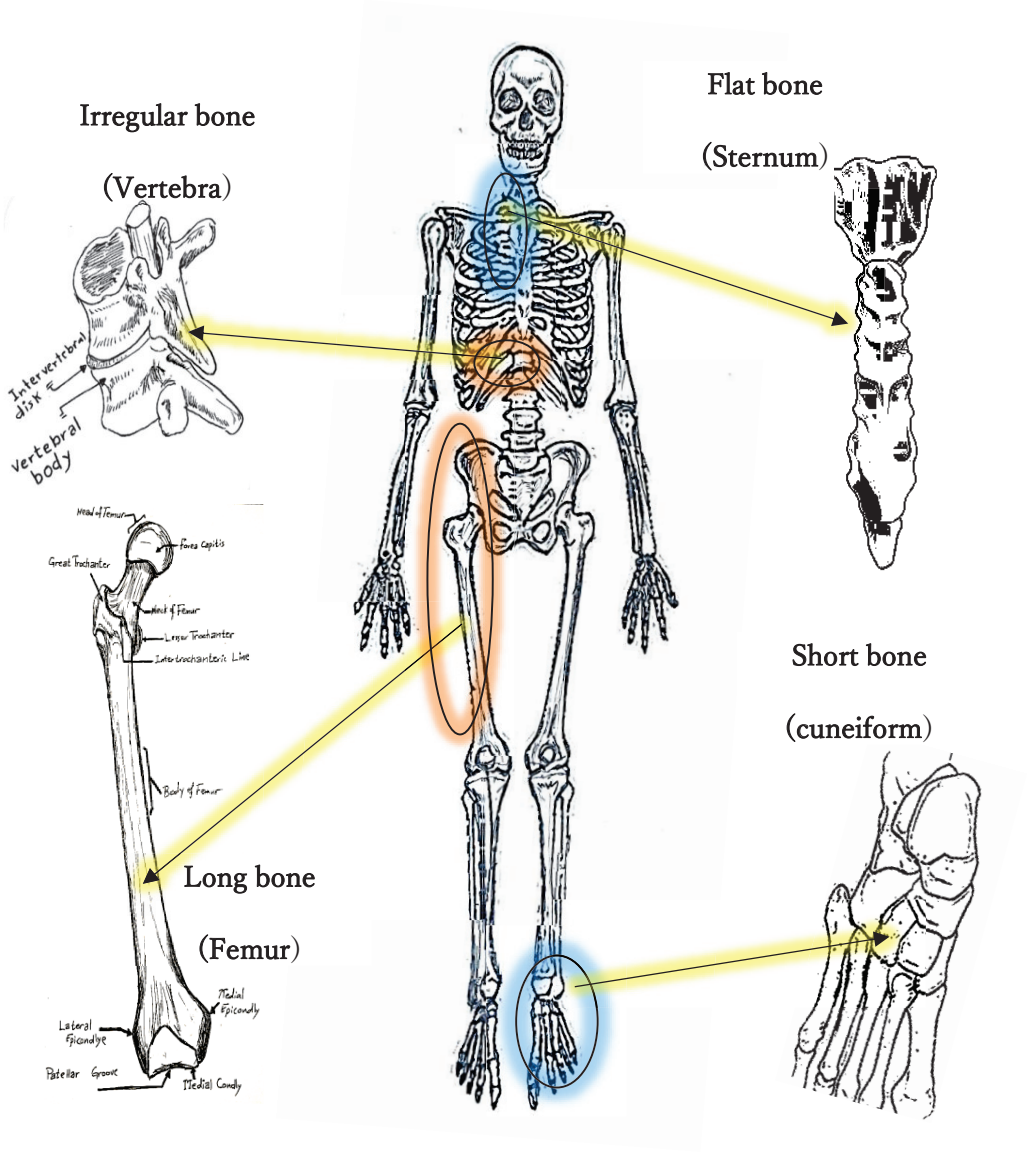

Figure 39 Bone type examples

treatment[78, 79] . Bone fractures have many classifications according to the bone location, the cause, and fracture complexity. Various classifications are used to ease choosing propitiate scheme of treating. One of classifications is Stress fracture, which happened due to abnormal trauma to the bone, usually caused by external intense stress field acting on trauma's area [80]. Fracture hematoma (Figure.40) is the first step to initiate fracture healing process by promoting blood capillaries sprouting within clot while fibroblasts, macrophage, osteoclasts, and osteogenic cells interstitially migrate from periosteal and medullary fracture sides.

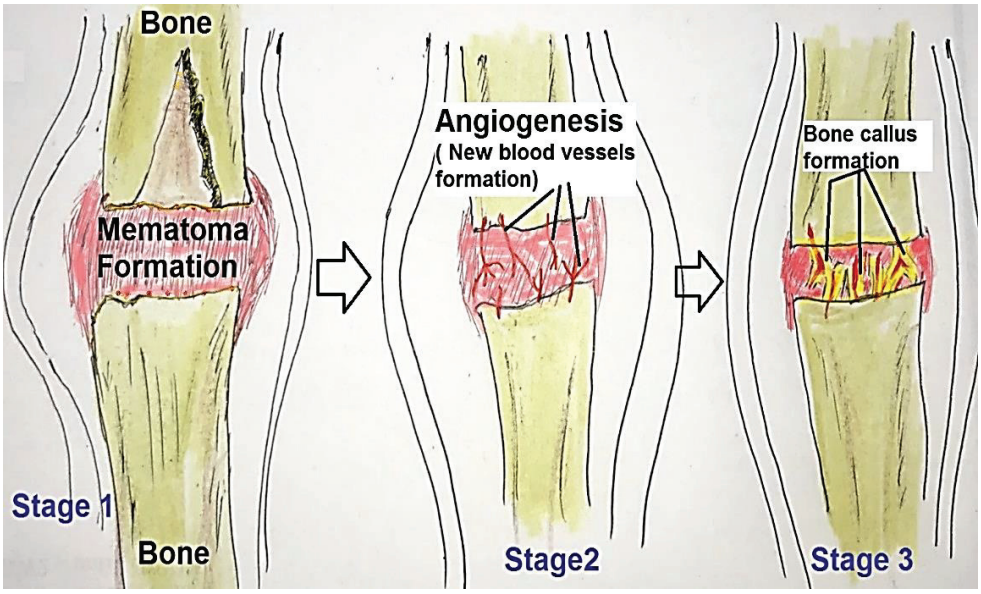

Figure 40 Bone healing principals

In order to make this process happened, bone sides should be aligned to gather. The aligned bone fragments are usually being guarded from external fields to ensure rapid healing without interruption. In case of open reduction [81], surgical fixation using plates, screws and pins are designed and implemented to fix the fragments and ensure mechanical stability during healing process. Healing process are patient dependent. Patient age, sex, health, and genetic condition are highly effective in the choice of fracture treatment method and the healing development. Mechanically, Bone brittleness is a factor determine the fracture treatment. Degree of brittleness vary due to age, gender, and patient's condition. Treatment sometimes cause over or under brittleness. Although open reduction with permanent implant can offer strong support and alignment, it has some limitation such as growth suppression for young patients, and the risk of infection. Temporary implants are considered as suitable and can solve such problem. The bone alignment is very important aspect of fracture treatment. The natural order of the bone topology is extremely vital to be followed and carefully addressed during treatment steps. In case of bad alignment or even small deviation in hard tissue relocation, the Malunions and Malocclusion are happened[82], which lead to full orthognathic workup[83] . Spector of infection is always being considered while treating mandibular fracture such that oral

cavity is a source of various infectious pathogens so, permanent foreign body within tissue is the last resort. Bone fracture is not the only the reason of using implants. Tumors in osseous, such as Osteosarcoma and Ameloblastoma [84-86], needs to huge excavation of the infected hard tissue. Immediate replacement of the missing bone is needed to retrieve bone functions.

2.2. Implant designing challenges

Implants may face the following major failure criterion [87-89], biocompatibility issues, and mechanical Issues. Biocompatibility for the implant is particularly important. Implant materials should not be toxic for short and long-term. Corrosion as much as it is physical phenomenon affect mechanical stability directly, but it affects the biological environment; leading to series of serious life-threatening problems. Less severe corrosion issue, which is Ion release also should be considered such that, undesired property which can lead to cellular abnormality problem. This is done by altering the chemical compounds inside the cells such as enzymes and the acidic ribose. Material allergy is a unique property for living body, in such case the implant trigger white blood cells to attack it. Mechanical stability, static and dynamic load resistance, fatigue and crack initiation and propagation, and wear are the major mechanical design aspects. Another problem raised which are stress shielding. One of the discussed solutions is to design composite implant to match mechanical properties represented majorly by the Young modulus of elasticity. The major problem of stress shielding is implant mobility, causing implant failure [90].

2.3. Orthopedic material selection

The aim of orthopedic surgery is to retrieve the functionality of the damaged body part. the design space for orthopedic prosthesis is limited due to body configurations. Human body parts have the property of mobility, which make the body substile to fatigue. As consists of collective tissues, most body organs are respectively renewing the structure by cells replacing. Such privilege is not available to foreign non-biological solutions such

as plastics, and metals. The need to long fatigue life material is necessary. The material should not be toxic and can withstand corrosion. The level of corrosion remittance is importance. The migration of ions from metallic prosthesis within body fluids can to happened. However, it might be not a mechanically noticeable corrosion. For example: With the migration of few ions of metallic alloy, the tribological functionality is acceptable for joints. many research's studied metallic alloys and their long-term biological compatibility. Laurence and Liberman [91] emphasize the relation between metallic implant corrosion and the severity of what so-called " bio-metallic interaction". Hueper at 1952 [92]studied investigated cancer tumors cases after Nickel injection in rats bone marrow. His work was driven by the notice of serious damage in respiratory system of workers of Nickel refineries. The work showed a noticeable chance of developing cancer taking into account the short lifespan of the rats. McDougall [93] studied several cases of rare cancer called Ewing's sarcoma which related to FeCrNi alloy in Human patient. Dube and Fisher [94] at 1972 linked abnormal blood vessel growth (Hemangioendotheliomas) with fixing plate made of stainless steel type 316. Titanium has good biomedical compatibility and good fatigue characteristics (physically and chemically)[95]. Despite the fact that hygral effect is damaging the composite integration, several studies addressed the use of fiber composites [96-98]. Composite martials in the classical view even with Nano composite interface[98], need long time research to exclude the long term biological effect.

2.4. Stress shielding problem and suggested solutions

Connective tissues have certain properties that may vary slightly from one patient to another and may change over time for the same individual. Bone is considered as a composite material. The mechanical properties of osseous tissues are governed by the topology distribution of the different tissues inside the bone. Bones majorly consist of an inorganic matrix (consisting mostly of mineral salts) and collagen (elastic fibers). Because of the nature of the living tissues, the mechanical properties change with environmental variation. Wolff's law is an example of bone adaptation under different stress conditions. For example, it been noticed that the Archery bone formation were

altered due the frequent using of the bow[99]. Implants are not far from such alteration, so the mechanical properties are varying hardly specially through the metal- bone interface area. The contact stresses are high, and the hardness of metals is larger than for bone. In orthopedic sense, stress shielding is the tendency of bone to dissolve in favor of the strongest forge body “the implant”. Some surgeons like to say, “there is a density incompatibility”. Because mechanical compliance of the implant is much higher than for the surrounding bone, stress shielding phenomenon happened and taking into consideration the dynamic response and biological optimization of living tissue. Accurate measurement were done to identify critical stress difference to start stress shielding [100].It has been noticed that for the In the case of orthopedic implants, the greater stiffness of metallic implants (which are the first to use historically) the greater the stress shielding is [52]. There are several engineering techniques used to decrease stress shielding. One solution involves the temporal aspect of the implant, by using temporary or biodegradable implants [101]. Temporary Implants will be remove after doing its purpose, so for metallic structure, long enough attachment is the important designing factor. Still the stress shielding occurs around the screws which used as fixations. Ernest and Grove [102] at suggested the use of wires instead of screw in plate fixation for fracture cause screws and due to tightening presents more stress shielding leading to losses of the fixation before the bone been healed. Another chose of biodegradation as property of the chosen material as calcium phosphate-based implants or Polycaprolactone (PCL) [103-110]. In some cases, long-term implant is a must. In such case, matching of the mechanical properties is a solution. This method suffers from serious drawback which is the fatigue life. Implant in the scope of modern medicine are not able to regenerate itself as the living tissue. This will lead to the accumulation of defects and the formation of cracks till failure. Metallic structures in the other hand have high fatigue life. This will force toward finding a solution of limiting stress shielding for metallic implants. The first suggested solution is treating the surface of the implant to promote the Osseointegration[111, 112], either by roughening the metallic surface, and /or adding Osseointegration agents as Polycaprolactone [5] and Hydroxyapatite [113]. This method is successfully implemented in teeth implant, but it is not efficient in terms of big bone replacement. Stiffness matching of the designed implant and the bone is a considerable

solution. Stiffness can be used as a design constraint for the implant, by calculating the stiffness the substituted bone and optimized the metallic implant till it has similar stiffness. Stiffness conditions can be introduced into the finite element as its opposite i.e. compliance ($C = \mathbf{F}^T\mathbf{U}$). In other words, compliance of the complete bulk design area (Ω) of bone as the material is the condition for the optimization process. Another solution is by using porous structure. A scaffold made of porous metallic structure (Figure. 41) with inner coating of biological material to improve implant rooting within bone [114, 115] is a suggested solution. The matching between the replaced bone desired mechanical properties and the metallic structure by designing the porous structure to achieve similar mechanical properties[116-118]. Such structures are manufactured with additive manufacturing[119, 120].

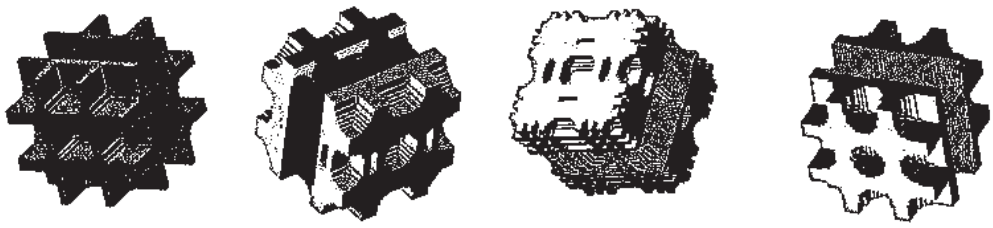

Figure 41 Lattice design examples for bone scaffold

The quality of the printed parts will vary with beam energy source (electron beam, and laser beam). Another issue is the orthotropy of the printed part due to layer by layer manufacturing. Additive manufacturing also suffers from relatively big surface roughness. Surface roughness is a desired for better Osseointegration. Still, it is affecting the fatigue life of the product[121]. Computer-based 3D geometric can be modeled in terms of lines, planes, boxes, etc. using different shapes of pore design, which and be chosen using experimental or optimization techniques for certain models. Modeling of pore done by many approaches with mechanical durability such as compressive strength objective function [113], or considering fluid flow through porous media models[5]. Regeneration of bone within the scaffold is porosity size dependent. Generally, bone composite unites element consists of the following, ordinated as [87]:

Neovascularization needs an average of 5 µm, fibroblast needs 5-15 µm, mammalian skin needs 20-125 µm, and finally, the Ostional growth needs 40-100 µm. Optimization of the porous structure should consider the Osteoconduction. Osteoconduction is the three-dimensional process which sprouting capillaries, perivascular tissue, and osteon cells grow. Capillary tube flow mathematical model [87] was adopted to describe healing of bone so that, the migration of sprouting cells and making the hematoma mass through the artificial porous media (influenced by Washburn's equation)from considered as the main objective function

$$\Delta P = \frac{2\gamma_{LV}(\cos\theta)}{r} \quad \ldots (73)$$

Where ΔP is the pressure difference creating the capillary action, γ_{LV} is surface tension,θ is the contact angle with the interface, and r is pore radius. Another model based on Darcy's equation which describe the flow through porous media [5]

$$Q = \mathcal{H}\Delta P/\mu L \quad \ldots (74)$$

Where Q is the flow flux,$\mathcal{H}$ is the permeability,μ is the dynamic viscosity of fluxed media, and L is the flux migration path. The third solution can be achieved by studying energy variation through the interfaces and the effect of pressure on the cell formation of the metal bone interface. The method is based on the phenomena f bone remodeling with the interface region. Bone remodeling under loading is been studied by Cowin and Hegedus 1976[122]. By establishing mathematical formulations based on Wolff's law. Blankevoort et al 1991 [106] studied contact stresses within contact bone surfaces. Husikes et al 1992 [123] studied hip replacements and stress shielding effect. Stress shielding was defined according to their work is represented by threshold average elastic energy per unit mass (energy density). The compatibility within living structures, in usual conditions, keep the stress distribution below the threshold. Introducing high stiffness difference leads to increase the stress that being applied to the bone, especially if contact stresses are taken into consideration. Contact stresses are a vital key to understand the phenomenon of bone density reduction around the implant, such that, the contact stresses are high. Total hip arthroplasty and stress shielding were studied by Makarand et al [124] evaluated von Mises stress around the implant, as a criterion for bone implant interface

failure. Localized stimulus stress is adopted in this paper. Stimulus octahedral stress. Stress stimulus approach of stress shielding propose that a threshold strain energy density can trigger bone dissolving process[125, 126] as in equation (75)

$$\frac{d\rho}{dt}=\begin{cases} c(\psi-\psi_{bone})+cw & (\psi-\psi_{bone}<-\omega) \\ 0 & \omega \le \psi-\psi_{bone}\le-\omega \\ c\ (\psi-\psi_{bone})-cw & (\psi-\psi_{bone}<\omega) \end{cases} \quad \dots (75)$$

Where c is an empirical rate constant, is the half-width of the central, normal activity region, the local stress stimulus provided by metal bone contact, is the maximum stress distribution within the same case of the healthy bone (before damage and implant), if the difference was smaller enough, it was assumed that no remodeling response would occur. According to that, topology optimization target should be set to minimize maximum strain energy of the bone surrounded by the implant. Another modeling is motivated by fatigue behavior[127]. This modeling is considering the stress shielding as a function of cementite destruction of the bone. This model is not compatible with remodeling process of the bone. Add to that the Osseointegration of tooth implant for example shows different results comparing to this modeling. The recent researches tend to introduce quantum behavior to describe the change done in bone formation[128]. Phenomenon such as quantum tunneling is not compatible with mechanical loading alone. Yes, mechanical loading will trigger the formation, but the mechanical look of failure is not compatible. This will lead to consider stiffness matching and decreasing the total strain energy are the best strategies to use for the current circumstances.

2.5. The intuitive of the design methodology of the prosthesis

There is a valid question which part of the orthopedic process is this work concern with? To answer this question. There are two different way of thinking in design should be discussed: First one is the surgeon and pathologist prospective, and the second one is the Engineering perspective. Starting with the medical point of view; First, the dimensional aspects of the implant and the surgical fixation should be accurate, so the original movements (Rigid multibody spatial description and transformation) [129] and the spatial topography of the bone will be the same as the original and healthy bone. Or

else, it will cause inflammation, lose functionality, and may need to remove the whole part in order to save the patient life. Material selection will come after to choose nontoxic and appropriate materials. The valid and easy to perform a Surgical technique is important to choose between different designs and / or improving an existing one. Anatomically variation and abnormalities are a challenge in performing surgeries, so the places of the various organs and tissues may have mild to severe variation from patient to another. Radiology is needed to plan the surgery. Radiology can be MRI or CT scan or 2D X-ray or ultrasonic.

Dimensional design

Ex. Malunions and Malocclusion

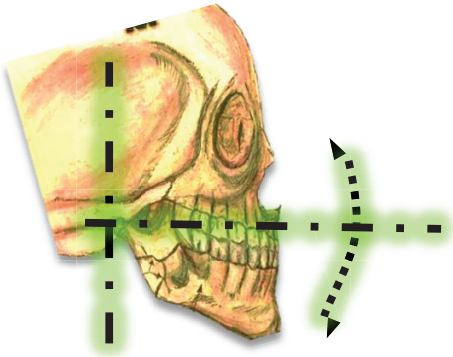

Material selection

Ex. Metal, polymer, ceramics, composites

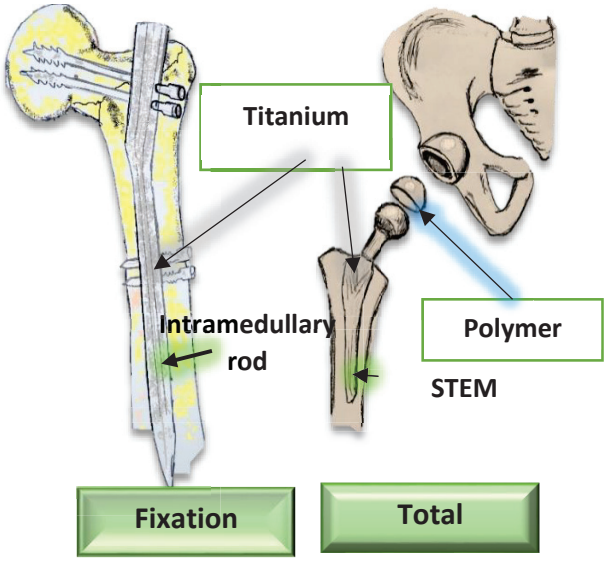

Surgical Methodologies

Ex. fixation by screw or wires, etc.

Radiology

Ex. magnetic resonance image, computed tomography, etc.

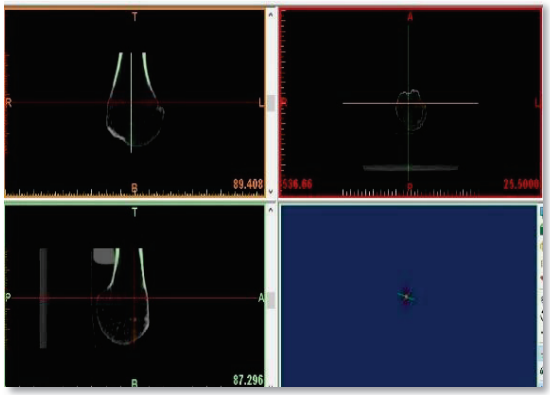

Figure 42 Surgical process and selections

Engineering design can be summarized as the criteria on which a product be outlined to perform a designated task in the most efficient and reliable way possible. The functionality is one aspect of the mechanical design. Mechanical design taking into consideration major and auxiliary criteria. The major criteria are: the safety, radiality, cost, manufacturability, and marketability. The auxiliary criteria are the ethics, legal requirements, consequences, time, the sociological aspects, marketing in tactical way (current demand) strategically (market saturation and product anticipated technical support revenue). The auxiliary criteria are not less important than the major criteria. Yet the auxiliary criteria need collaborative work of non-engineering expertise. The most vital aspect irreversible aspect of patient management is time. Time of the diagnostic, treating, response, mending and healing is a matter of necessity and utmost importance. Most of the surgeons demanding fully customized orthopedic solution, in shorter time as possible. It is being mentioned that there is a huge demand for one surgery only at which the pre-fixation and the fully customized orthopedic insertion. The technology of computerized imaging, and rapid prototyping may be well developed in the near future to deliver the orthopedic before the pre-operation ends. So, the orthopedic will be inserted and the

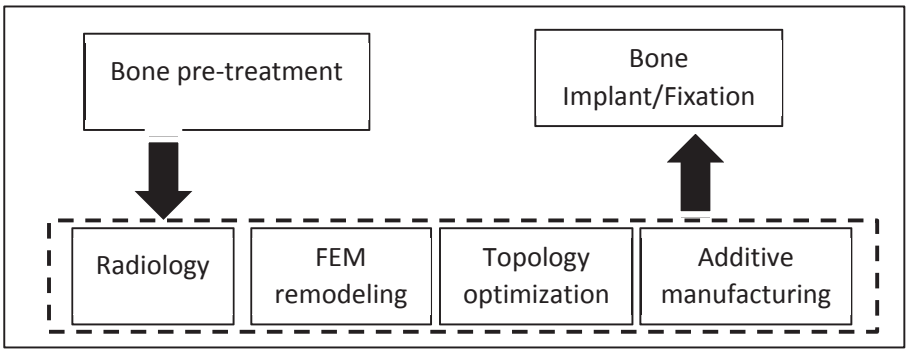

Figure 43The suggested single reconstructive surgery Algorithm

healing time will be short. Add to that the cost and the medical resources can be optimized in the time of crises (such as earthquake, mass transportation accidents, wars, etc.). Operation type depends on the type of Injury. Bone treatment does not necessitate an outer stress as a cause of injury. It can be caused by diseases such as malignant tumor, or bone decay. In case of malignant tumor, resection is needed. Resection is the proceed of cutting the tumor with safe margin of nonaffected tissue. No less than 2.5 cm in general and 1 cm in oral cavity. In case of bone degeneration, an excavation process is used. In

this case the hard tissue turned to be soft tissue due to a disease. After healing process, the patient may need scar correction, sensitive area to be desensitize. The area of amputate needs to subject to bearing exercise. The long-term aim of this research is to investigate the recent ideas and perspective of advanced orthopedics and study the ability of delivering such product with the up to date available and practical technical solutions.

Chapter 3 The intuitive of the design methodologies of the prosthesis using topology optimization

3.1. Topology optimization possible schemes investigation

Topology optimization as non-parametric design methodology uses cascade approximations stating from the design variables Such as SIMP method and through the discretization method, objective criteria, and ended with design variables update. In the other hand, orthopedic design facing mechanically many challenges one of them the is the stress shielding, and mechanical life (fatigue life) which are the main purpose of the current research. Stress shielding propose to have two main approaches. First one is matching stiffness. In this proposed approach, the metal is proposed to be springy enough to store the energy inside by deflection before it transfer it to the surrounding tissue. Of course, surface hardness in this approach is not addressed, so contact stresses is being eliminated in the calculations. The main philosophy behind that is that the Osseointegration process (bone formation around the implant) are adaptable to the loading condition in some extent, so the bone around the implant will have strong bone formation specially with the use of Osseointegration agents [130-132]. Second approach is by decreasing the maximum strain energy in the bone as much as possible by redistribute the topology of the implant. This approached is based on stress stimulus approach of stress shielding propose that a threshold strain energy density can trigger bone dissolving process[125, 126]. The non-parametric approached is optimality criteria approaches. Topology optimization and shape optimization been studied. Topology optimization using SIMP method is been adopted by many companies (Such as Autodesk, ANSYS, COMSOL, Dassault, Altair, LSTC, Quint and CAESS) in their commercial software so it proven its adaptability and relatability for the common problems. Topology optimization according to the objective criteria are compliance based, and stress based. The proposed approaches of prosthesis design are based on two methods, first is matching

stiffness of the prosthesis and the surrounding bone. The second methodology is decreasing the maximum strain energy inside the bone exerted by the prosthesis. Topology optimization best scheme for design is needed to investigate in order to use for enriching the possibilities of produce the best designs. The study regarding topology optimization is dividing into three main mesh type dependency of the design, the best objective functions and the minimization of stress, Shape optimization and layout optimization comparison. The results will be the axiom for the prosthesis design approach. The Investigation will be divided for several steps. First one is testing the finite element dependency and impact on achieving mathematical convergence, and mechanical design. The second part is to test aspects of topology optimization. The aspects of topology optimization are divided into the methodological parts of the topology such as mesh dependency filter, penalization of artificial density. The other part is testing the impact of the objective function. This will lead us to the final part of the testing which is implementing shape optimization and compare the results.

3.2. Objective functions

3.2.1. Compliance based objective function

Finite Element discretization of linear elastic continuum mechanics is taking the form of displacement approach as

$$\mathbf{K}(\rho)\mathbf{u} = \mathbf{F} \qquad \ldots (75)$$

Here, **K** is the structural stiffness matrix depending on density function. **u** is the nodal displacement vector, and **F** is nodal force vector. Stiffness is the measurement of structure to withstand certain load. It can be introducing in term of finite element analysis as its opposite; i.e. compliance. So, minimizing compliance will mean maximizing stiffness. Conditional objective function based on compliance is

$$\begin{aligned} &find \quad \rho \\ &\min \ \mathbf{F}^T\mathbf{u} \qquad \ldots (76) \\ &s.t. \ \int_{\Omega_d} \rho d\rho \le V_d \quad , 0 < \rho_{\min} \le \rho \le 1 \quad \forall \rho \in \Omega_d \end{aligned}$$

V_d is a volume fraction, ρ is elemental density, Ω_d is the design domain. Power (p) that satisfies the condition of 2D SIMP set to be within[13]

$$p = \begin{cases} \left[\dfrac{4}{1+\upsilon}, \dfrac{2}{1-\upsilon}\right] & in \quad 2D \\ \left[15\dfrac{1-\upsilon}{7-5\upsilon}, \dfrac{31-\upsilon}{21-2\upsilon}\right] & in \quad 3D \end{cases} \qquad \ldots \quad (77)$$

3.2.2. Stress-based objective function

Stiffness maximization will not necessitate stress minimization. Compliance function is being used successfully for the past three decades associated with SIMP method.

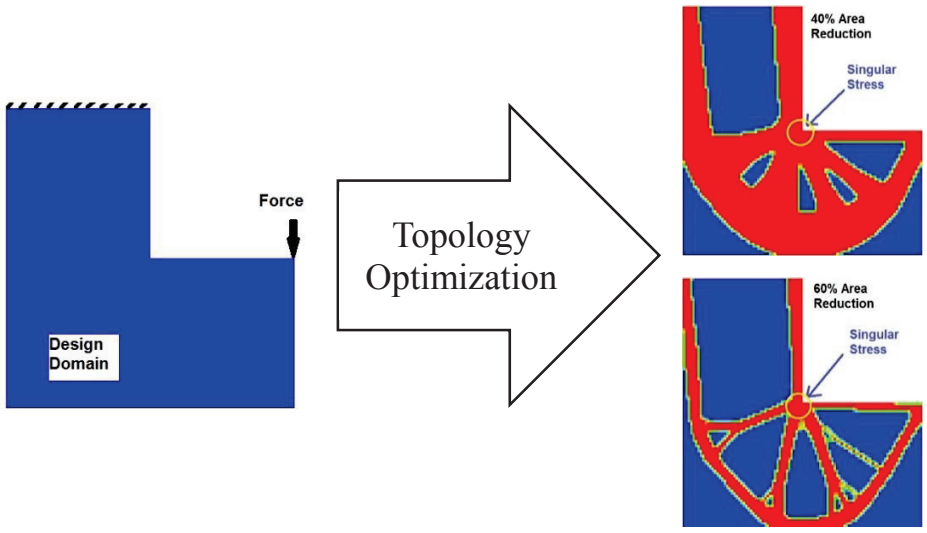

Figure 44 Stress singularity areas with compliance objective function

Stress can be addressed as an effective objective function to minimize the singularity topography (stress concentration parts). Using finite element as discretization method for topology optimization is imposing the use of nodal displacement to calculate the strain then the stress. The nodal displacement effect will be discussing later in this chapter. The stress itself, they are the direct translation of force action with related nodal displacement.

The translation is done in terms of stiffness matrix and displacement matrix. In the core of this matrices multiplication is the property matrix that is model in term of the artificial density function. The stress in the scope of finite element destination is not far from sharp change in value due to the jumping of nodal addressing in calculation procedure[133]. Another issue is the stresses to be addressed are in 2d case are three for each element. This will impact heavily in computational power specially with the use of numerical sensitivities. These aspects need to address a minimal stress entity that is statistically averaged in acceptable way to be the target of optimization as objective function or a constrained. stress function, and the second one is the aggregative approach (p-norm function). Single stress is considerably easier to program and handled. However, it can be computationally costly. This approach identifies the maximum stress parts easily, yet singular stress parts can theoretically[134, 135], leads to the non-convergence solution so, the singularity is problem face topology optimization[134]. In this work, two stresses based objective function (SBOF) are addressed, first is single Elastic failure criteria are used as an averaging method which gives single stress to be measured in order to achieve the safe design. One of these yielding envelopes is the maximum shear strain energy per unit volume criteria which usually refer to with Maxwell von Mises stress (σ_{vms}). The maximum allowable von Mises stress could be identifying for certain material. In order to establish stress criterion as a valid objective function to be extremum, the relationship of scaled stress should be formed to satisfying the following; simplicity to decrease unnecessary commotions, physical coherence, and address material discretization directly. qp-approach is satisfying the above; which take the form

$$\rho^{p-q}(\sigma_{avg}) \mid \sigma_{avg} = \begin{cases} \sigma_{vms} \\ \sigma_{U\max} \end{cases} \quad \ldots (78)$$

p-norm stress function[136] is used to overcome some of the limitations of single stress approach. This approach is based on choosing the Lebesgue space (equation (79)) as continuous objective function [137]

$$\ell^P(\Omega) = \left\{ \sigma_{avg} \in M(\Omega) : \int_{\Omega} | \sigma_{avg}(t) |^P dt \right\} \quad \ldots (79)$$

With *norm* defined by

$$\left\|\sigma_{avg}\right\|_P = \begin{cases} \sqrt[P]{\ell^P(\Omega)} \ , \ 1 \le P < \infty \\ \sup\left\{\left|\sigma_{avg}(\rho)\right| \ \rho \in \ [0,1]\right\} \end{cases} \quad \ldots (80)$$

Optimization will consider the first part of norm Eq. 9. Theoretically, efficient optimization could be achieved for a higher value of *P* as the need for computational power. In other words, maximum stress region can be recognized by p-norm function with increasing the value of the power *P*. This will lead to magnifying maximum stress of the system and then it be addressed intensively in the optimization process. The objective function that used is taking the form in equation (81)

$$\begin{aligned} &find \quad \rho \\ &\min \left\|\sigma_{avg}\right\|_P \\ &s.t. \int_{\Omega_d} \rho d\rho \le V_d \quad , 0 < \rho_{\min} \le \rho \le 1 \quad \forall \rho \in \Omega_d \end{aligned} \quad \ldots (81)$$

$\left\|\sigma_{avg}\right\|_P$ is wildly known as pnorm function, or sometimes KK function refining to Park K. and Kikuchi [135, 138]. Due to discretization nature of topology optimization, mesh quality and type play vital role in pre-and post-processing of design. As mentioned previously, stress-based topology optimization affected by FEM accumulative analysis history. High order elements may increase the odds "theoretically "of better design, and higher resolution designs as well as increasing element geometric density. However, computational and time cost may be a serious problem along with convergence.

3.2.3. Fatigue constraint-based topology optimization

Fatigue life is a cycle counter. In other words, the modeling and the consideration of fatigue are not for the time of operation rather than how many stress cycles is predicted. Many researchers studied fatigue concentrating based topology optimization [123, 139, 140]. The results were similar to stress-based topology optimization, in shape, design methodology, and results. For the work in hand, the optimization objective function is minimizing the volume, with fatigue life calculated by the famous model introduced by the rain flow method[141]. The generalization of the problem is used Goodman approach.

$$\min \textit{Volume}$$

$$s.t. \sum \frac{n}{N} \geq \eta \mid n = \frac{\left(1 - \frac{\sigma_m}{\sigma_u}\right)^{\frac{1}{b}}}{\sigma'_f} \quad \ldots (82)$$

The order of the various stress amplitudes is not considered in the rain flow method which impacts on the accuracy of the fatigue life prediction. However, the optimization process will follow the nature of the fatigue problem. The shape is rather convex; thus, smooth optimization is anticipated.

3.3. Sensitivity analysis

Sensitivity analysis plays a major role in achieving converging results while minimizing computational and time input. First order sensitivity analysis is required to be performed for each iteration. The adjoint variable method is used to develop a unified formulation for representing response variation in terms of variation design. Iterative Lagrangian process in term of design variable needs building sensitivity analysis by adopting first order sensitivity analysis. Sensitivity analysis of constraint depending on designated design variables can be achieved by derivative techniques (exact, and Numerical approaches). For exact approach;

Let the design variable be

$$\rho = \{\rho_1 \quad \ldots \quad \rho_m\} \quad \ldots (83)$$

m is number of elements

Let C is compliance function

$$C = \mathbf{F}^T \mathbf{u} \quad \ldots (84)$$

Adding $\lambda^T(\mathbf{F} - \mathbf{Ku})$ as zero function to equation (85) as

$$C = \mathbf{F}^T \mathbf{u} - \lambda^T(\mathbf{F} - \mathbf{Ku}) \quad \ldots (85)$$

Taking the derivative to the equation

$$\frac{dC}{d\rho}(\mathbf{F}^T - \lambda^T \mathbf{K})\frac{d\mathbf{u}}{d\rho} - \lambda^T \frac{d\mathbf{K}}{d\rho}\mathbf{u} \quad \ldots (86)$$

Using Adjoint operator such that

$$\mathbf{F} = \lambda \mathbf{K}^{-1} \quad \ldots (87)$$

$$(\mathbf{F}^T - \lambda^T \mathbf{K}) = 0 \ \rightarrow \lambda^T = \mathbf{u} \quad \ldots (88)$$

This leads to

$$\frac{dC}{d\rho} = -\mathbf{u}^T \frac{d\mathbf{K}}{d\rho}\mathbf{u} \quad \ldots (89)$$

The final form proves that compliance function is a self-adjoint function. Stress-based objective function Sensitivity analysis**.** Considering stress based objective function, Cascade function [134] $f(\sigma(\rho), \rho)$

$$\frac{df}{d\rho} = \frac{\partial f}{\partial \sigma_{avg}}\frac{\partial \sigma_{avg}}{\partial \boldsymbol{\sigma}}\frac{\partial \boldsymbol{\sigma}}{d\mathbf{u}}\frac{d\mathbf{u}}{d\rho} + \frac{\partial f}{\partial \rho} \mid f = \begin{cases} \rho^{p-q}\left(\dfrac{\sigma_{avg}}{\sigma_{yield}}\right) : qp - approach \\ \sqrt[P]{\displaystyle\sum_{i=1}^{n}\left|\frac{\sigma_{avg}}{\sigma_{yield}}\right|^P} \ : p - norm \ approach \end{cases} \quad \ldots (90)$$

$\dfrac{d\mathbf{u}}{d\rho}$ can be replaced by the adjoint operator to be

$$\frac{df}{d\rho} = \frac{\partial f}{\partial \sigma_{avg}}\frac{\partial \sigma_{avg}}{\partial \boldsymbol{\sigma}}\frac{\partial \boldsymbol{\sigma}}{d\mathbf{u}} K^{-1}\left(\frac{d\mathbf{F}}{d\rho} - \frac{dK}{d\rho}\mathbf{u}\right) + \frac{\partial f}{\partial \rho} \quad \ldots (91)$$

Using Adjoint operator such that

$$\left(\frac{\partial f}{\partial \sigma_{avg}}\frac{\partial \sigma_{avg}}{\partial \boldsymbol{\sigma}}\frac{\partial \boldsymbol{\sigma}}{d\mathbf{u}}\right) = \lambda \mathbf{K}^{-1} \quad \ldots (92)$$

The final derivative is

$$\frac{df}{d\rho} = \lambda^T \left(\frac{d\mathbf{F}}{d\rho} - \frac{d\mathbf{K}}{d\rho}\mathbf{u} \right) + \frac{\partial f}{\partial \rho} \quad \ldots (93)$$

3.4. Mesh type impact on topology optimization

Achieving smooth convergence is not a straightforward process. The searching algorithms moving the limits of the design variable (here is the penalized artificial density function). The complications of the objective function will lead to the needs of decreasing the incremental movement of the design variables. Discretization using finite element method theoretically does not needs to increase the numbers of the polynomial complexity over the optimal limit. Yet the complexity of the shape is impacting the formation of the overall woven polynomial into the stiffness matrix. The mesh effect on the convergence is needed to be investigated. Figure.45 shows the stopping criteria of the optimization process (which is the convergence of change to zero) versus the objective function history. In this case, it is a test of stress-based function. It is being noted that the stress-based function is highly susceptible to a degree of freedom of the element that used. In case of four node elements, the stopping criteria reached its goal, yet the objective function is not converged to the global minima. By decreasing the design variable update to smaller value [142](as shown in Figure.46), The objective function converged efficiently. However, the time consumed is large. For the purpose of studying the meshing impact, a comparison of benchmark problem for three types of elements (3 nodes, 4 nodes, and 8 nodes elements). The benchmark problem that been chosen is compliance minimization of the 2d cantilever. For fare corporation, the overall degree of freedom is matched for the three examples. The test starts with increasing the resolution of the convergence. The test also shows shown elimination of non-feasible members with

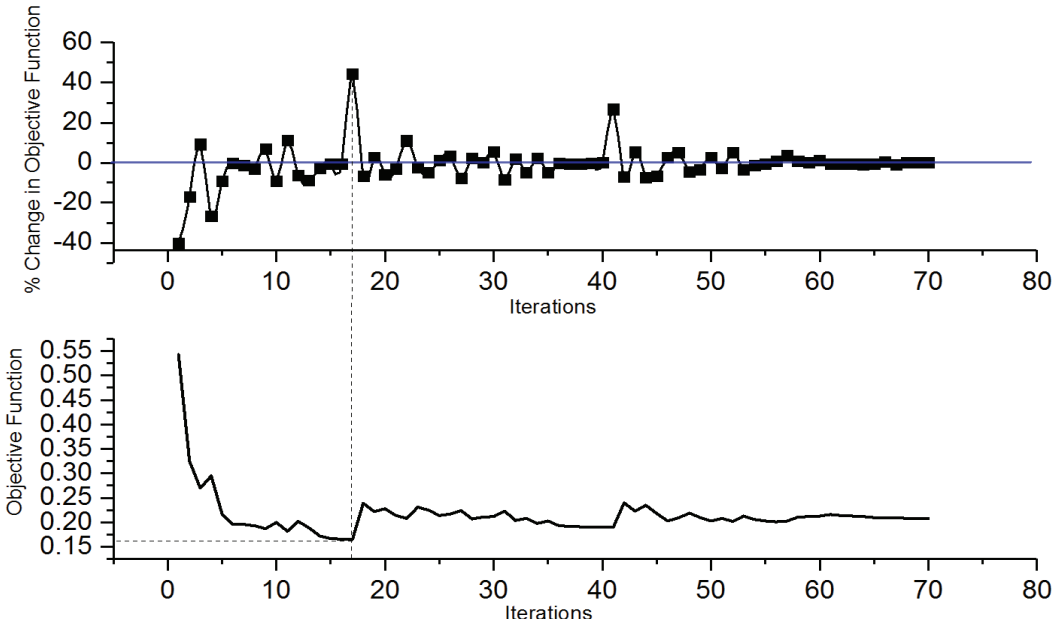

Figure 45 The behavior of Stopping Criteria of Topology optimization versus objective function history

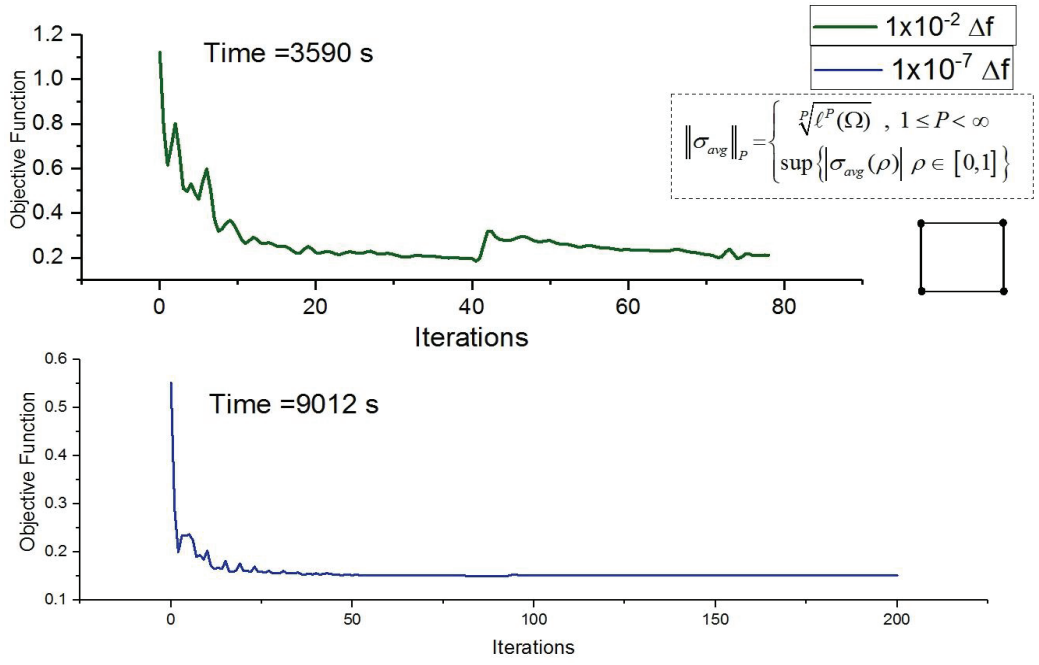

Figure 46 objective function convergence with respect to percentage change of the objective function

increasing the degree of freedom for the element. 8 nodes element showed the better results.

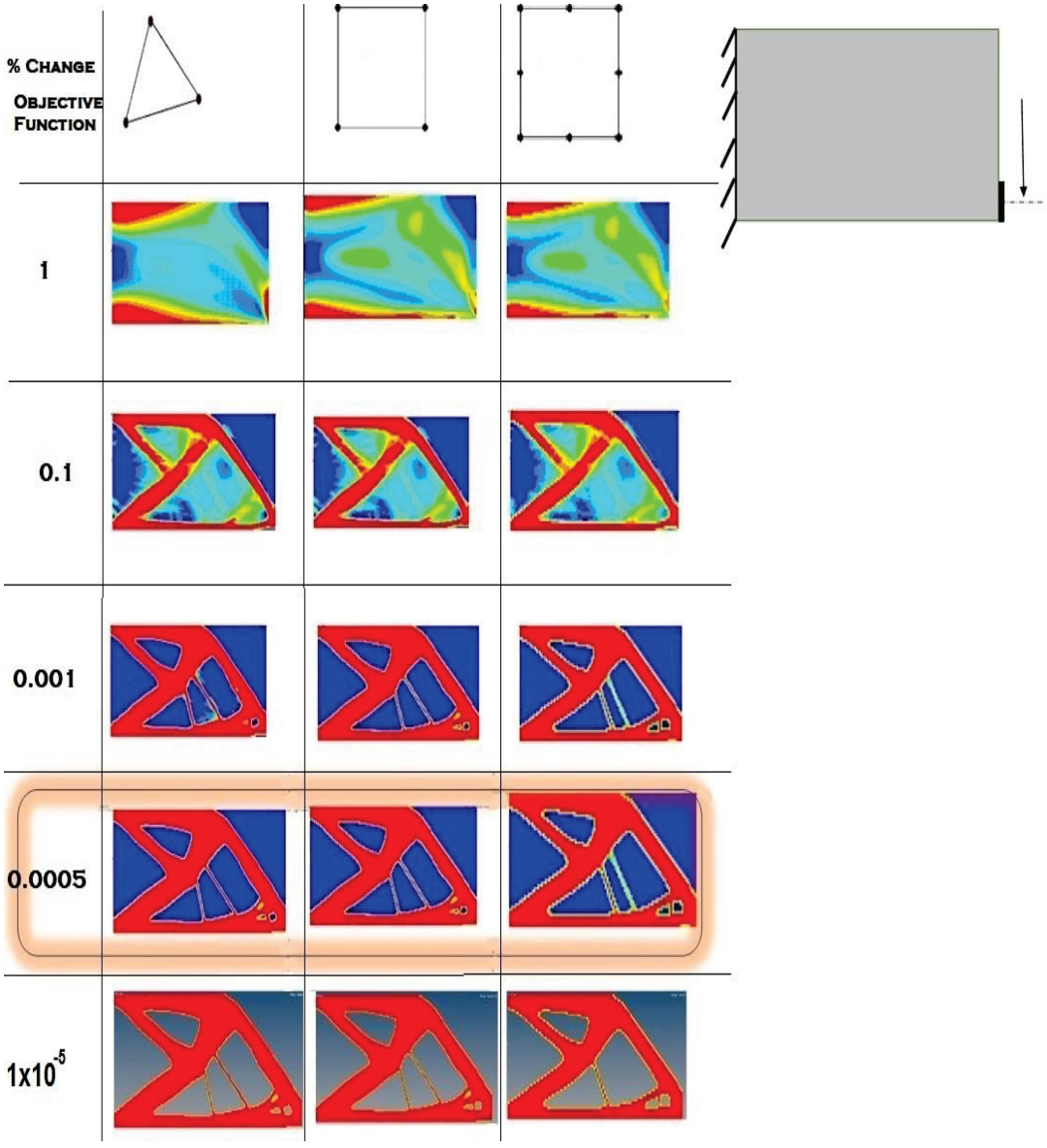

Figure 47 Comparison of element types with % change in objective function of benchmarking problem

3.5. Mesh in dependency filter

Mesh independency filter effect on the resulted structure is been tested. First is the use of 8 node square element shows no checkboard area without the use of mesh independency filter.

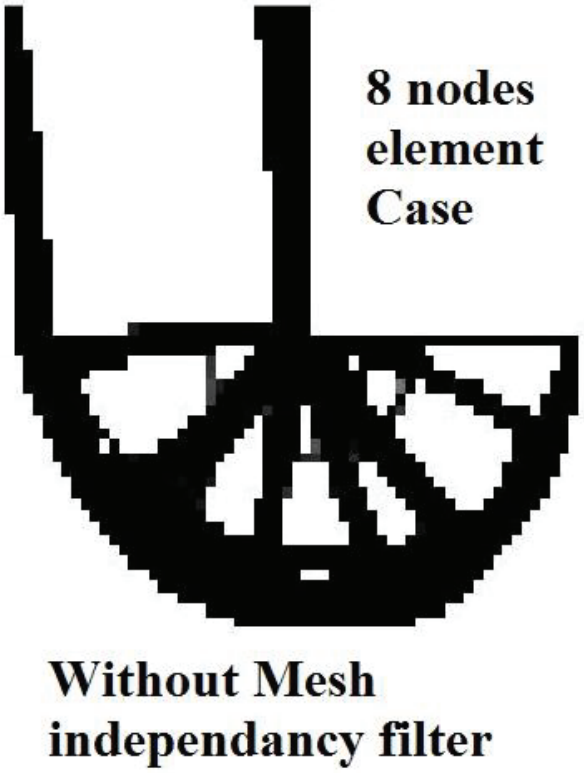

Figure 48 topology optimization without mesh independency filter for 8 node element

Increasing the number of element been predicted to limit the checkboard effect. To check the prediction, MATLAB based program was used to check. By increasing the number of the element for linear quad nods element. Checkboard is being limited significantly with increasing number of the element as shown in figure.50-56

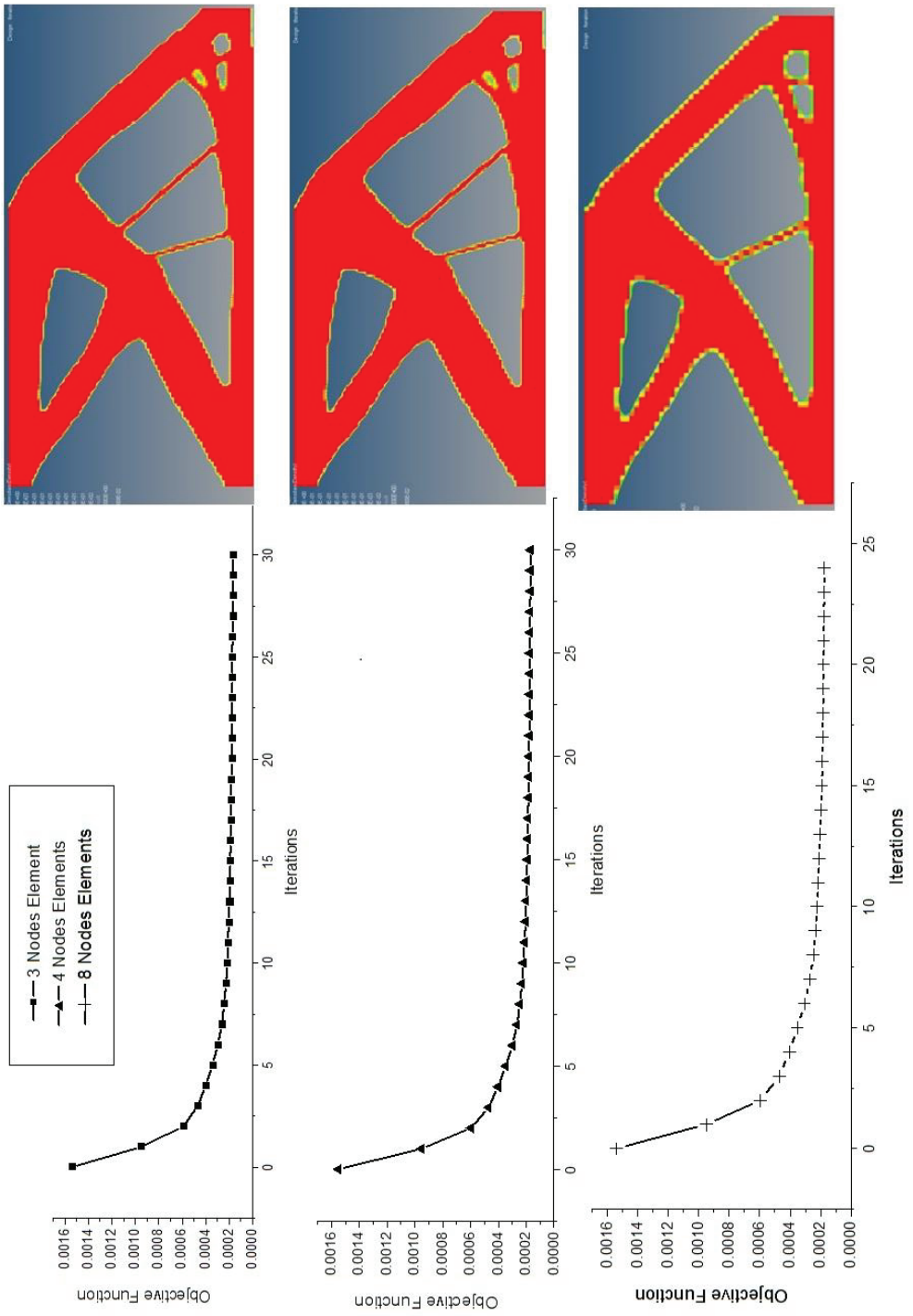

Figure 49 Objective function for diffrerent elemnt types

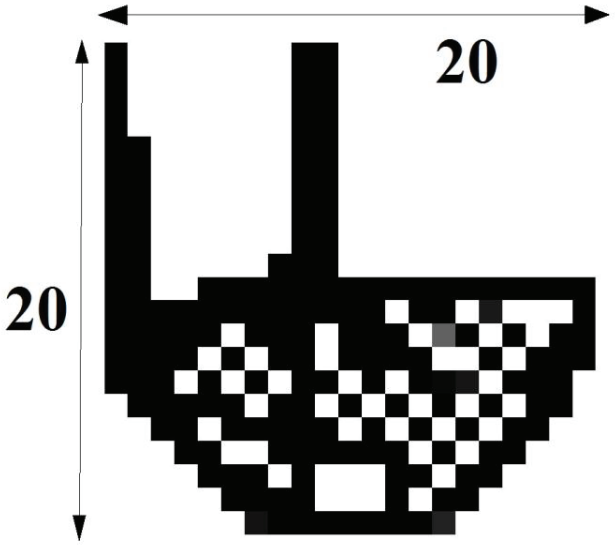

Figure 50 20x20 topology optimization results without mesh independancy filter

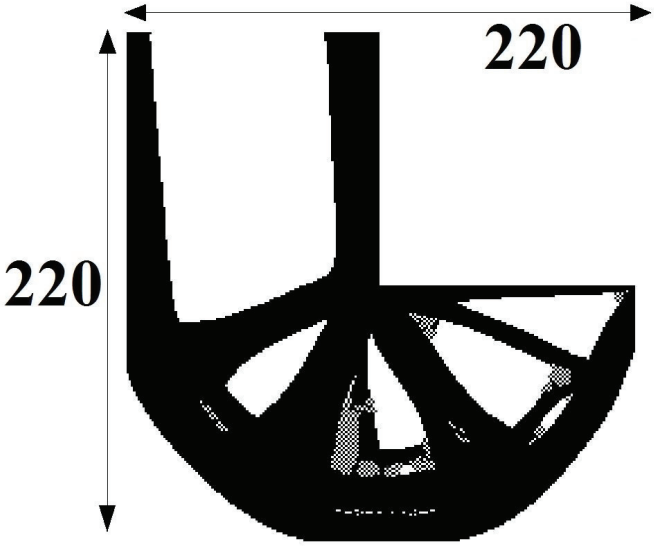

Figure 51 220x220 topology optimization results without mesh independency filter

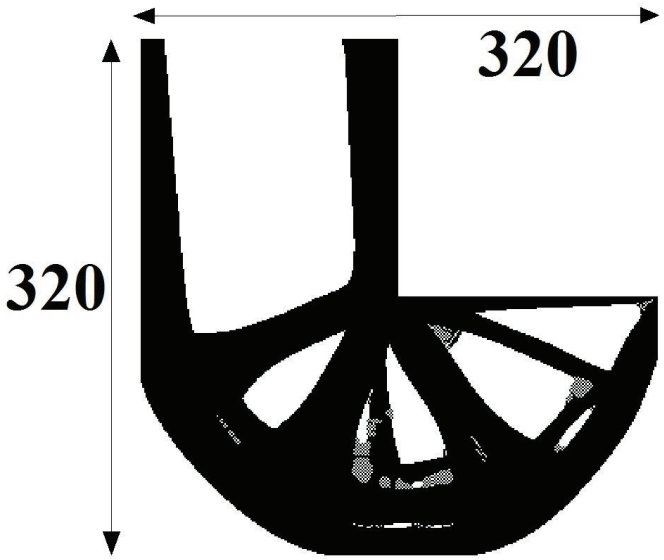

Figure 52 3 20x320 topology optimization results without mesh independency filter

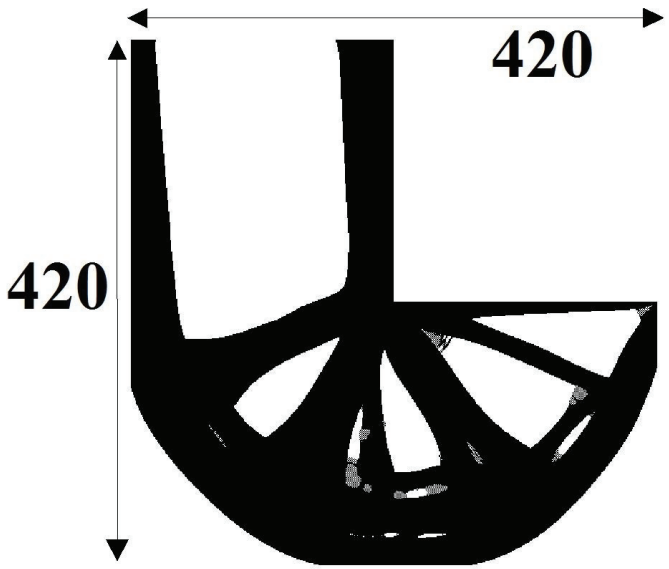

Figure 53 420x420 topology optimization results without mesh independency filter

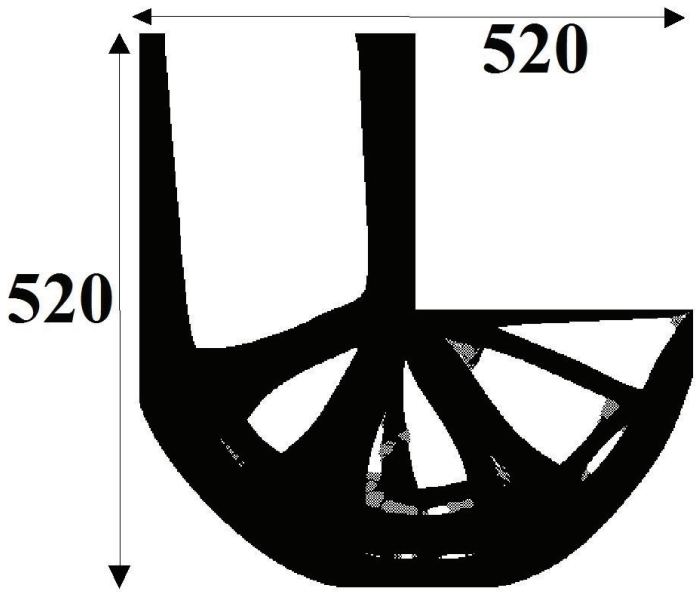

Figure 54 520x520 topology optimization results without mesh independency filter

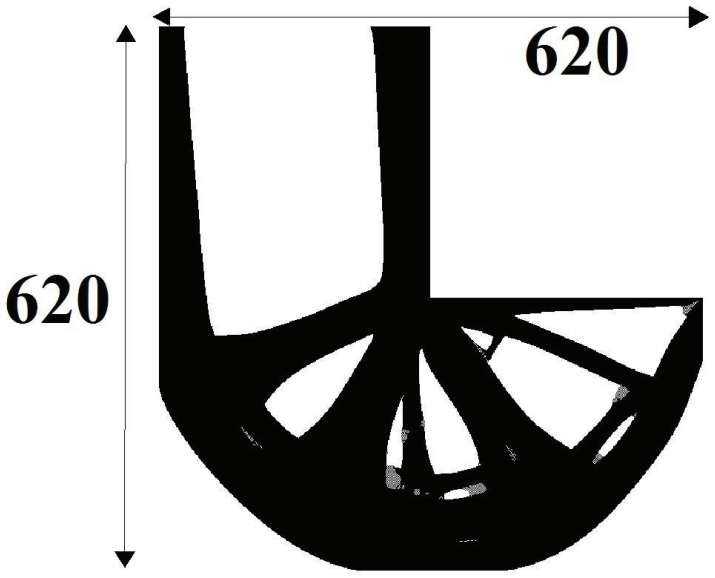

Figure 55 620x620 topology optimization results without mesh independency filter

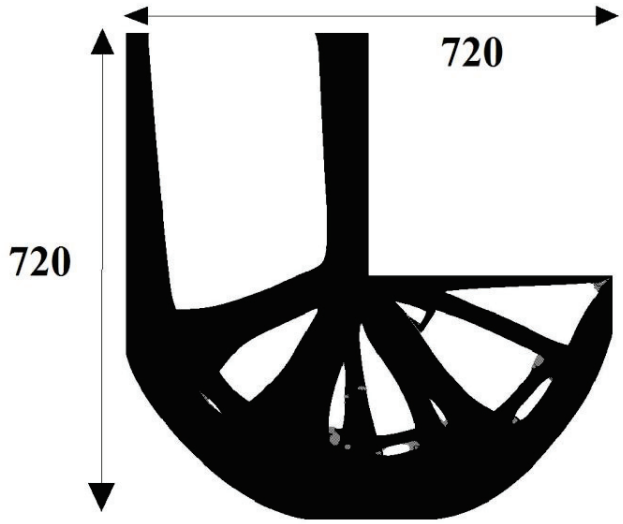

Figure 56 720x720 topology optimization results without mesh independency filter

Using the mesh independency filter is been tested. The first test is the identify the behavior of the produced design under different areas of filtering, as shown in Figure.57

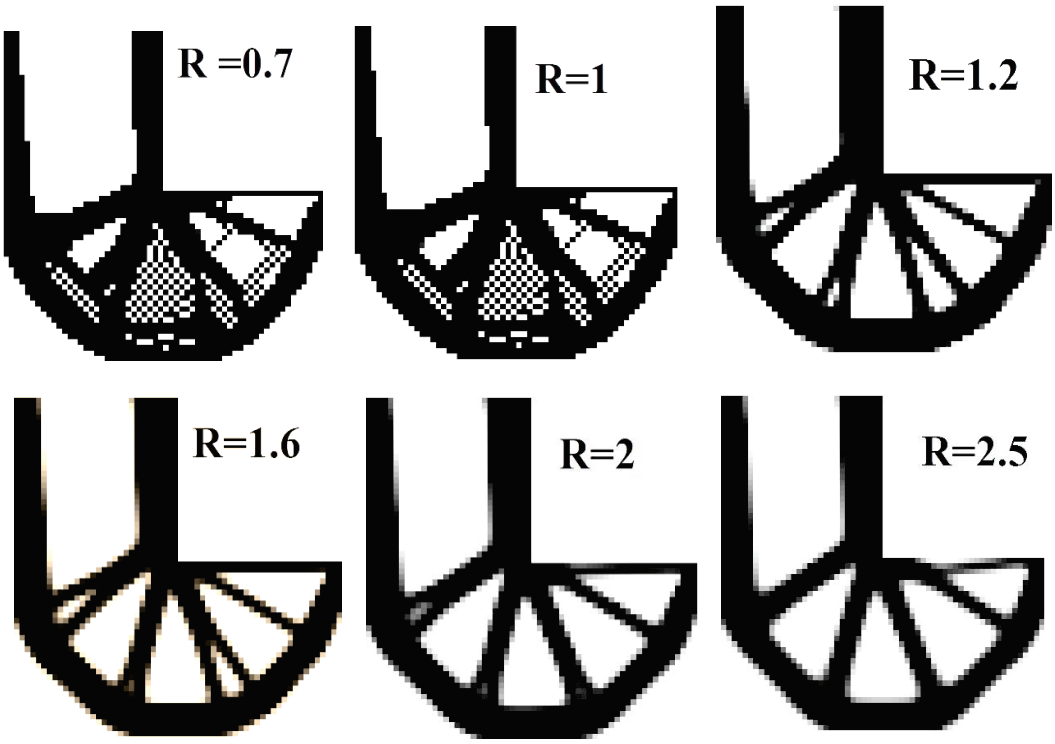

Figure 57 Mesh independency filter study 60% area reduction, 60 by 60 number of elements

It has been anticipated that the filtering will react with the optimization problem, another test is done to by increasing the number of the element with fixing the radius of mesh independency filters. From the filtering tests, it is logically good for the design to increase the resolution of the design (despite the fact that it is computationally expensive). However, it is impacting the solution that been developed and adopts to withstand topology optimization problems. The suitable dwindling number of elements will guarantee good layout optimization. Changing the filtering scheme will improve the result for a certain case yet it is not guaranteed that the best setting for different problems will be the same. From Figure 57. There is a change in link creation such that it shows softening in stress singularity are (case R=2.5). This can be a door of addressing stress minimization while increasing the stiffness of the designated structure, without increasing the computational cost. There are some work discussing the use of the stress based adaptive filtering to control the creation of stress singularity areas in FEM models[143].

3.6. Penalization impact on topology optimization

Penalization for most metals (Poisson ration =0.3) according to Bensdson et al [13] should exceed 2.95 in 2d case simulation and 1.5 in the 3d case for using in SIMP method. To investigate the effect of density penalization

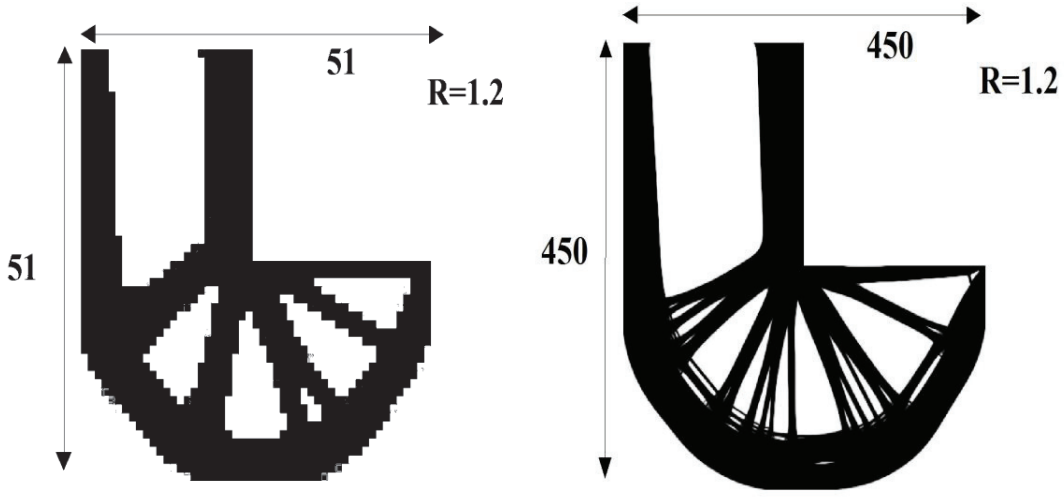

Figure 58 Mesh independency filter effect on the member formation

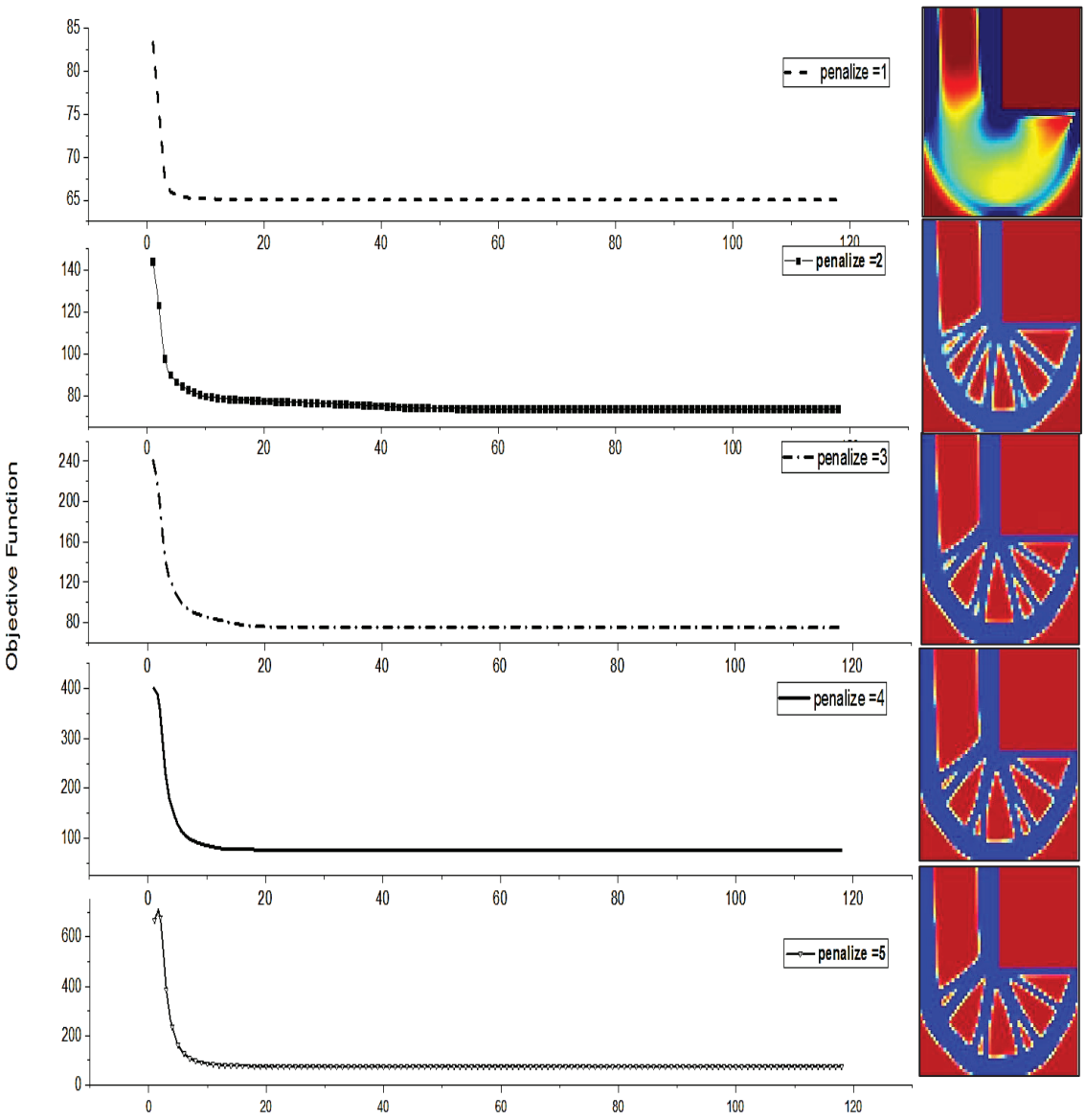

Figure 59 topology optimization design with diffrenet penalization values

3.7. Stress compression of topology optimization with the various objective functions

Compliance minimization approach is giving the optimize stiffer structure. However, stress localization is a problem that row compliance function cannot address. Several conditional optimizations approach been introduced[104]. However, stress-based function noticed to normalized singularities efficiently. For stress-based function, aggregative stress gives a smooth function, avoiding singularities, however, for microscopic(localized) stress, a minimum stress can be achieved in some cases. For examples, comparing the topology optimizations cases that were shown in Figure .60.

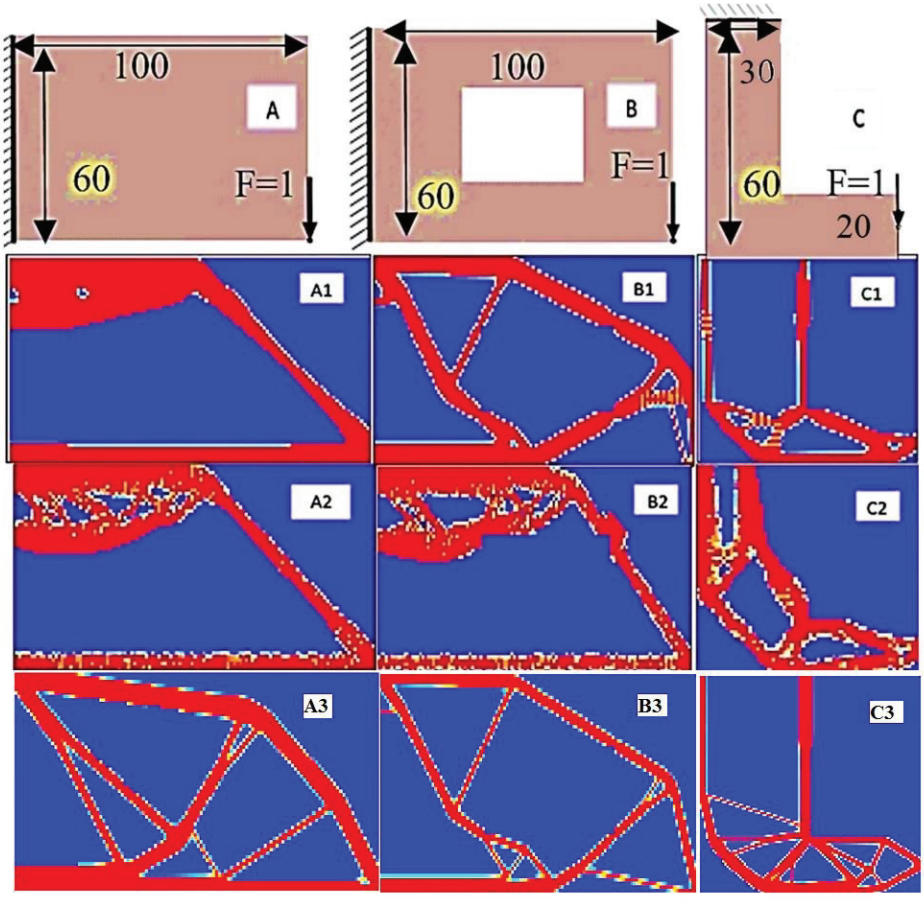

Figure 60. Topology optimization example using stress objectives: A, B, C are topology problems and boundaries. A1, B1, C1 are local stress optimized structures. A2, B2, C2 are pnorm optimized structures. A3, B3, C3, are compliance function optimized structure.

Table 1 von Mises stress results of the optimized 2d cases

Objective function	**A**	**B**	**C**
Compliance	1.3188	1.4391	8.4841
Local Stress	1.5232	1.4775	1.53
pnorm	1.4651	1.8719	1.7598

The results show a variance in best optimization objective function, in the favor of the design boundary conations and geometry. While the diminishing of elements, the stress constraint be discontinuing. This will lead to singularity of the function The local stress around the diminishing areas tend to high due to the nature of stress function[134]. It will be a similar case of stress constriction areas. Relaxation function [144]is used to solve such problem, yet the relaxation is not a radical solution. This is the purpose of the trail of generalizing the stress optimization. The generalization is done by using aggregative method such as pnorm [136] and KS function[145]. In this work pnorm is been taking as the aggregation objective function. Mathematically speaking, p-norm function tends to be convex. This is not promoting its superiority of optimizing the discretized domain. To study the behavior of the normative function. The power of the pnorm function has a big impact on the shape of the function itself. For example, figure.61 shows the function tend to take the largest point of the aggregative data as the main curve. This will theoretically show that the increasing in the normative power will leads to the addressing of the regions of high stress and then modify them or even diminish them. It is being predicted that the impact of discretization will affect the process, so it is not a straightforward process. In addition to that, the design problem of orthopedics is consisting of two different materials enclosed in design and no design domain. Both of these domains have their own traction and support.

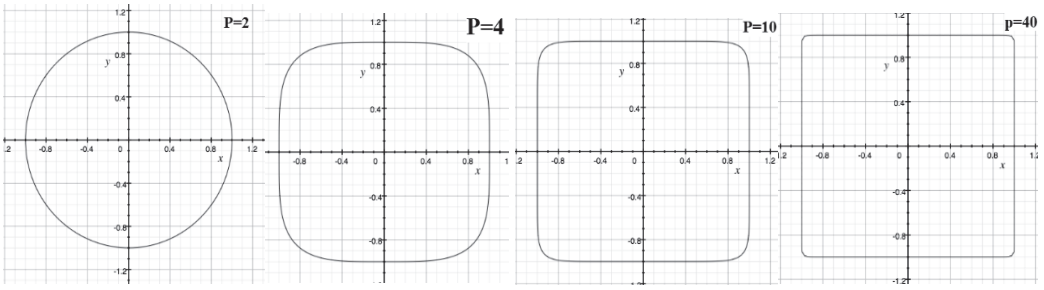

Figure 61 pnorm functions of various normative power (*P*)

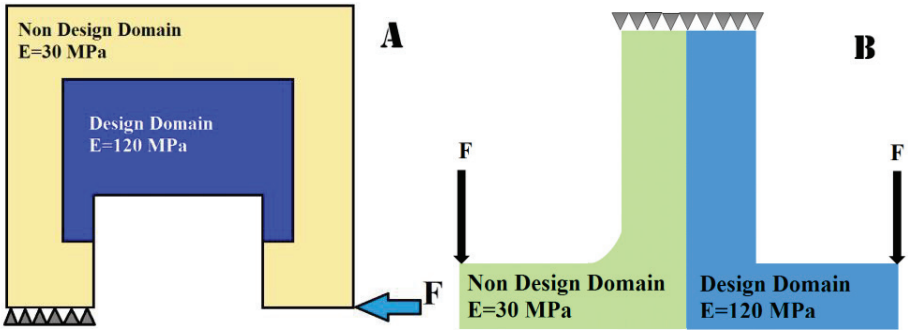

Figure 62 pnrom test design domains

There are two factors in pnorm function, first one is the normative power which is hugely impacting the behavior of the function, and the second aspect is the normalization factor i.e. The normalized stress (σ_{yeild}). Figure. 62 shows a test problem that been introducing to study the effect of discretization on the behavior of normative power of normative power, and the normalizing stress. The normalize stress is took from the preliminary test (Figure (63)). The yield stress of case A is $5.302x10^3$, and for case B is $6.52x10^4$. The normative power changed from (2 to 40). This change in normative power where done for (0.8,0.9,1,1.1,1.2) multiply by normalization stress σ_{yield}.

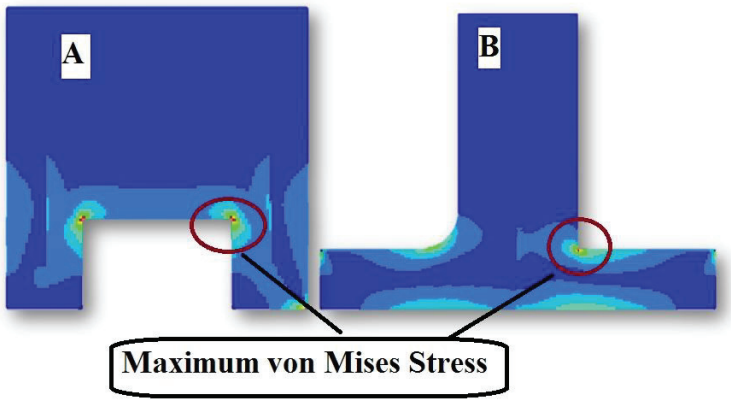

Figure 63 Stress analysis of pnorm test design problems

The two problems represent the action of the enveloped non-design domain on the design domain as in the inner plate of maxillofacial fixations (Figure (62-A)). The second problem is the mutually felid affected problem such as in the hip joint replacement (Figure (62-B). The results are shown in the table (2) - (11)

Table 2 Normative power effect for 0.8x The Normalized stress (Case A)

Normative Power	Maximum Displacement (mm)	Maximum von Mises Stress(N/mm^2)
2	1.26E+01	4.81E+04
4	1.27E+01	4.96E+04
6	1.27E+01	4.94E+04
8	1.26E+01	4.81E+04
10	1.26E+01	4.81E+04
12	1.36E+01	5.79E+04
14	1.35E+01	6.64E+04
16	1.34E+01	5.75E+04
20	1.45E+01	7.31E+04
24	1.32E+01	6.31E+04
28	1.26E+01	5.12E+04
32	1.29E+01	4.74E+04
36	1.41E+01	7.15E+04
40	1.39E+01	1.09E+05

Table 3 Normative power effect for 0.9x The Normalized stress (Case A)

Normative Power	Maximum Displacement (mm)	Maximum von Mises Stress(N/mm^2)
2	1.26E+01	4.92E+04
4	1.33E+01	6.51E+04
6	1.30E+01	6.26E+04
8	1.26E+01	4.91E+04
10	1.26E+01	4.91E+04
12	1.41E+01	6.02E+04
14	1.32E+01	5.91E+04
16	1.28E+01	4.96E+04
20	1.32E+01	6.16E+04
24	1.28E+01	4.72E+04
28	1.31E+01	5.02E+04
32	1.35E+01	6.18E+04
36	1.29E+01	6.18E+04
40	1.30E+01	6.08E+04

Table 4 Normative power effect for 1x The Normalized stress (Case A)

Normative Power	Maximum Displacement (mm)	Maximum von Mises Stress(N/mm^2)
2	1.36E+01	7.62E+04
4	1.25E+01	5.10E+04
6	1.24E+01	7.76E+04
8	1.36E+01	7.62E+04
10	1.36E+01	7.62E+04
12	1.36E+01	6.79E+04
14	1.32E+01	6.11E+04
16	1.35E+01	5.41E+04
20	1.36E+01	5.75E+04
24	1.36E+01	5.46E+04
28	1.28E+01	5.03E+04
32	1.38E+01	6.34E+04
40	1.36E+01	5.65E+04

Table 5 Normative power effect for 1.1x The Normalized stress (Case A)

Normative Power	Maximum Displacement (mm)	Maximum von Mises Stress(N/mm^2)
2	1.36E+01	6.88E+04
4	1.45E+01	9.67E+04
6	1.45E+01	8.56E+04
8	1.36E+01	6.88E+04
10	1.36E+01	6.88E+04
12	1.45E+01	8.56E+04
14	1.36E+01	5.88E+04
16	1.35E+01	5.89E+04
20	1.37E+01	5.65E+04
24	1.33E+01	5.48E+04
28	1.23E+01	7.66E+04
32	1.36E+01	5.73E+04
36	1.35E+01	5.23E+04
40	1.36E+01	5.67E+04

Table 6 Normative power effect for 1.2x The Normalized stress (Case A)

Normative Power	Maximum Displacement (mm)	Maximum von Mises Stress(N/mm^2)
2	1.36E+01	6.88E+04
4	1.45E+01	9.67E+04
6	1.33E+01	6.25E+04
8	1.36E+01	6.88E+04
10	1.36E+01	6.88E+04
12	1.45E+01	8.56E+04
14	1.29E+01	5.79E+04
16	1.35E+01	5.89E+04
20	1.37E+01	5.65E+04
24	1.37E+01	6.67E+04
28	1.35E+01	5.76E+04
32	1.36E+01	5.73E+04
36	1.37E+01	5.50E+04
40	1.36E+01	5.67E+04

Table 7 Normative power effect for 0.8x The Normalized stress (Case B)

Normative Power	Maximum Displacement (mm)	Maximum von Mises Stress(N/mm^2)
2	1.319	5.11E+03
4	1.319	4.85E+03
6	1.318	4.56E+03
8	1.317	4.69E+03
10	1.317	4.69E+03
12	1.318	4.67E+03
14	1.318	5.35E+03
16	1.318	5.07E+03
20	1.317	4.84E+03
24	1.319	4.77E+03
28	1.318	5.25E+03
32	1.318	5.52E+03
36	1.317	5.31E+03
40	1.316	5.33E+03

Table 8 Normative power effect for 0.9x The Normalized stress (Case B)

Normative Power	Maximum Displacement (mm)	Maximum von Mises Stress(N/mm^2)
2	1.318	5.18E+03
4	1.318	4.77E+03
6	1.316	4.76E+03
8	1.318	5.18E+03
10	1.318	5.18E+03
12	1.318	6.03E+03
14	1.318	4.91E+03
16	1.318	4.90E+03
20	1.317	4.59E+03
24	1.317	7.03E+03
28	1.32	4.88E+03
32	1.317	4.48E+03
36	1.319	4.65E+03
40	1.32	5.18E+03

Table 9 Normative power effect for 1x The Normalized stress (Case B)

Normative Power	Maximum Displacement (mm)	Maximum von Mises Stress(N/mm^2)
2	1.32	5.65E+03
4	1.317	4.69E+03
6	1.315	5.09E+03
8	1.32	5.65E+03
10	1.32	5.65E+03
12	1.317	4.96E+03
14	1.317	4.37E+03
16	1.315	5.18E+03
20	1.316	4.87E+03
24	1.318	4.22E+03
28	1.312	7.04E+03
32	1.32	5.77E+03
36	1.307	4.46E+03
40	1.317	4.07E+03

Table 10 Normative power effect for 1.1x The Normalized stress (Case B)

Normative Power	Maximum Displacement (mm)	Maximum von Mises Stress(N/mm^2)
2	1.317	4.51E+03
4	1.319	6.16E+03
6	1.318	5.22E+03
8	1.317	4.51E+03
10	1.317	4.51E+03
12	1.317	4.48E+03
14	1.316	5.40E+03
16	1.318	5.04E+03
20	1.316	4.66E+03
24	1.316	4.74E+03
28	1.316	4.70E+03
32	1.318	4.56E+03
36	1.319	4.56E+03
40	1.316	4.54E+03

Table 11 Normative power effect for 1.2x The Normalized stress (Case B)

Normative Power	Maximum Displacement (mm)	Maximum von Mises Stress(N/mm^2)
2	1.318	4.88E+03
4	1.317	5.24E+03
6	1.316	5.21E+03
8	1.317	4.88E+03
10	1.318	4.88E+03
12	1.312	4.84E+03
14	1.32	4.62E+03
16	1.319	4.41E+03
20	1.312	5.28E+03
24	1.318	4.78E+03
28	1.319	6.61E+03
32	1.318	4.44E+03
36	1.319	4.27E+03
40	1.321	5.03E+03

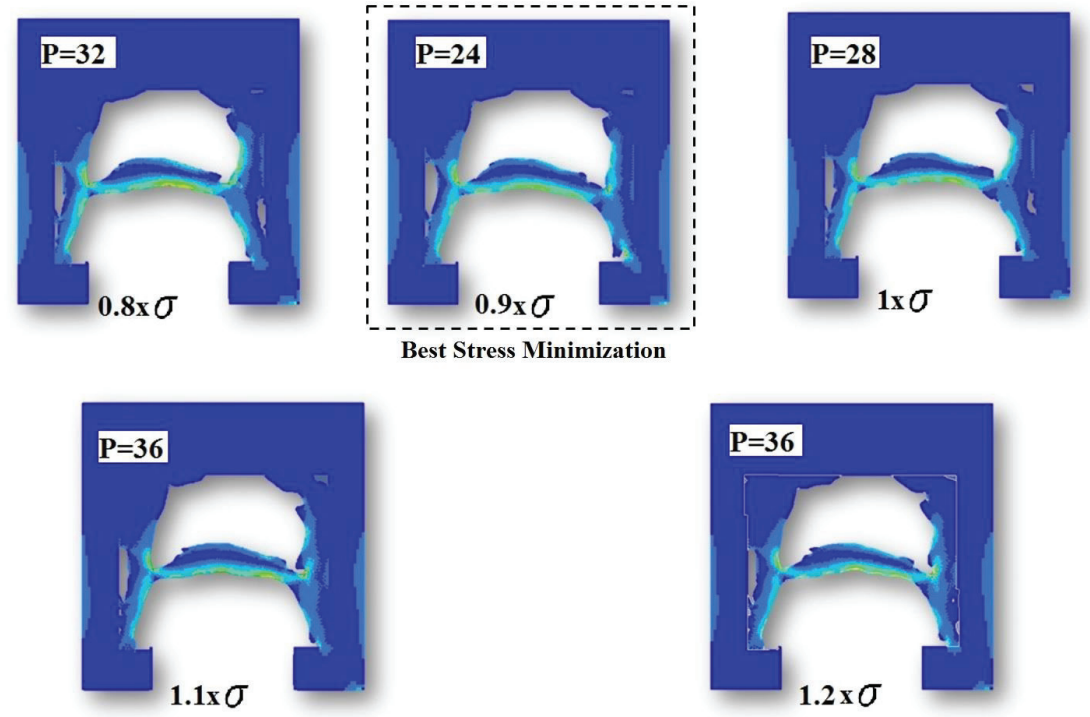

Figure 64 Best results of Case (A)

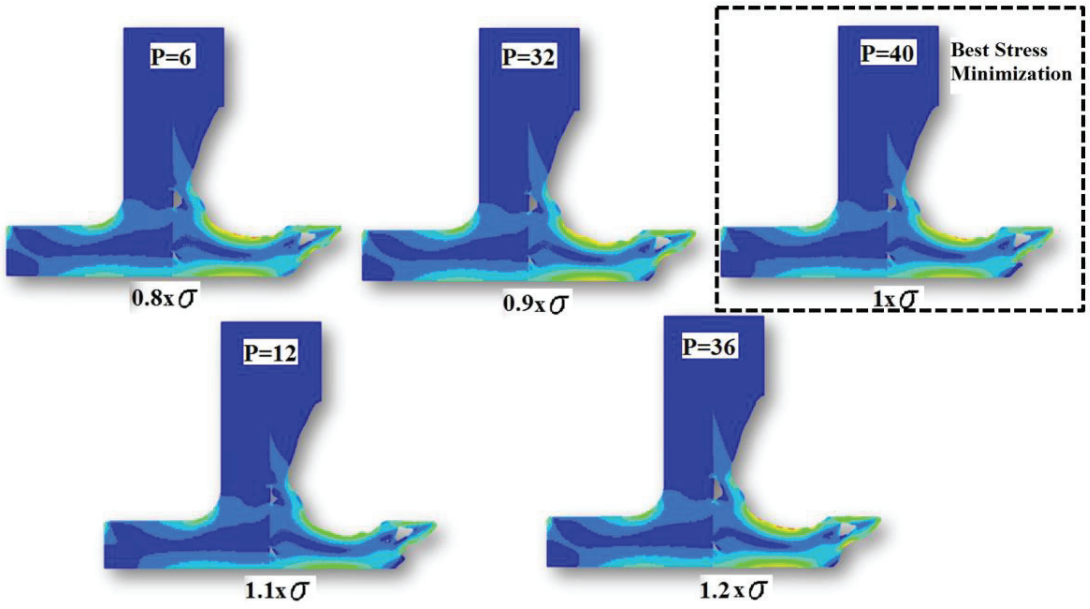

Figure 65 Best results of Case (B)

Increasing the normative power is not associated with getting the best results, as shown in Figure (64), and (65). From the previously mentioned characteristics, and results; it is concluding that topology optimization using pnorm objective is the safest approach.

3.8. Shape optimization versus layout optimization approach

3.8.1. Mesh morphing shape optimization versus topology optimization

Many researchers been implemented and tested shape optimization with boundary growing approaches (Phase field, Level set, etc.). Shape optimization face the problem of computational power and time. Mesh morphing is a technique uses the entire meshed domain or a discretized one. It has the ability of be perform in an impressively short time. the stiffness matrix will be altered only by changing the spatial configuration of the nodes due to the adaptive extrusion process. To test the mesh morphing performance, the following numerical simulation been performed. 3, 4, and 8 nodes elements are used to describe the problem individually. L-bracket problem was chosen (Young's modulus is 210 GPa, and Poisson's ration of 0.3) to perform stress-based optimization. The dimensions and loading conditions are shown in Figure.66. The problem is divided into two parts, the first part is the design domain, which is enclosing the maximum stress area of the whole domain, and the other part is the non-design domain. Optimization is certainly addressed the design domain only. The first step of performing optimization is the preparation of appropriate discretization of the domain. Finite element convergence test was performed by increasing the number of elements and measuring maximum von Mises stress. Three node elements were chosen, to ensure getting properties element number for the lowest number of nodes as possible in the 2D case. Due to stress singularity, maximum stress which is located on the inner side of the elbow is increasing with increasing element number indefinitely. However, it will reach acceptable slope which means, increasing element number will slightly increase maximum stress.

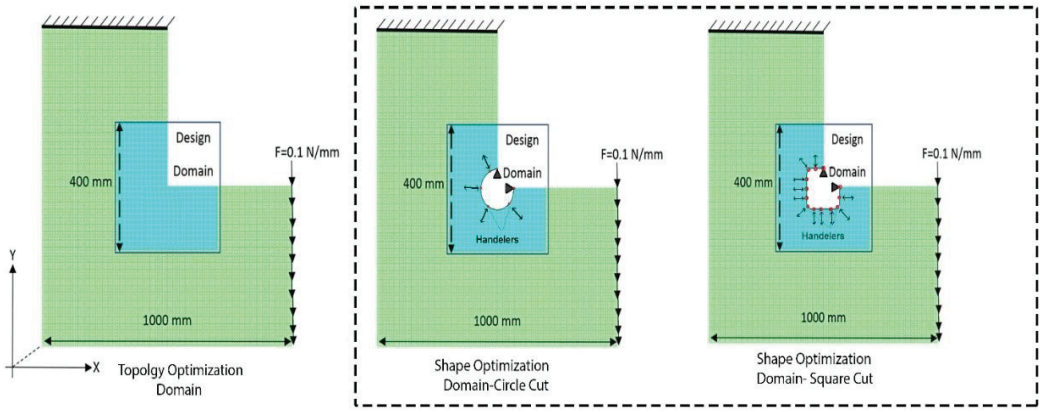

Figure 66 L-bracket problem

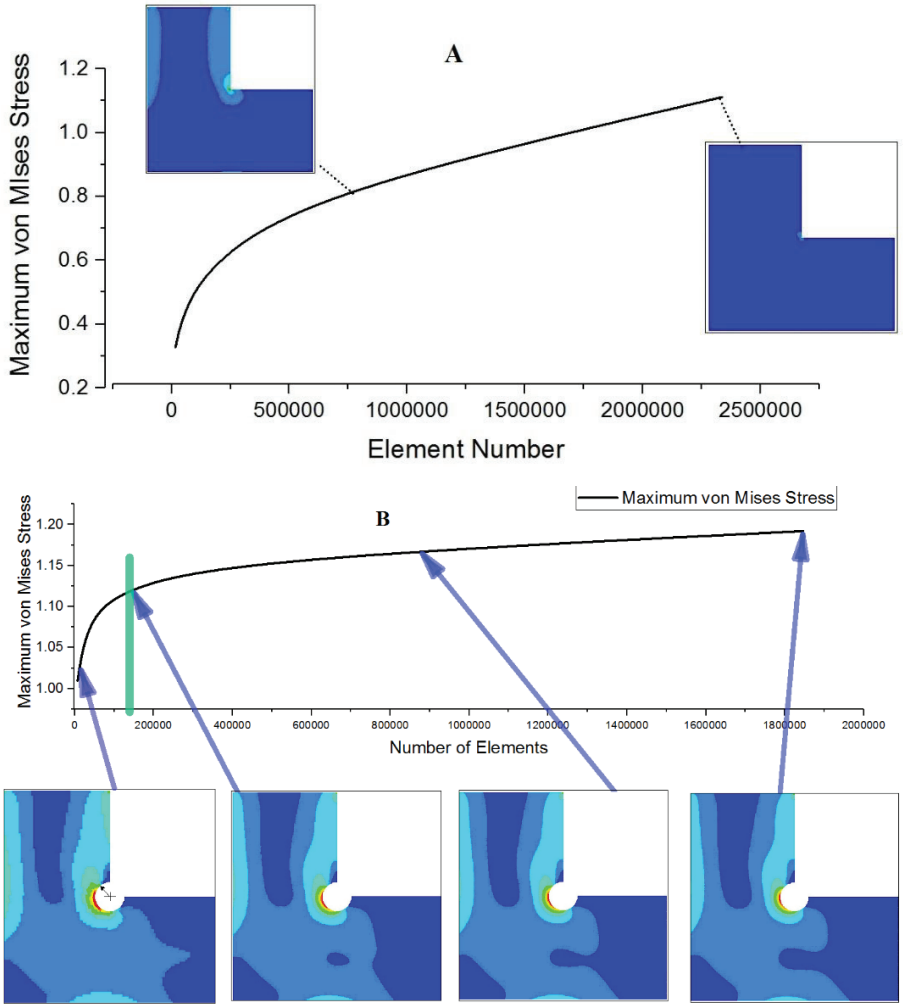

Figure 67 FEM convergence test with 3nodes element. A) the test of sharp angle; B) is the test of circular hole cut.

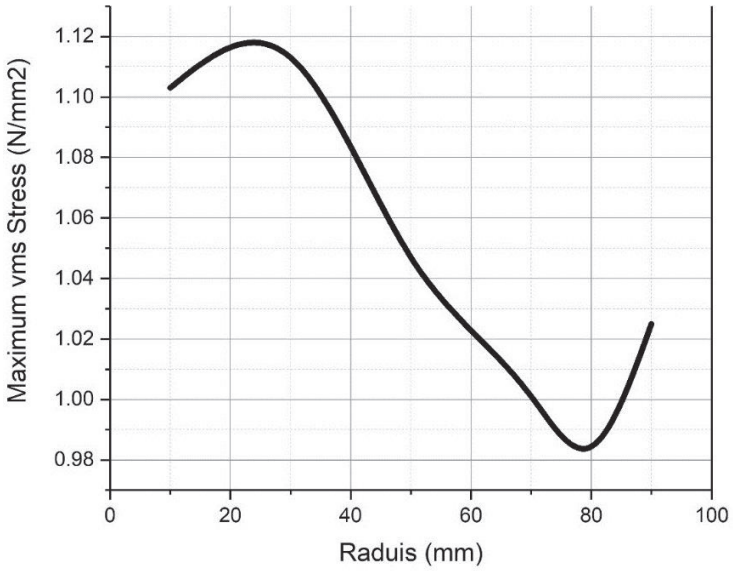

Figure 68 Circular cut radius convergence test

Optimization is a computationally demanding process, so choosing the lowest element number is crucial. Figure 67 show the results. The best element number to be chosen is theoretically the maximum number at which the slope of the graph is constant. In this case, it should be more than $1.2x10^5$, but for topology optimization process, it will take incredibly long time to the optimization, especially with stress objective function. Under the assumption of strong convexity of the objective functions; moving step of the function could be increased without affecting the results so much (In other words, the point that represents the function fitting can be reduced as much as it shows the original domain boundaries with acceptable resolution). Stress is extremely sensitive to the special configuration, so it is high around the areas of sharp angels (Figure. 67-A), so in structural design, the engineers, try to limit sharp edges of the design in order to limit stress singularity. Improving surface finish to elongate fatigue life, is an advanced approach of such principal, which usually done by removing some of the specimen outer layers. Addressing stress singularity is an engineering problem, which is usually referred to in simple form as stress concentration. If there is sharp angle space confinement, stress will rise numerically to a huge value. The remedy is by avoiding sharp confinement by adding or removing materials around singularity issue. Practically and for the case of engineering structures (excluding tribological aspect of the design), sharp inclusions usually be big

enough so the need for adding materials usually done by thermal methods. The structure of the added layers or part will have different microstructure. If it stays without proper treatment, it will promote failure chemically (for example; corrosive induced spots) and physically (for example; residual stress). Cutting the surrounding metal will have a less

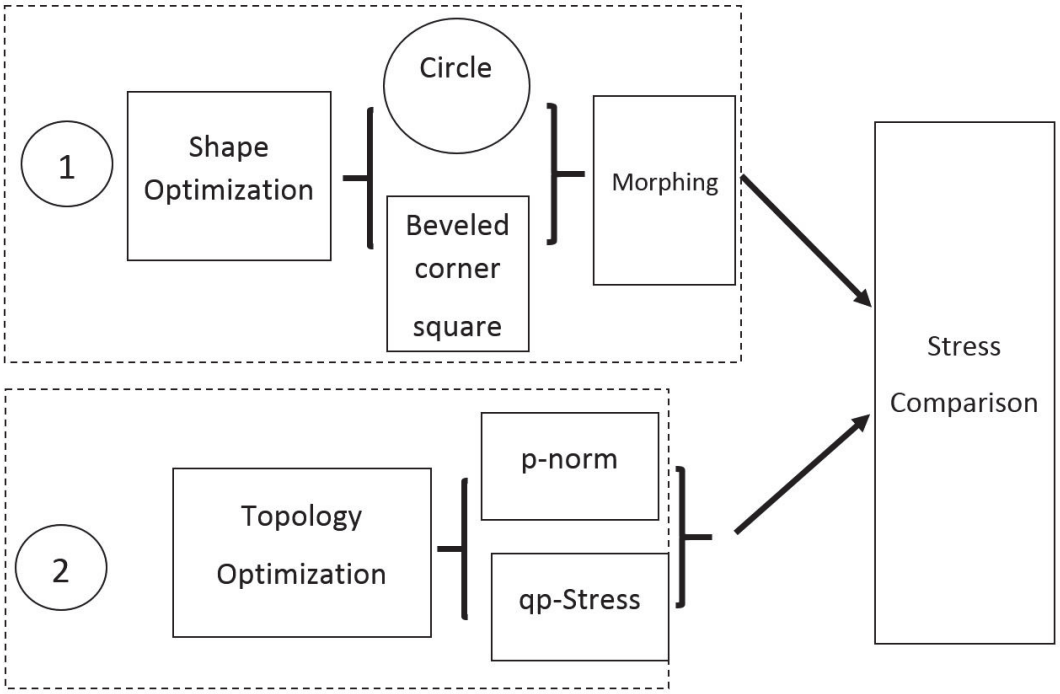

Figure 69 The algorithm of the optimization and evaluation process.

severe change in the processed area, add to that the easiness and energy saving of post-processing. The method of cutting areas to decrease the singular stress is used for limiting crack propagation efficiently[146, 147]. The optimal shape of cut will vary with the confined place itself, but the best surface tension is for the adequate round cut. In this work, cutting areas around the singularity point is been adopted as the method of reducing the stress concentration. First, a circular cut was made. The circular cut was done with various radii, to find out the optimal radius (Figure. 68) which shows that the best radius (78 mm). Shape optimization is being performed for the cutted boundary to enhance stress

reduction. The edges of the cut are fixed. The circumference of the hole is set to move normal to the boundary inward (lower limit) and outward (upper limit). Another cut shape is chosen for comparison. The cut is beveled edges square cut; mathematically similar to norm function of power20. The upper and lower limits were chosen to be in the period (500, -40). Movement period has been chased such that, negative Jacobian is not happening for the elements. Objective functions for shape optimization are qp-approach and p-norm functions. Topology optimization with artificial density approach and shape optimization using mesh morphing is being performed using qp approach and p-norm approach for the three element types. Figure. 69 shows the algorithm of the optimization process. Optimization results Figure. 70 showed varying in results with different element types. The cases have similar node numbers in order to keep the conformity of degree of freedom. Figure.70 shows maximum stress reduction being performed by averaging stress method (p-norm. Best results are shown for 4 node elements. This is regarding increasing the number of elements that the objective function can modify. Results of Figure. 71 shows that the increase of area reduction is not necessarily associated with minimum singular stress (The case of three node element of p-norm function). Figure.72 shows the results of pnorm function for the used three types of elements.

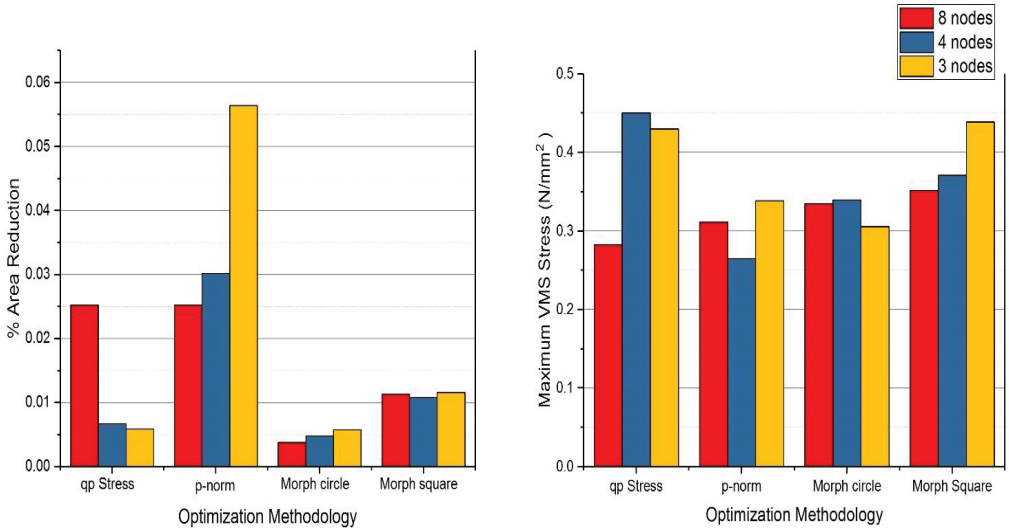

Figure 70 Area reduction and maximum von Mises stress for optimization methodologies

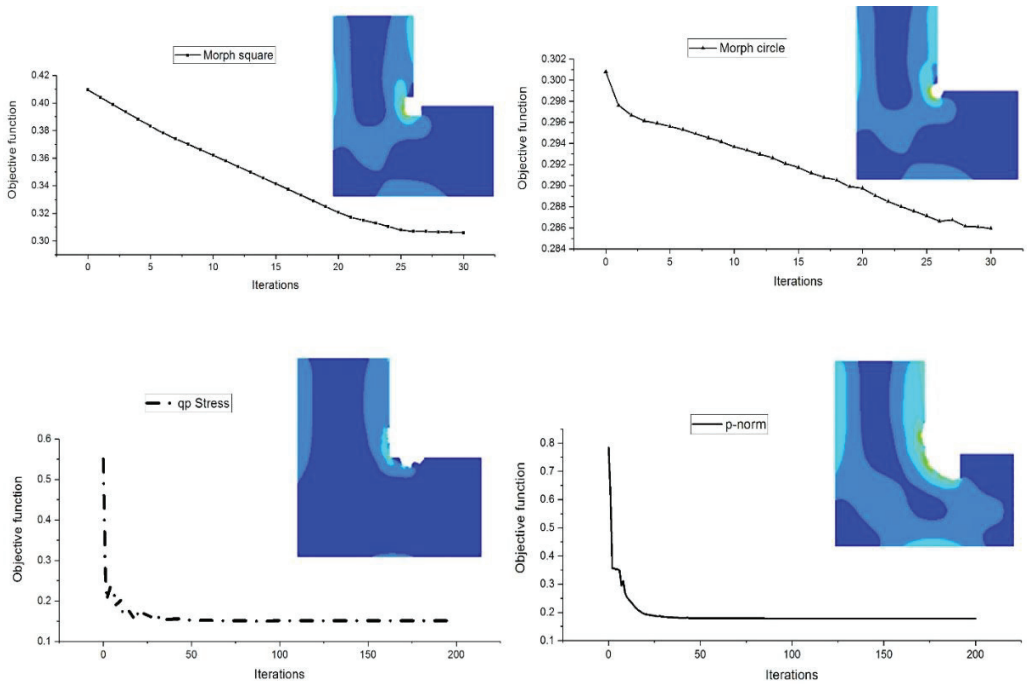

Figure 71 Objective function convergence for 4 node elements with different optimization methodologies

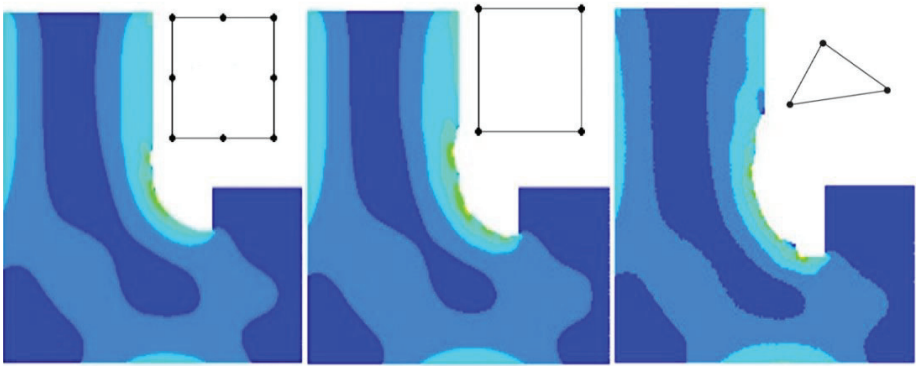

Figure 72 Pnorm function final results for the three types of elements

3.8.2. Topology optimization versus Fatigue based shape optimization

The results that were presented in the section 3.8.1. promoted pnorm stress optimization as a methodology of design in the case of L bracket case with a relatively high number of elements. Pnorm is also a stable methodology of design and been advised to use by many researchers, so it is a normative function, which aggregates the stresses.

Another study is being performed using fatigue concentrate shape optimization. Free shape optimization was performed for the shame study case as shown in the figure. 66. The results are shown in the figure. 74. The stress comparations showed in Figure. 73.

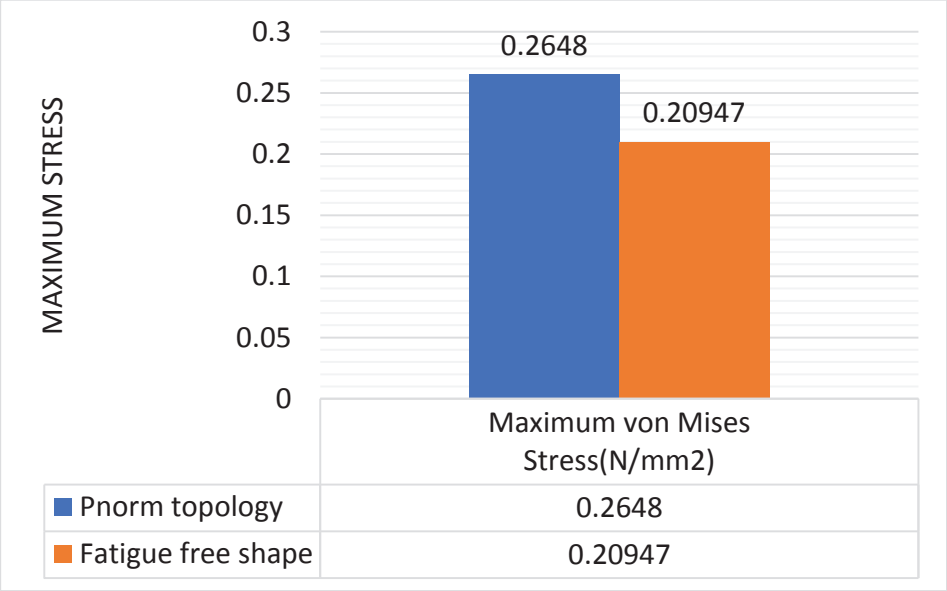

Figure 73 Results of pnorm topology optimization and free shape fatigue baes optimization

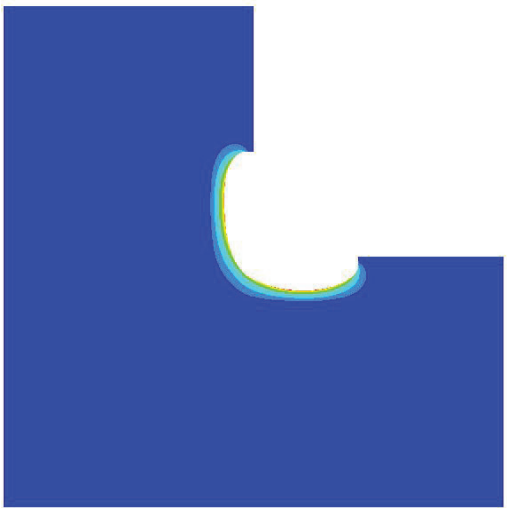

Figure 74 Ftuige objective function based shape optimization.

3.9. Cascade model approach

Another approach was tested which is the mix between topology optimization and shape optimization. The Idea is to introduce the weigh minimization based on the compliance function, then the results will be optimized interim of stress minimization in order to make the design more fatigue resistance. Figure.44 shows the topology optimization using compliance as objective function[57] then it is transferred to phase field shape optimization program[142]. These programs written in MATLAB and use 4 node structured element.

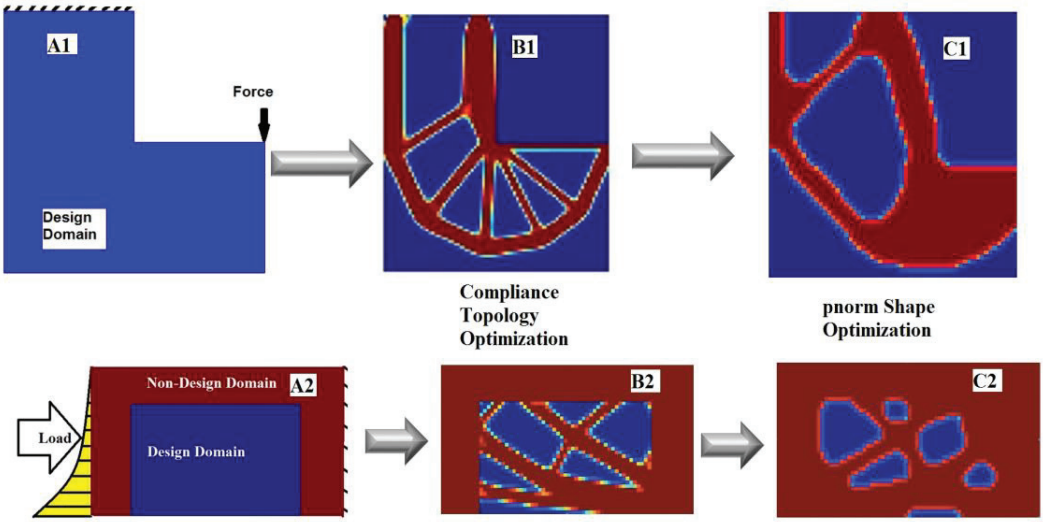

Figure 75 Case 1: L-shape cascade mode Case 2: U-shape cascade model

It is being shown in Figure.75, that the areas of sudden change are softened to rounded for the problem. However, the problem of orthopedic design is a stiffness sensitive. The stiffness is altered using this methodology. It is a valid methodology to address the stiffness (or the equivalent compliance) in the shape optimization as a constraint. This will lead to the following argument: why not address the compliance and stress in shape or topology optimization, so this will lead to less complication in designing process and the computational time. Another possible strategy is to reverse the situation. So, the first stage is done by shape optimization to smoothen the stress concentration areas. the second stage is the compliance optimization. Stress concentration elimination is valuable for increasing the implant lifespan, especially the stress concentration areas will promote not

only the crack initiation due to high stresses, but also due to the engorgement of corrosive various action[148-150] (Hydrogen embrittlement, ions migration, oxide film irregularities, etc.) in the implant metal itself induced by body fluids and high stress variation of the implant. Shape optimization is chosen to by fatigue based. So, it can focus only on the high-stress areas effectively and fast such that the fatigue curve is a convex curve, making the optimization process is smooth and straightforward.

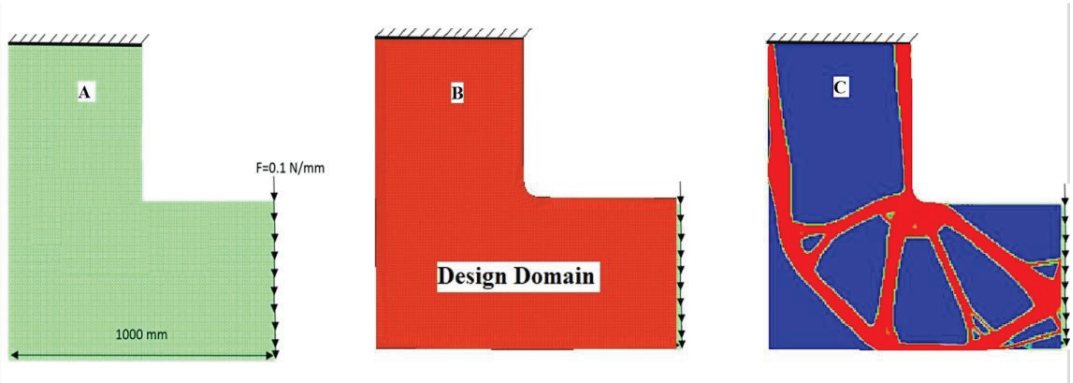

Figure 76 Cascade Model (A) Design Domain, (B) Fatigue based Shape Optimization, (C) Compliance based Topology Optimization

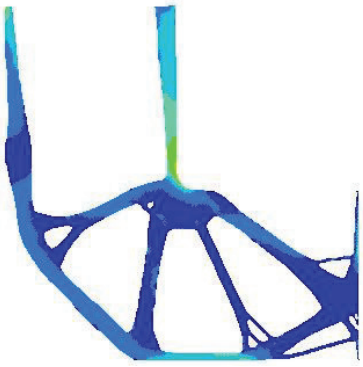

Figure 77 von Mises Stress Analysis of the Shape-layout optimization model

As a comparison of Figure. 44, and Figure.77; the fatigue shape-compliance topology optimization model shows a topology of stress friendly areas (minimal stress concentration) for the specific loading condition that the bracket suffer from.

3.10. Conformal lattice structure approach

This approach is been introduce into the OptiStruc solver and been investigated by researchers[151-153]. In this method, optimization is done on two stages (cascade approach). First, topology optimization is performed using SIMP method. Density ρ is lower- penalization (i.e. $\rho^{1\sim1.5}$) to allow the existence of gray areas (as shown in figure 59). Gray area is no desired aspect of traditional topology optimization caused it gives the undetermined status of the design, such that SIMP method as a blunt abstract of homogenization approach, is not considering any possibility except the isotropy of the material as one material (in general); so, it will be difficult to determine whether there is or there is not material (Figure. 78).

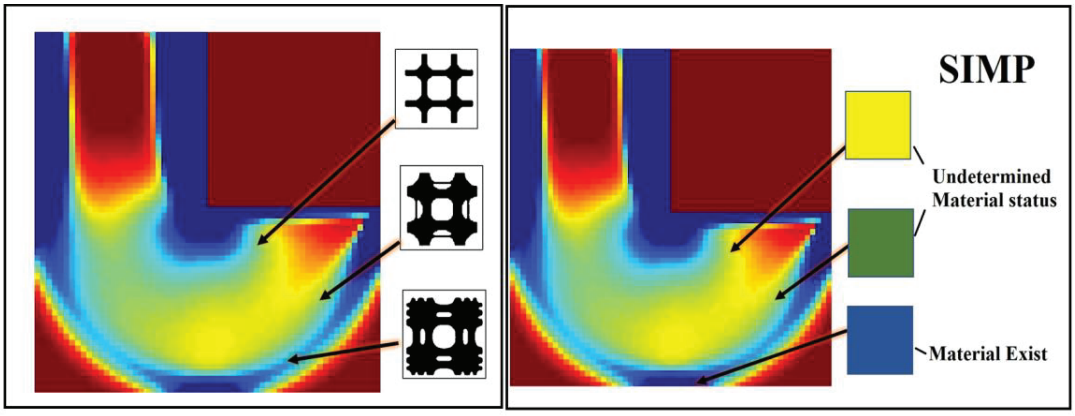

Figure 78 Homogenization versus SIMP approach

However, in CLS method, ray areas are translated to truss shape by replacing the element edges with truss members. After identifying the truss locations, another optimization is performed to find out individually, the best truss cross-section in the overall design. Figure. 79 shows the various linkage radius of a designed case.

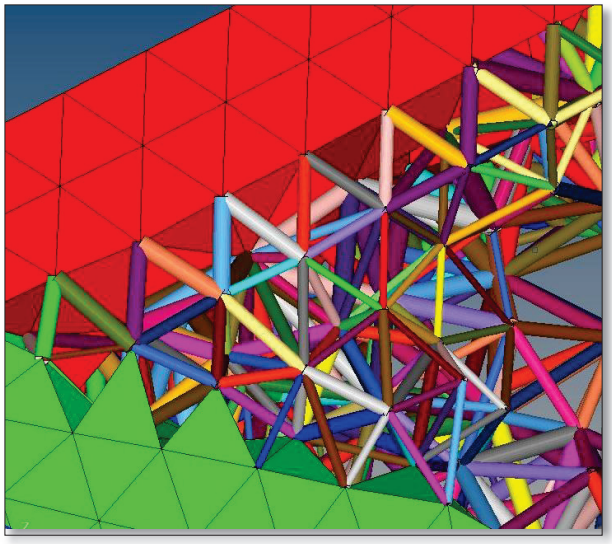

Figure 79 Conformal lattice structed design

3.11. Selection of topology optimization methodologies

In this work topology optimization is addressing the stress shielding in order to increase the medical lifetime of the implant. The robustness of this goal promotes challenge comparing to the performed researches topology optimization in medical prosthesis. The vast majority of the researches addressed the prosthesis itself to have long mechanical life span[154], or the computer aided design of complex prosthetic with weight minimization of the design structure[155-157]. The separation between the engineering side and medical side in the favor of spatiality claims is not in the favor of the patient. The engineers in these researches lakes the access to the problem data in the short and long term. The medical experience lacks the ability of performing structural optimization design and introducing objective function by its own due to lack of engineering experience. The scientific criticisms of the previous topology optimization views are the pillars of the design hypothesis that is introduce in this work. Two major goals to be satisfied. The first one is introducing design methodology to address stress shielding, to increase the medical life time of the prosthesis and keeping the mechanical life time as long as it could be achieved. The second goal is to identify the possibility of

doing one surgery in which the surgery is implemented while the design till CAM specialized prosthesis is implanted successfully.

From the experience of chapter two and topology optimization study which is been perform in this chapter, the selected design algorithm is as follows:

First: the objective function.

Compliance objective function seems a valid idea such that, the metal prosthesis is much stiffer than the bone, so maximizing the compliance will lead to less stiff orthopedics. This will obey the first approach of stress shielding, i.e. stiffness matching of the orthopedic and the surrounding bone. Real-time bone stiffens can be calculated by building finite element model and using the calculated modulus of elasticity that is measured from radiology images such as CT scan. Pnorm function with compliance constraint is another optimization criterion of stiffness matching approach.

Second: the non-paramedic design approach (Topology, and the shape optimization)

This related to the design domain topographic, and physical constraint. Aesthetically, the design domain should obey the specific topology of the patient body has been mentioned in the section 2.1. Aesthetic constraints forced to have the outer shape fixed. The design will be performed inside the implant. This will promote topology optimization as a generalized method in the scope of the current non-parametric optimization methodologies, and the commercial software adaptability. In case of inside implant such as femoral stem road design, it is been noted that the designs using shape optimization is decreasing the bone material surface interaction[158]. In the scope of the pervious recaches and experience, topology optimization is the valid option to be general optimization methodology for prosthesis design.

Chapter Four: Medical challenges examples

4.1. Introduction

The patient specialized prosthesis is the scope of this chapter. This will promote strong biomechanical integration. Temporomandibular joint prosthesis and total hip joint replacement are studied with the different stress shielding approach. The first approach is stiffness matching. This is done in temporomandibular joint design. Minimizing bone stress which is induced transfer by the implant is been studied in the total hip implant. Dipole vision of additive manufacturing products surface finish is discussed in the last part of this chapter.

4.2. Temporomandibular joint prosthesis design

Mandibular fracture is expected and common for facial injury. Body and angle fractures are more often to be expected. Sportive like cavities, mandibular thickness, and location, promote such fractures to happen. Infection highly frequent with oral cavity related fractures; which makes addressing surgical intervention be exceptionally thorough. Although Medical treatment keep improving, in a similar way to computer integrated circuits (Moore's Law), Surgical techniques are lagging. Two kind of fixation used as fixed and flexible fixation. , However flexible fixation gives portion of freedom for trading team, fixed fixation in some cases be the best option[80] . Orthodox maxillofacial fractures fixing techniques including wire/plate/screw osteosynthesis and maxillomandibular fixation (MMF) [159-162]. Michelete et al[159] studied osteosynthesis technique using strip plates (mini-plate) fixed by screws. Plate design based on surgeon view of approach the requirements of maxillofacial region as possible; taking into consecration remodeling of facial safekeeping of functions and correct occlusion. S. Choudhari et al[163] investigated temporary fixation in view of biodegradable close regarded fixation. Plate design stay within orthodox way of thinking

however revolutionary material been used. Fracture line stability reviewed by Jones et al[160]. Cases of skewed path of screw, may use for better attachment, and fracture line fixation. Fracture hematoma stability is vital for healing process. In general, design and chose open reduction materials, is based on surgeon “common sense” and “experience” [164]. Aiding surgeon better judgment with mechanical analysis emerge in finite element analysis[165-167]. As in structural analysis, stress singularity may appear in bone finite element representation especially with complexity of bone topography. Stress singularity in shade of surgical assessment may not needed to be addressed, such that displacement can be determined with existence of singularity. Due to complexity of bone structure in head and neck in anatomical point of view, facial treatment is often take a considerably more time to address problem carefully. Facial construction is difficult to construct accurately with taking the surface scan for the face. It is filled with air cavity, soft tissue spots, as arteries, and facial nerves. Individual variation also a fact which should be consider. Computer tomography (CT) and Magnetic resonance imaging (MRI) is effective way to construct 3D modeling of domain to have design within [168-171]. MRI capable of giving high resolution –high contest image[172], however, it is still considered an expensive diagnostic Tanique. In the other hand CT scan, more cheap and reliable source of data[173]. Also, for some cases in which, patient has metallic implants or tooth filling, MRI is not an option any more. 3D construction from CT imaging Technique allow to get appropriate design for the case in hand and lowering probability of the Malunions and Malocclusion, taking in consideration surgeon adjustment. Another advantage of such modeling technique is to limit Nerve injury[174] within design domain. So, critical locations can be identified and set as conditional design domains. So, fixing parts such as screws and wires will nor contact nerval system or any vital soft tissue areas. The Domain will be selected with both the surgeon and the engineers in order to lower the risk of pre-/post- risks, such as infections elevator spots, soft tissue collateral damage, best available fixing, and enclosure. Desired cavities, appropriate loads, and can be taking into consideration more efficiently [156]. A several cases of optimized plate fixation for fractured mandibles been studied. Designing orthopedic implant as extraskeletal in topographic nature. Loading condition simulate real joint degree of freedom and actual closure pursue in addition to muscular tension forces [175-177]. Orthopedic implants

need precision in preparing. Both bulk and surface [178-182], characteristics are addressed with noticeably concern. Bio-Tribological characteristics are beyond the scope of this research. Computer-aided design (CAD), gives good database for better precision of workpiece making. Additive manufacturing controlled by computer-aided manufacturing (CAM) protocols, gives the ability of control implant mechanical and topological aspects. Different biomaterials were studied with particle (electrons) or energy wave buckets (laser) rays,[183-187]. As design done by topology optimizations leads sometimes to rather complicated design, Additive manufacturing seems important choice. Automating custom orthoepic implant with real-time surgical operation is a target, might seems extremely difficult to achieved practically nowadays, but with the advance of CAD-CAM process with TO laying within the core of such processes, it could be achievable target in the scope of near future.

4.2.1. Fatigue life

Because of shape complexity of prosthesis designed by topology optimization; rapid prototyping expected to be used in machining of such structure. Additive manufacturing using Laser 3D printing gives rather acceptable surface finish with metal constancy due to unique characteristics of laser welding. Surface finish is very important to determine life printed peace. Associated with microstructure. Residual stresses due to laser thermal processing are in minima, because of high heat dissipation of localized heat. Under such assumptions, surface finish and residual stress will not be highlighted addressed in fatigue model. Averaging stress should use in the 3D case. Signed Von-Mises is a suitable equivalent state for Titanium Alloys.

4.2.2. Numerical examples

An in vitro case study was simulated and studied involving a major excavation of the mandible, simulating jaw cancer, as shown in Figure. 80.

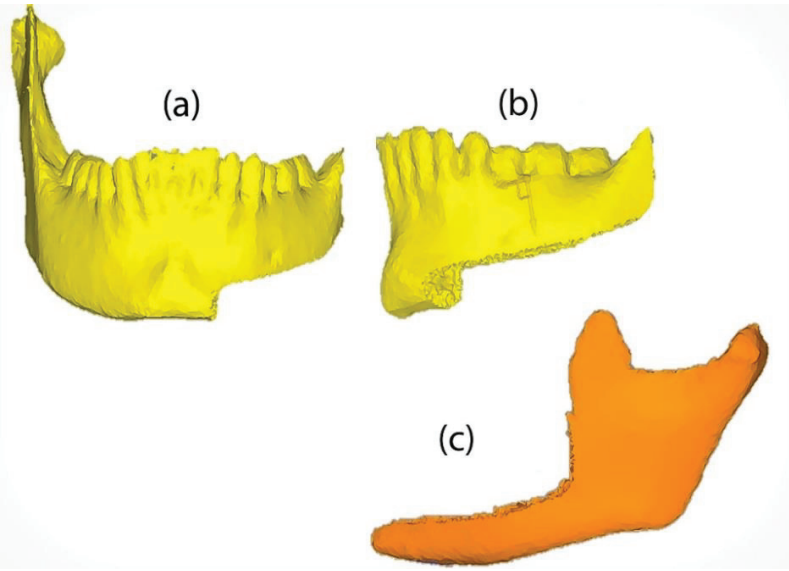

Figure 80 In vitro case study: (a) front view of the mandible, (b) side view of the mandible showing the remaining jaw, (c) missing section of the mandible

Temporomandibular (TM) prostheses are commonly used in major reconstructive surgery. An orthodox reconstructive prosthesis based on a design simulation, using a Vitek-Kent prosthesis body with an AO/ASIF TM joint condylar prosthesis, is shown in the figure. 81

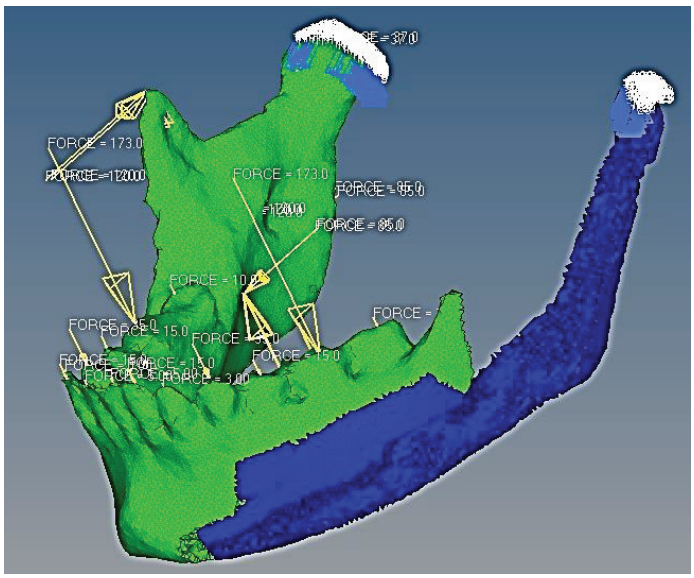

Figure 81 Orthodox mandibular TM prosthesis

The core is the design domain. Bone density varies from 1.5 gm/cm^3 to 0.9 gm/cm^3 compared with approximately 4.53 gm/cm^3 for titanium alloy. Such a difference necessitates coverage of a smaller region of mandibular space to overcome excessive weight. In this case study, the orthodox prosthesis occupied 28.72% of the original replaced bone. The prosthesis material used was titanium alloy (Ti-6Al-7Nb). To perform finite element analysis, constraints and loads on the mandible need to be defined (Figure. 82). Individual variations in biting condition have been ignored. Suitable adaptive loading values are listed in Tables 12 and 13.

Table 12 Biting forces

Number	**Tooth**	**Average model force (N)**
1	central incisor	5
2	lateral incisor	15
3	canine	35
4	first premolar	1.2
5	second premolar	15
6	first molar	173
7	second molar	6.3
8	third molar	0

Table 13 Mandibular muscular forces

Symbol	**Muscle**	**Average model force (N)**
M	Masseter	170
MP	medial pterygoid	180
LP	lateral pterygoid	37
T	Temporal	170

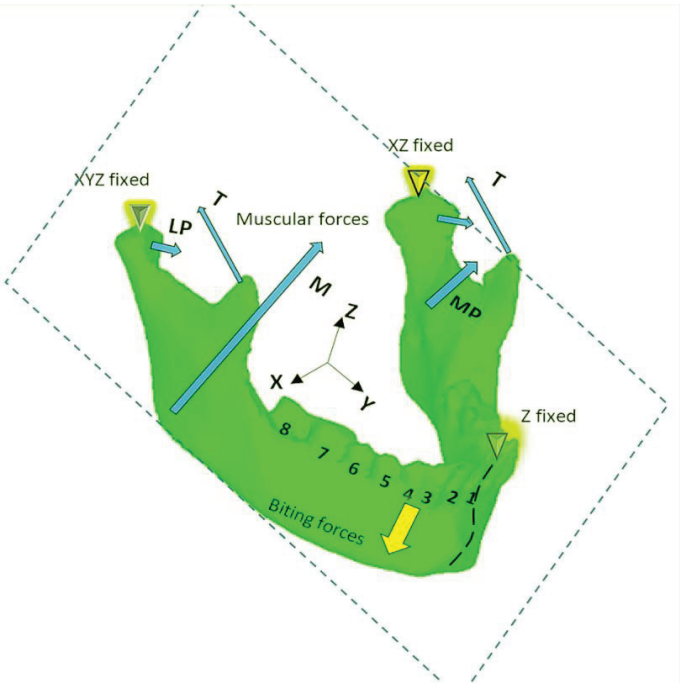

Figure 82 Mandibular model

The design problem that is considered in this work is divided into two regions: the design in which the optimization process will occur; and the non-design domain which is needed to satisfy medical conditions, such as an occlusion mismatch. The implant is made of materials with a high modulus of elasticity, such as titanium alloy. The implant domain is within the boundary domain of the lower modulus of elasticity (bone). This boundary domain will eliminate the need to extract a design model for certain applications as it is being done within the conventional topology optimization design process. The design takes into consideration the original state of the finite element analysis of the mandible (i.e. FEM undertook with the OptiStruc solver). Objective function has been investigated was compliance, and p-norm. Power effect on SBTO function was studied. Power used are (50). In the present computer simulation, a major temporomandibular joint prosthesis reconstruction of the mandible should be done for most of the left-side damaged jaw as shown in Figure 83a. This case simulates resection of the jaw for treatment of bone cancer, necessitating an immediate large-scale implant. Because of the complexity of the mandibular anatomy, the reconstructive prosthetic part is shaped based on information

from the CT scan. The implant consists of a non-design domain and a design domain of titanium alloy. The purpose of the non-design domain is to mimic the actual replaced bone shape to avoid malocclusion. Malocclusion can lead to chronic headaches and serious joint inflammation if it is not treated. Cloning of the actual shape will certainly eliminate malocclusion. As shown in Figure. 84b, the full prosthetic outer shape has been determined by the non-design domain, while the design domain is within the core of the implant.

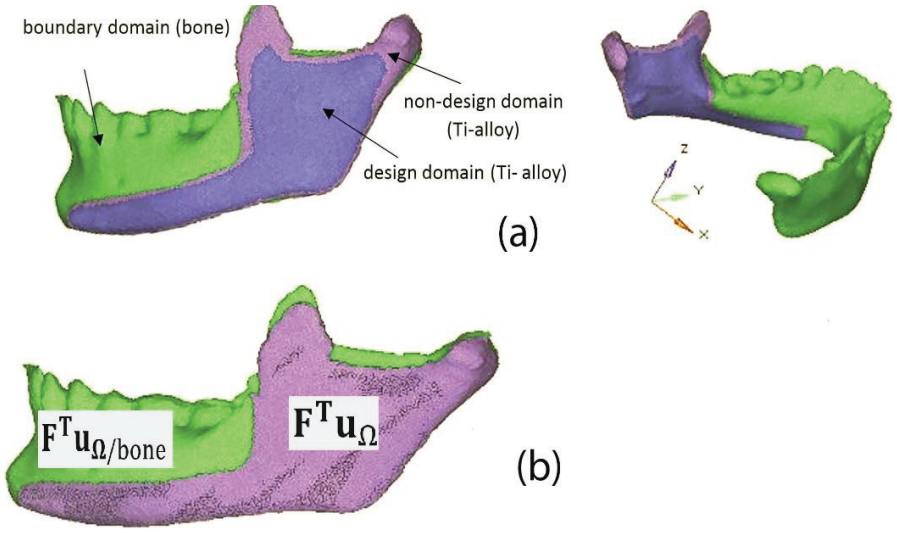

Figure 83 Temporomandibular reconstructive design problem

(a) Cross-section of the mandibular substitution implant design problem

(b) Mandibular substitution implant design problem – metal-skinned version

The target volume fraction in topology optimization was set to be equal to the volume fraction of the orthodox prosthesis compared with the original bone; in this case, it was 0.2872. To maintain the structural integrity, the pre-design space is skinning the design area as well as a presumably place of fixing pins. As a solution to stress shielding, an additional constraint was added which is compliance constraint to topology optimization based on compliance and SBTO functions. It is necessary to calculate what compliance (C) would be for healthy bone structure. This compliance would be an additional constraint to the upper boundary of the volume fraction. In the case of compliance

maximization based objective function, the design scheme follows Equation (94).

$$\begin{aligned} &find \quad \rho^3 \\ &\max \ \mathbf{F}^T\mathbf{u}_\Omega \\ &s.t. \ \int_{\Omega_d} \rho d\rho \le V_d \ , 0 < \rho_{\min} \le \rho \le 1 \quad \forall \rho \in \Omega_d \\ &\mathbf{F}^T\mathbf{u}_\Omega \to \mathbf{F}^T\mathbf{u}_{\Omega/bone} \end{aligned} \quad \dots (94)$$

In the case of minimizing the averaging stress aggregative equation, i.e. p-norm, the design scheme follows equation (95). In this case, the compliance condition which is the compliance of the missing bone in case it exists, was measured as 34.04 of 247.27 (the total compliance of the complete healthy mandible).

$$\begin{aligned} &find \quad \rho \\ &\min \left\| \sigma_{vms} \right\| \\ &s.t. \ \int_{\Omega_d} \rho d\rho \le V_d \ , 0 < \rho_{\min} \le \rho \le 1 \quad \forall \rho \in \Omega_d \\ &\mathbf{F}^T\mathbf{u}_\Omega \to \mathbf{F}^T\mathbf{u}_{\Omega/bone} \end{aligned} \quad \dots (95)$$

A fatigue life estimation was performed for the designed prosthesis. The strain-life method was adopted for its accuracy and suitability for the loading conditions. Loading variation was considered as full revisers of 10% of the overall maximum strain, linear variated within the simulated biting time. Modeling of the strain-life is calculated as in equation (96)[188].

$$\varepsilon_a = 0.015381572(2N_f)^{-0.095} + 0.35(2N_f)^{-0.69} \quad \dots (96)$$

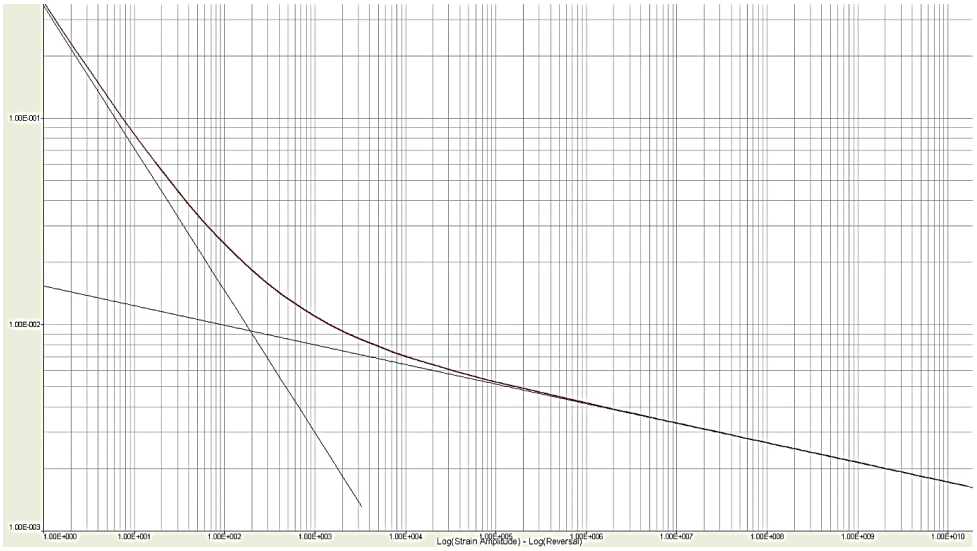

Figure 84 Strain-Life of Ti-6Al-7Nb

Hydrogen embrittlement is a phenomenon that can lower the fatigue life of metallic structure significantly[189-192]. The modeling of hydrogen embrittlement and other interstitial behavior as much as it is effective to lower the fatigue life significantly, it can be considered as a correction factor within the fatigue simulation, so it is not significantly altering topology the fitted fatigue function[193]. The correction factors are not considered in this work. The suggested optimal design procedure started with imaging the case to create a 3D FEM model (Figure 85). In the case of a pre-existing hole, jaw topological similarity can be used to create missing parts within the FEM model.

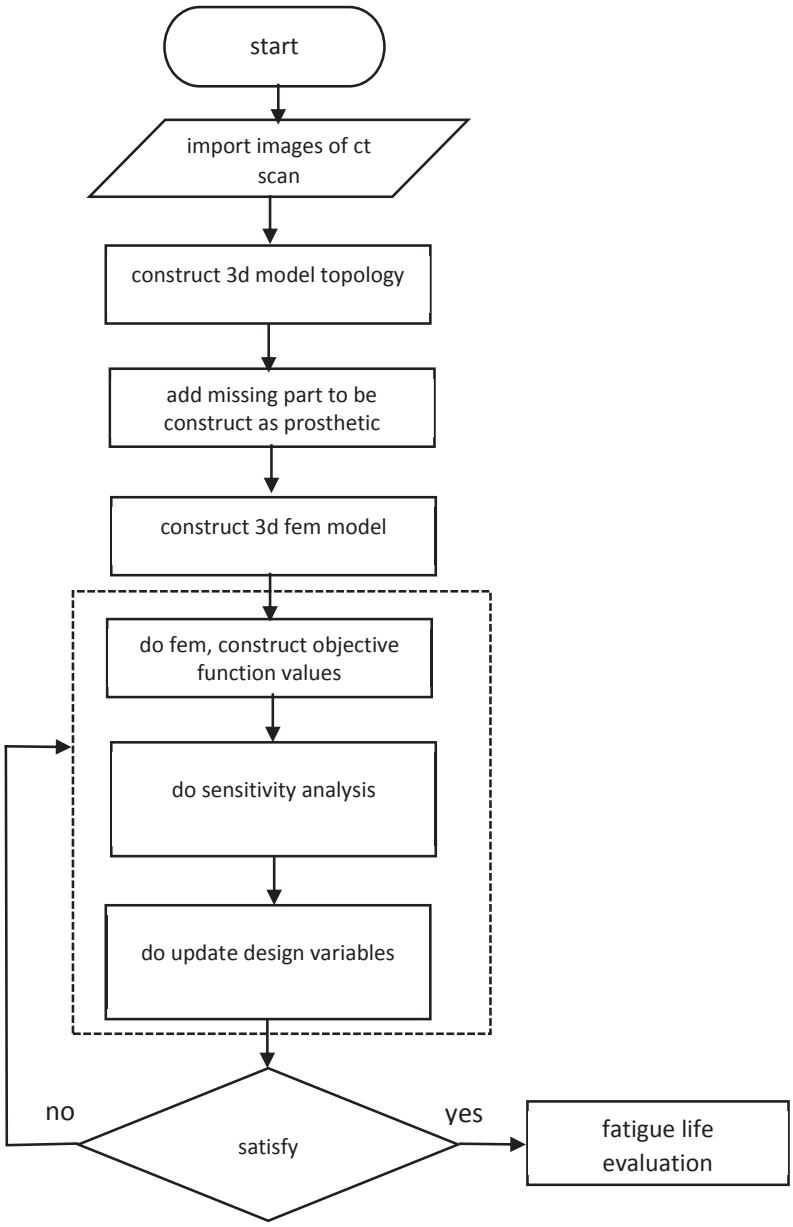

Figure 85 Design and evaluation flow chart

After constructing the topographical model, the dentist will identify the muscular orientation and move on to the non-design domain associated with some desired design features. Topology optimization will be conducted. Finally, fatigue simulation is undertaken as a reference to evaluate the design. Now the design is ready to be 3D printed to use in surgery. The medical and engineering points of view are separated during the

whole process to theoretically maximize the design speed. The FEM design and setting of boundary conditions requires a knowledge of anatomy (major aspects of the organ mechanical boundaries), and topological aspects of making holes for blood vessels or marking dangerous places to be avoided (nerve clusters etc.).

4.2.3. Results

3D design of the design domain was conditioned to approach bone compliance. Different powers of p-norm showed similar results for the chosen volume fraction. Results of the higher power (50) were chosen to ensure approaching (Figure. 86).

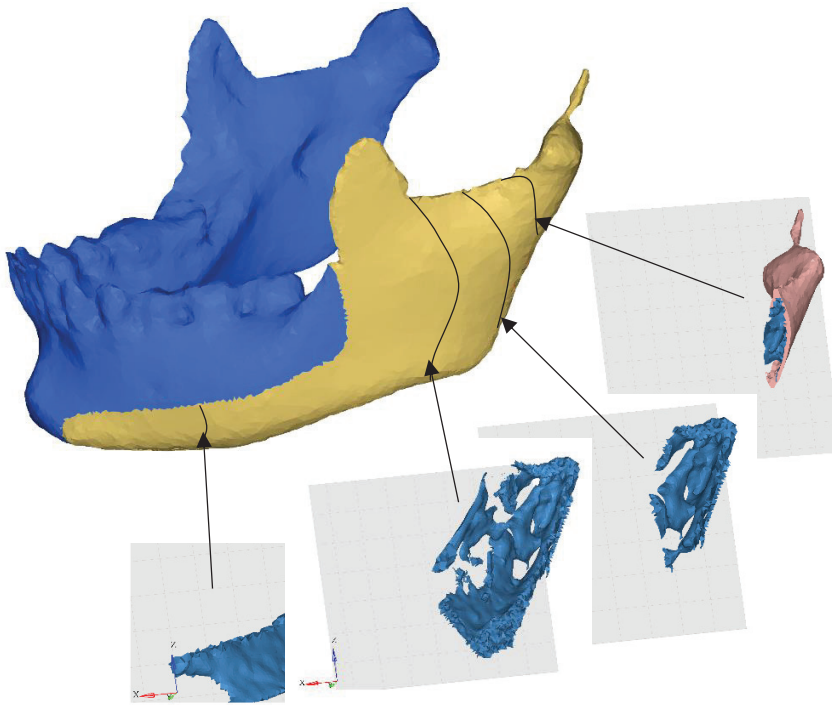

Figure 86 p-norm topology optimization skinned mandible

The objective function history for both objective functions is summarized in Figures 87 and 88. Optimization in the case of SBTO was achieved by minimization of the norm function, while in the case of the compliance objective function, the metallic prosthesis stiffness was minimized by maximizing compliance itself to meet bone

compliance. Figure. 89 shows the location of the maximum von Mises stress within the designed prosthesis.

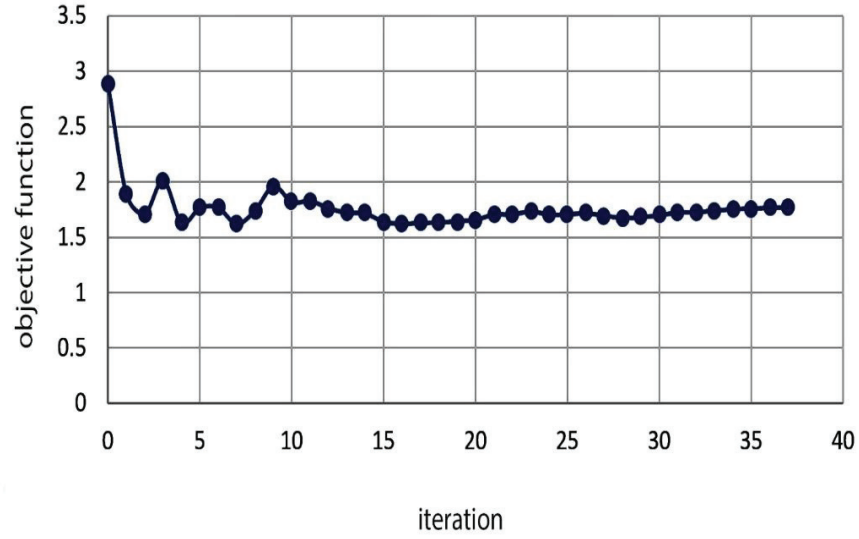

Figure 87 SBTO objective function history

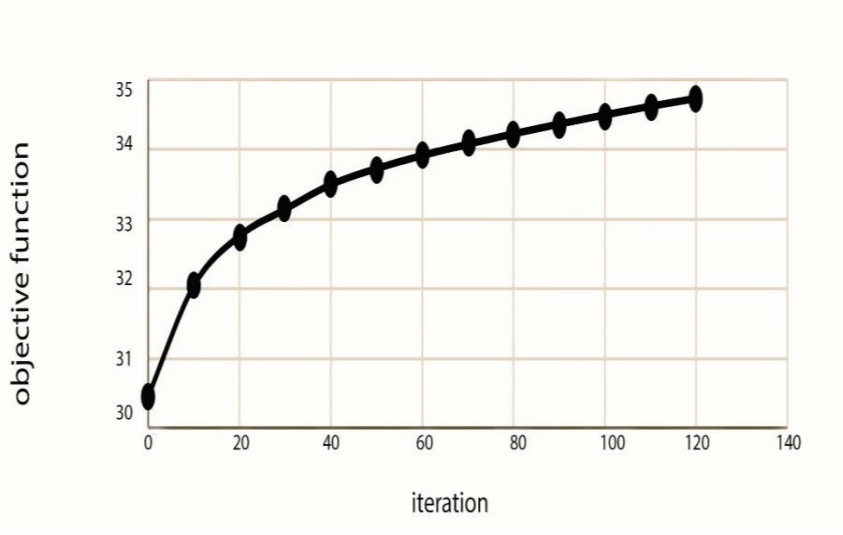

Figure 88 Compliance objective function history

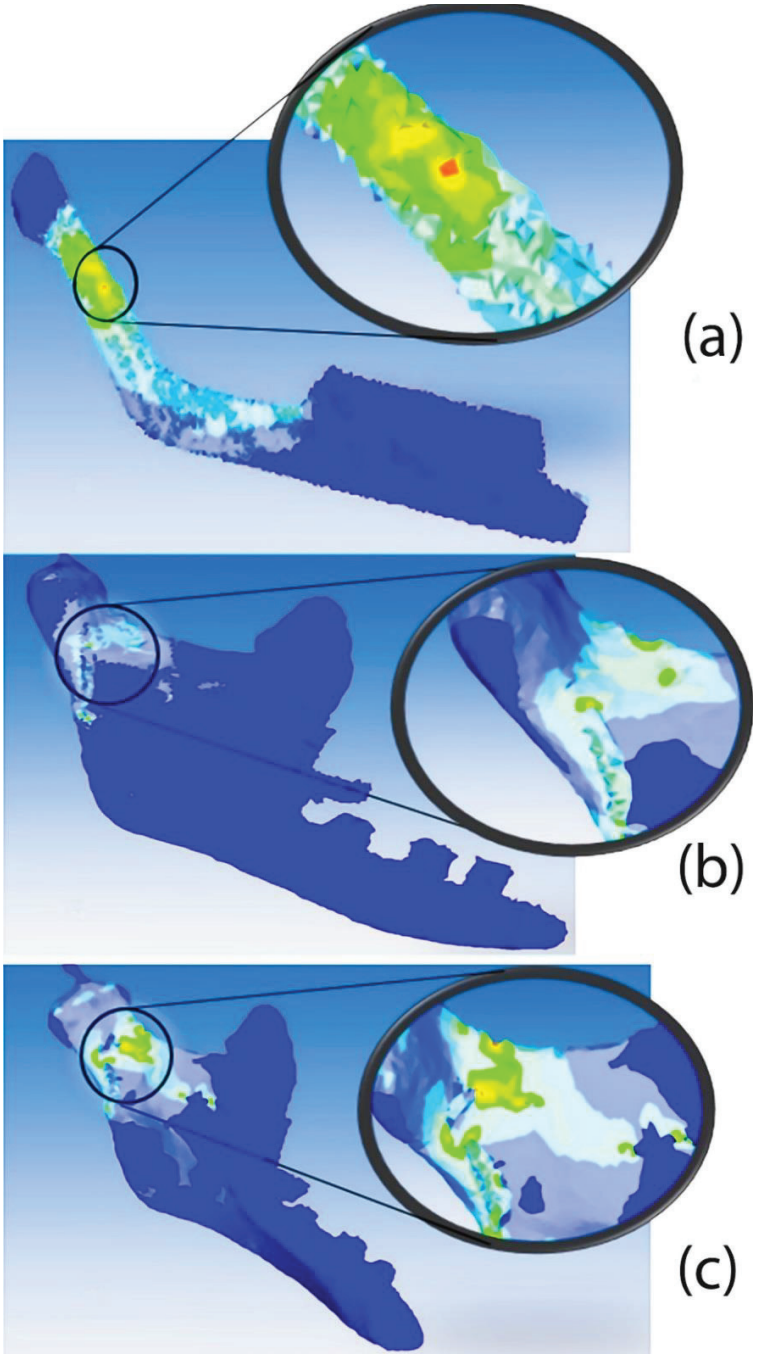

Figure 89 von Mises Stress distribution of the orthopedic designs (a) Maximum von Mises region within the orthodox prosthesis; (b) Maximum von Mises region within topology optimization and compliance-based objective function; (c) Maximum von Mises region within the SBTO-based objective function

Table 14 shows the decrease in life expectancy of the prosthesis implant designed with SBTO compared with the compliance function-based topology optimization. Fatigue assessment based on the strain life approach takes into consideration strain hardening within the complicated shape of the produced design domain.

Table 14 Average fatigue analysis results of the P-norm objective function

case	average life (5% damage) of the artificial mandible
pnorm	2.767E+11 cycle
compliance	3.122E+10 cycle
orthothox design	4.115E+09 cycle

The SBTO design shows almost 100% improvement in life expectancy for the reconstructive prosthesis compared with the orthodox design. However, the orthodox design of the reconstructive prosthesis usually marginalizes stiffness compatibility. This is because of the lack of individuality in general surgical solutions, so in this case, compliance of the orthodox prosthesis is 107.513, and normal bone compliance (34.04). Von Mises Stress Distribution for designed Prosthesis are shown in figures 91, and 92. Figures 93, and 94 show the damage and life prediction

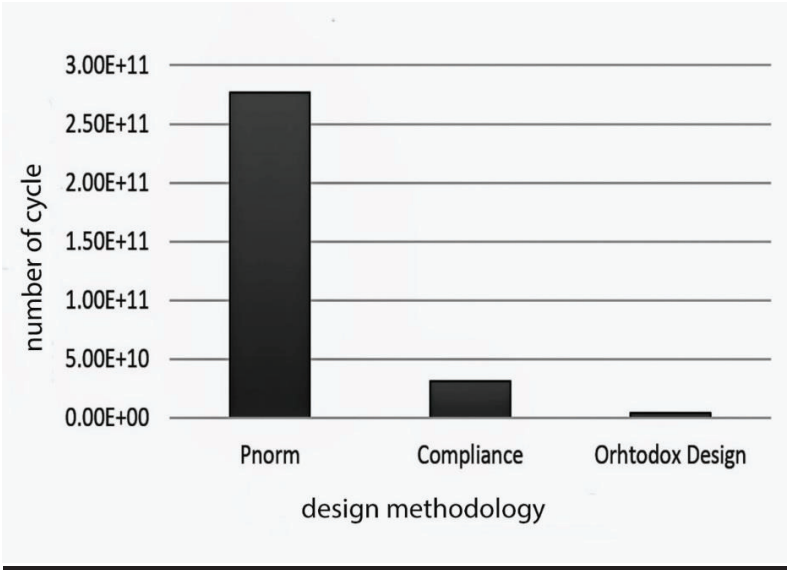

Figure 90 Number of cycles for SBTO, compliance and orthodox designs

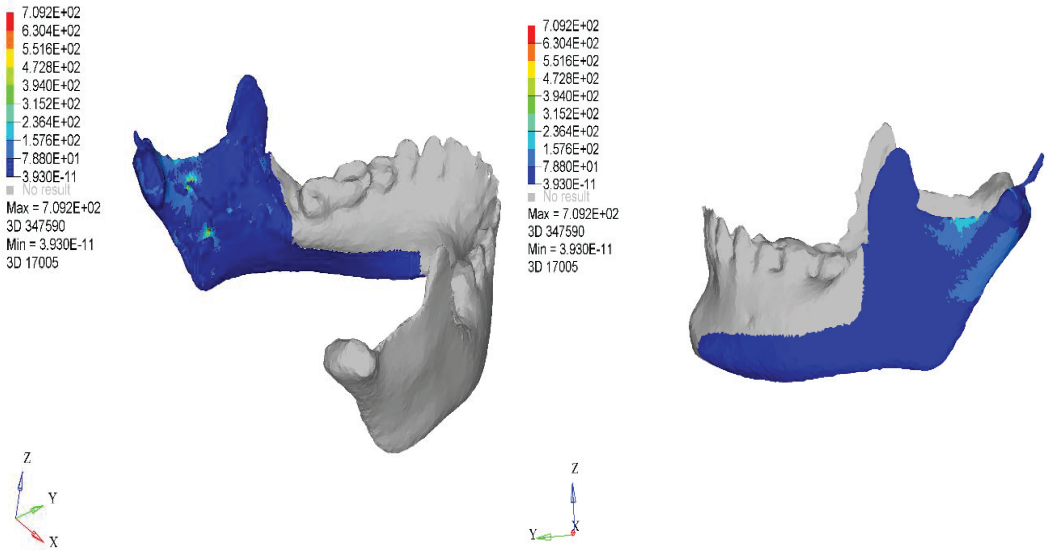

Figure 91 von Mises Stress representation of P-norm topology optimization design.

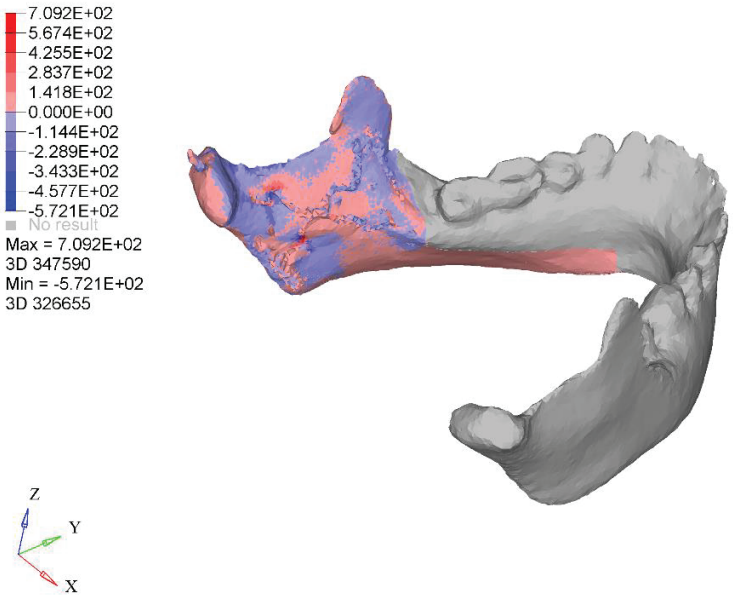

Figure 92 signed von Mises Stress representation of P-norm topology optimization design.

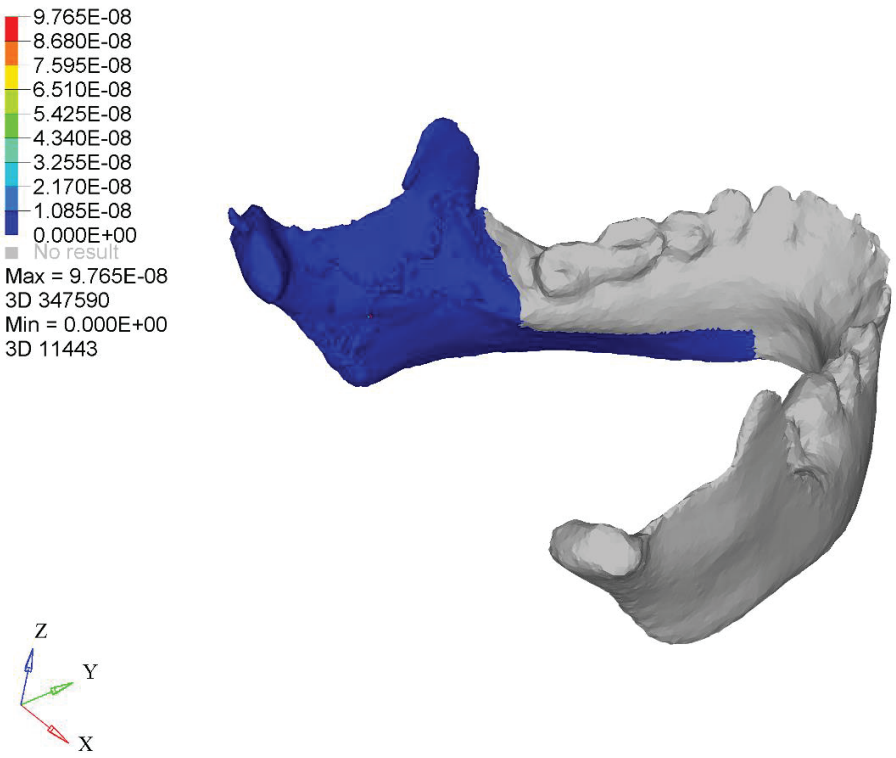

Figure 93 P-norm topology optimization design fatigue damage

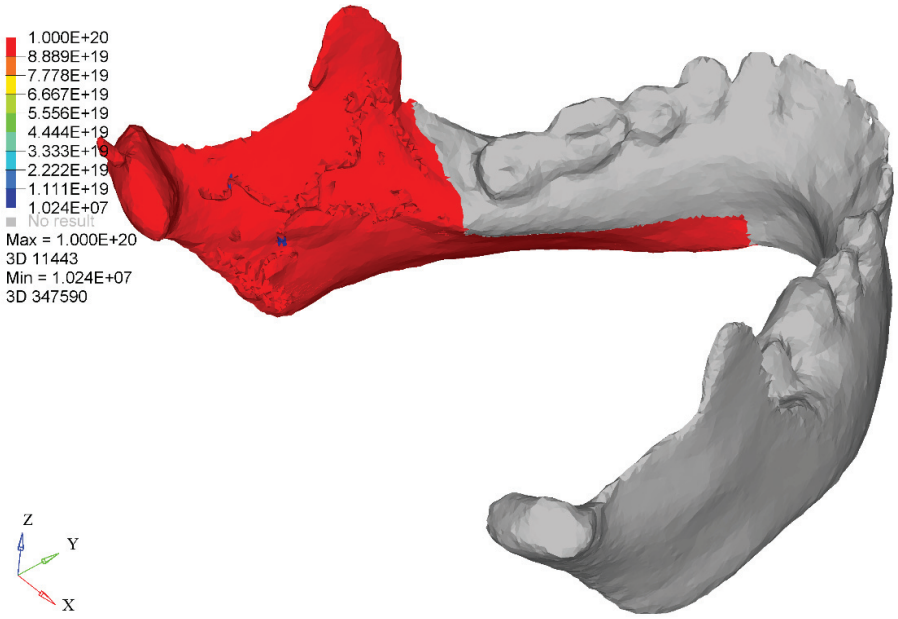

Figure 94 P-norm topology optimization design fatigue life

Osseous tissues functionality varies for its location. For Mandible, Biomechanics and mobility [194-196], are vital for healthy prosthesis. Finite element analysis based on up to date patient Images (such as CT scan) describe actual geometry, and boundary conditions that can set the basis of highly geometrically compatible prosthesis. Suitable occlusion can be achieved also for manufactured prosthesis build based on such constructed 3D model. Prosthesis Design has three major factors, which are Functionality, Compatibility and Aesthetic aspects. Functionality set tissue original major task, i.e. it can be set by the organ to be replace directly, by Imaging process. For Aesthetic Aspect is surgeon issue. It could be considering as surgeon vision of the case in hand which lead to identify secondary non-design region of the implant, which was done in the current work. Matching stiffness as a solution for stress shielding, in the current case, simply means making structure less stiff. SBTO basically tends to maximize stiffness with taking into consecration the important point of applied solid mechanics design, which is order in stress distribution within the boundaries of yield surfaces; in this case, Von- Mises. Large-scale Surgical removal of Tamer such as Osteosarcoma, which needs prosthesis to overcome largescale tissue removing; value time aspect of the process. Optimizing manufacturing time depends on squeezing the period of sequential design process. Pre- and post-operation CT scan which take roughly 20 minutes per process will provide data for image processing. Some software such as Materialise software takes around two hours to produce finite element model as a base of designing and evaluation with high performance standard office computer. Noticing that it depends on integrity of solid state components and Database clarity. Performing optimization needs discussion to identify selective design domain. After setting all topology optimization aspects, running extrema criteria depends on the properties of discretized optimality function.

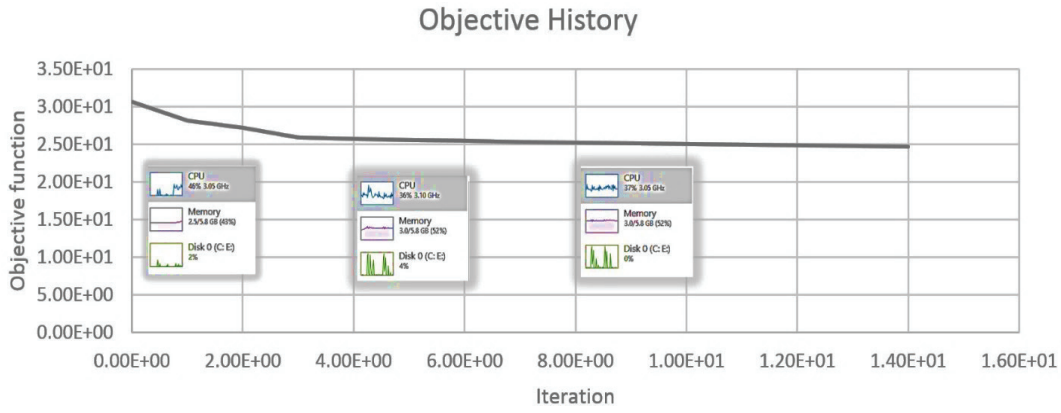

Figure 95 Computer resource consuming during the optimization process

Increasing element number creates more design variables to be addressed especially in case of stress-based function. Averaging method is the key to decrease computational time. The topography of orthopedic is rather difficult to make without additive manufacturing. Laser additive manufacturing could perform SBTO complicated topography. Stress shielding compatibility has been approached by adding original bone compliance as design target associated with decreasing volume of orthopedic alloys in order to decrease its weight. Fatigue results show slightly more life expectation with lower volume fraction. The argument of that is, however stress concentration optimizes within selective design domain; still, compliance condition tends to design to follow stiffness minimization path in order to reach bone compliance condition. This led to complicated shapes which affect fatigue life due to accumulating damage.

4.3. Designing femoral implant using stress based

4.3.1. Stress shielding based optimization

Several works were done to study femoral stem effect in terms of stress distribution of femoral stem [197, 198]. The stem design takes two major tendencies, first one is mechanical design aspects based on size optimization aspects, and the second view is material bone interaction point of view. The optimal size of femoral stem been studied by many researchers for the past few decades. Abdellah Ait Moussa et al [127] studied stress shielding and femoral stem diameter. von Mises stress was the main characteristic stress that was studied. M Reimeringer et al [199] studied the mechanical immobility improvement in terms of stem length. MY Shishani et al [200] studied the length factor of the stem in the bone. The second design point view gained increasing attention in the recent decades. D R Sumner et al [100], studied material tissue interaction, the recommendation of porous coating of matching material was introduced. van Rietbergen et al [198] studied material selection option by introducing bone-friendly material coating to the stem surface. F schmidutz et al [201] introduced ceramic outer shell as stem design. Considering mechanical structure biocompatibilities, Stress shielding is an important topic which can be controlled by mechanical properties matching.

4.3.2. Mathematical meddling and optimization

Total hip replacement is performing due to hip deterioration [202, 203]. Hip replacement divided into two major mechanical structures, the femoral head which

concerned more with the tribological aspect is the drive of the design, and the femoral stem, which supports the body load on the femur and distributed within inner space of femoral cavity. However, in this study, tribological loads are not been considered. Figure. 96 shows the model used in this study. The first step is applying topology optimization to design the stem for minimizing bone stress induced by the stem bone interaction. Topology optimization design is done using the following design strategy-

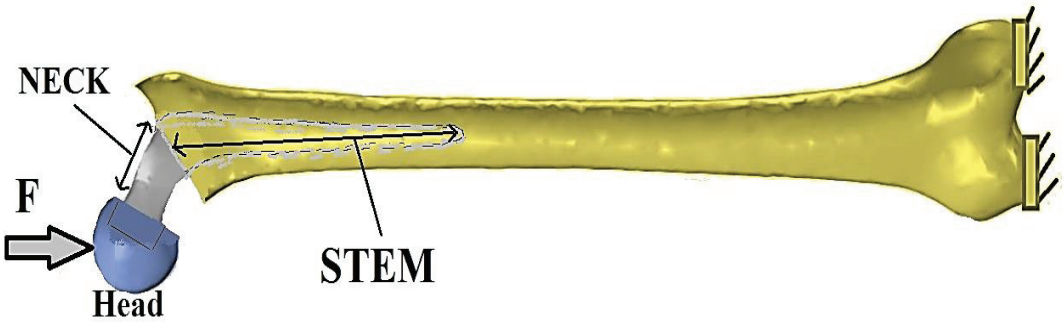

Figure 96 Femoral implant simulation

4.3.3. SIMP topology optimization

Topology optimization will be performed directly for the density function which is penalized to power 3. The p-norm function is used to minimize the bone Sant Venant stress. This is to minimize bone degeneration (equation (75)). The objective function that used in topology optimization is shown in equation (97). The volume fraction is set to be 40% of the original volume. This is to reduce the weight of the implant.

$$\begin{aligned} &find \quad \rho \\ &\min \left\| \sigma_{U\max} \right\| \\ &s.t. \quad \int_{\Omega_d} \rho d\rho \le V_d \quad , 0 < \rho_{\min} \le \rho \le 1 \quad \forall \rho \in \Omega_d \end{aligned} \qquad \ldots (97)$$

Conformal lattice structure method is performed for the objective function shown in equation (97). After identifying the truss locations, another optimization is performed to find out individually, the best truss cross-section in the overall design. The problem is simulated using tetrahedral, first-order mesh using OptiStruc solver. The material in use is Titanium alloy (Ti-6Al-7Nb).

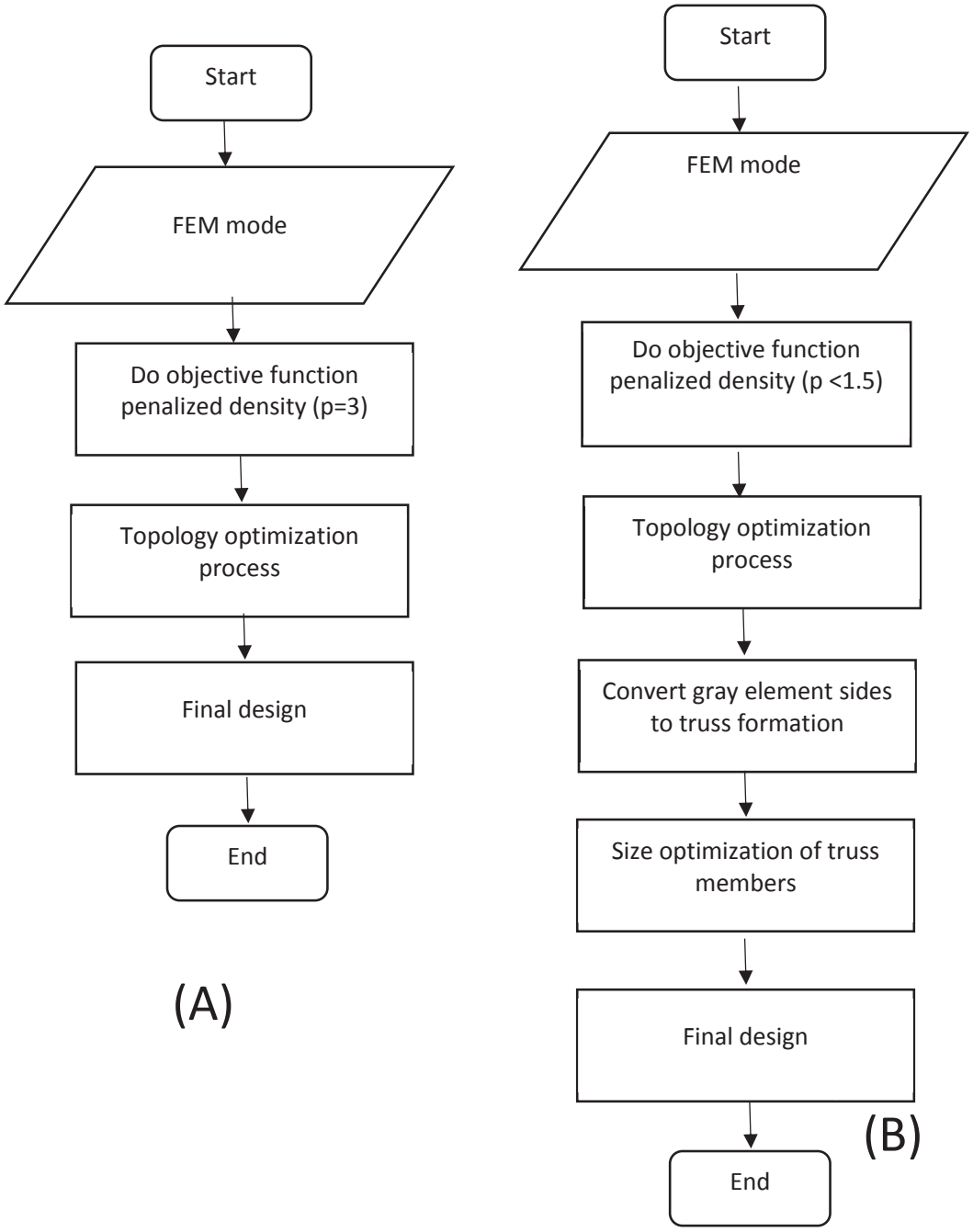

Figure 97 Femoral case design algorithms. (A) Topology optimization process. (B) conformal lattice structure process

4.3.4. Results

The numerical example as the following. Femoral loading is 600 newtons. CLS- topology optimization is performed in two stages, the first trail is to identify the gray area elements, then followed by the second trail which is optimizing truss links cross-section. Figure. 99. Showed the objective history of the optimization processes (First Stage of CLS). Figure. 99 also is the final design objective history of CLS. The p-norm method is also performed to achieve an optimal design. Table 15 shows the stress in the bone for the designed methodologies. Table 15 showed the prevailing of p-norm optimization comparing to CLS design. SIMP design showed better results regarding inducing stress shielding. Volume fraction of the designed cases is 40%. Stress shielding is being anticipated for the higher stress of the bone that was imposed by the implant. However, the tribological aspects are not been addressed in the optimization process, but the results showed the tendency of averaging stress method (p-norm, functions) to produce good results, due to function convexity.

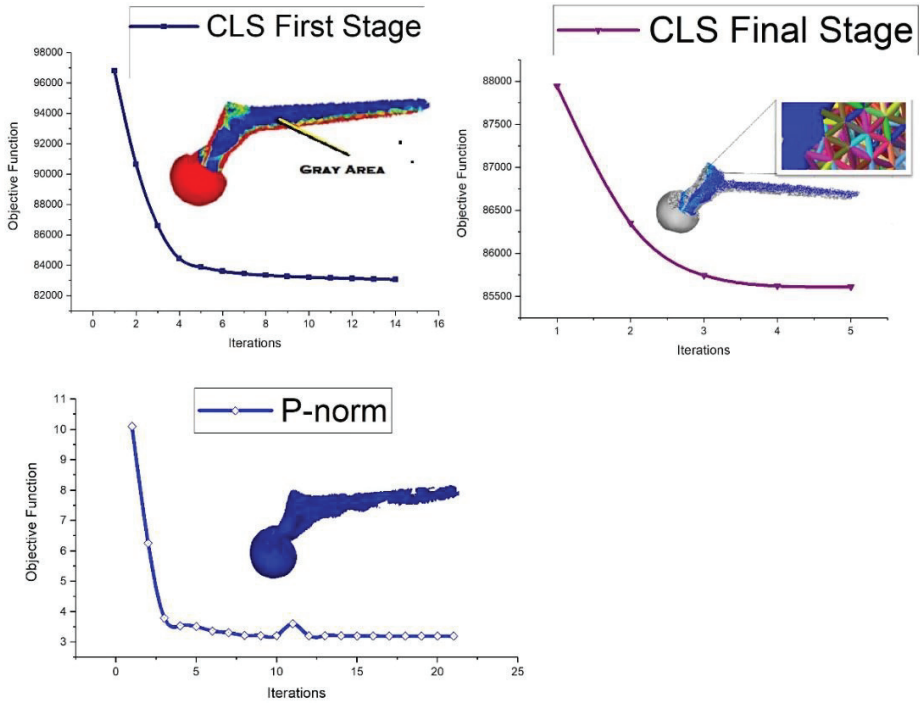

Figure 98 Objective function history of pre-CLS based topology optimization, final CLS stage, and p-norm topology optimization

Table 15 Bone stress for the designed methodologies

Model	Maximum octahedral stress in the bone (N/mm^3)	Volume fraction 100%
Non-optimized case	7.103e2	100%
CLS optimized case	1e3	40%
p-norm optimized case	1.533e2	40%

4.4. Surface enhancement of rapid prototyping orthopedic

Additive manufacturing is the desired method of computer-aided manufacturing of producing the customized. Energy beams- metallic powder interaction is the most addressed method by companies and laboratories. Particle size[204], beam type[205], and related interaction aspects are been studied[206, 207]. The surface roughness of the additive manufactured parts has to opposites consideration in biomedical applications. In term of implant stability, the surface roughness is a desired aspect. That is because it is anticipated increase the strength of implant-bone integration. Mechanically, a rough surface is a rich culture of crack nucleation. This will impact fatigue life in a negative way. Form the above, surface roughness should be high for a medical reason and should be low for a mechanical reason. The following work is discussing Method of surface roughness modification using electrochemical polishing. The reason of that is; If the implant surface roughness can be tuned with the controlled additional process, it can be customized for the selective bone to match the cell cluster size (so, cell cluster in the mandible is different than for femur). Electrochemical polishing is chosen for three reasons. The first ration is it can be done in the inner surfaces for complex orthopedics, such as scaffolds due to electrolyte infiltration. The second reason is it can be easily controlled and tuned comparing to chemical etching. The final reason is the idea of adding material to the implant will theoretically increase the length of the crack journey to be harmful, add to that filling the hidden manufacturing faults.

4.4.1. Electroplating principal

Electrochemical cell is used for metallic surface modification for a various application[208]. The electrochemical cell is consisting of an electrolyte, anode, and cathode. It is a reverse of galvanic cell concept, such that the chemical action is been induced by electric current. Electrochemical surface modification can be done by two opposite methods. One is by extracting the ions from the target workpiece and precipitate it on a target. The other method is by precipitate layers of metallic ions on the workpiece by set it the cathode. The plating is biomechanically desired for orthopedics, so the material will slightly increase in size which theoretically increase the lifespan of fatigue to grow. The second desired point is that it is easy to control material precipitation in order to control the smoothness of the surface asperities. The purpose is to have matching of surface roughness with the bone cluster formation. The optimal of surface roughness matching is differ for the various bones for the same patient. This work is not considering the tribo-medical matching; however, it is a study of the ability to simulate the surface modification by plating in order to have accurate surface cell setting for the futuristic medical application.

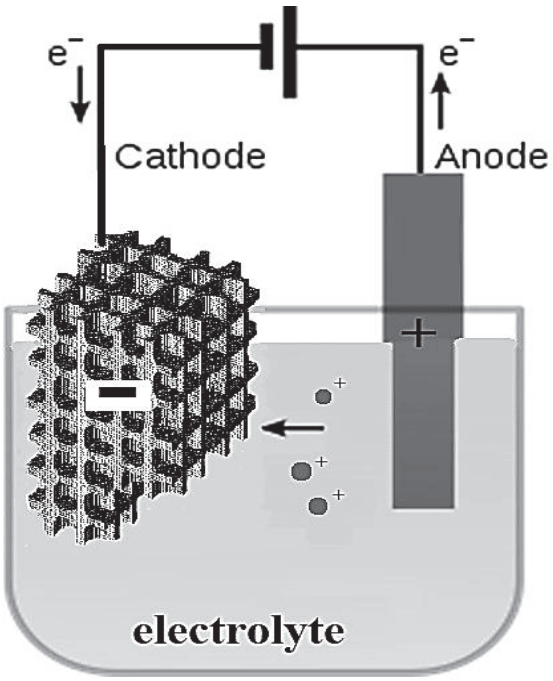

Figure 99 Electrochemical polishing by precipitation

4.4.2. Electrochemical polishing process simulation

Surface finish plays important role in mechanical stability and life expectations. Small inclusions lead to maximize stress filed within small size leading to localized deformations, crack propagation till final failure. Although, implants surface roughness is used to intersect within surrounding tissue, making better fixation in order to speed up healing process; some researchers show some desired characteristics of the smooth surface implant [209]. One of the cheap and considerably stress-free methods is an electrochemical polishing process. Electrochemical is the process of surface modification to reduce surface roughness, by dissipation of metals within design electrochemical cell. The unit cell is usually consisting of three major parts, which are, the workpiece, the precipitation source, and the transfer media (electrolyte). Electrolyte composition plays an important role in the speed of playing, purity, and homogeneity [210]. An electric source is needed to extract the molecules from the source to the substrate. The speed of this process control mainly by current density. Current density value should be applied carefully, so for high values, inhomogeneous precipitation and in severe cases, the undesired chemical reaction can happen, which damage the substrate. The arbitrary Lagrangian-Eulerian (ALE) [211, 212]finite element formulation is used to simulate the problem. Underestimation of current density value could not give the desired results making the process inefficient. Determining material precipitation rate can be modeled by acquiring the depletion redelegation rate is been considered as the proportional relation between material freed from the anode and the current density, which is the characteristic of electrolyte and chemical cell design configuration. The updated velocity U of ALE is proportional to the normal current density of the cell ($I.\bar{n}$).

$$U = C.I.\bar{n} \quad \ldots (98)$$

The coefficient of proportionality C can be calculated from

$$C = \frac{m}{\mathbb{C}\rho N} \quad \ldots (99)$$

Here, m is atomic mass of the targeted material. $\mathbb{C}$ is Faraday's constant, ρ is the targeted material density, and N is valence number of the targeted material. The simulation was done for the simple 2D case in order to evaluate the effectiveness of electrochemical

polishing by adding layers of materials. The additive process is being anticipated to decrease the severity of sharps inclusions which is done by 3D printing process. The domain is shown in Figure 100 A. Two holes were cut in the domain, circular shape with two depths, 0.15mm and 0.3 mm. The addressing area of polishing is the inners walls. The outer sides of the cells are simulated to be hold by conducting gripper (Ground surfaces) Figure. 100B shows a cell without cutting howls in general formation of grounding. So, the cellular structure is assumed to be gripped from the outer boundaries, so the inner cells have internal ground points. $\mathbb{C}$ is being calculated as 1.69×10^{-10} m^3/A.s..

4.4.3. Simulated Example

Simple unite cell design is been chosen as the testing model. The simple cell study is being divided into two categories. Category one is to study the smoothness ability of electrochemical polishing on smoothing grove inside the inner wall of the cell. The second case is to study the overall smoothing of the cell especially the sharp angles of inclusions.

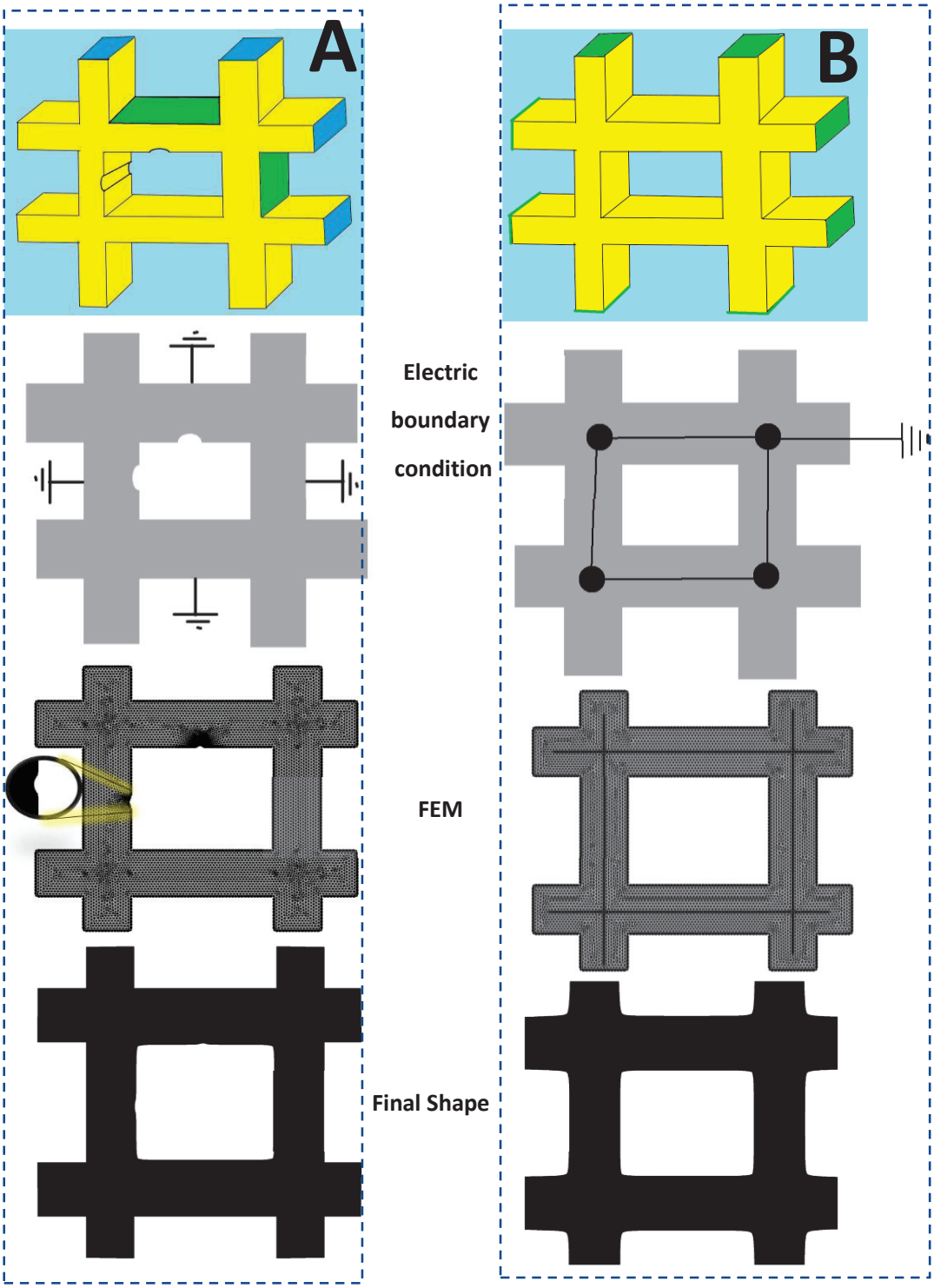

Figure 100 case study of electropolishing model using ALE. Case A is the process of smoothing inclusion inside the lattice. Case B is the smoothing of the lattice shape angles.

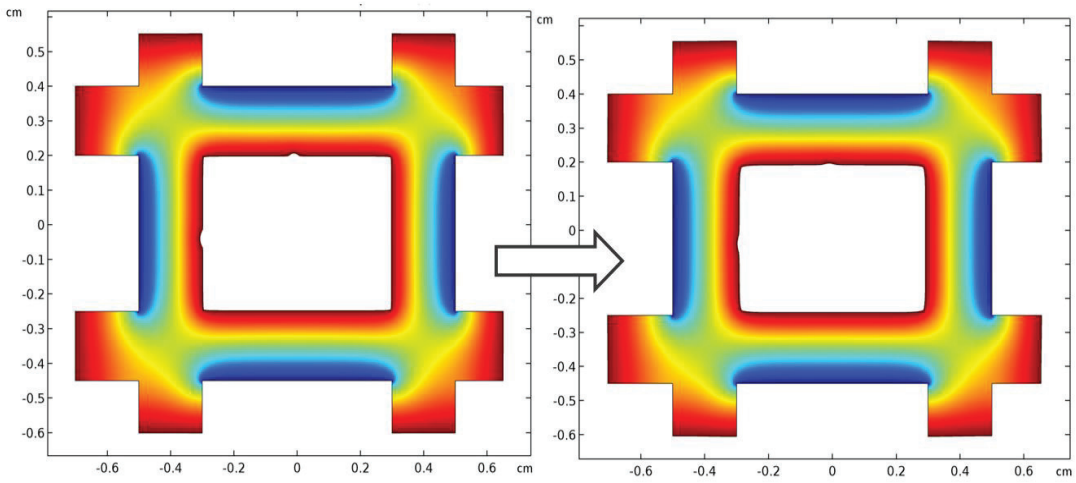

Figure 101 Electropolishing simulation of case A.

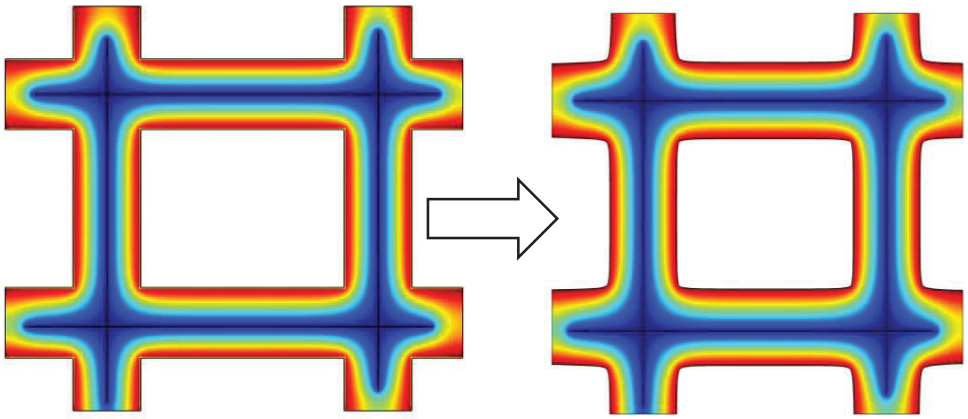

Figure 102 Electropolishing simulation of case B

Table 16 Maximum von Mises stress reduction of case A, and B

Case	Before polishing (N/m^2)	After polishing (N/m^2)	% Change
Case A	0.022197	0.022197	3.8677E-09
Case B	0.022206	0.022161	0.20261362

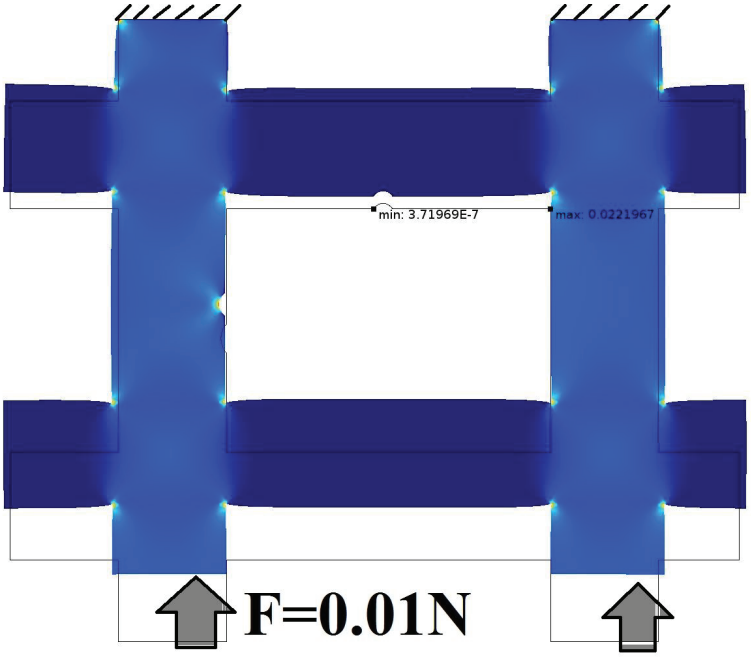

Figure 103 von Mises stress of Case A Before smoothing

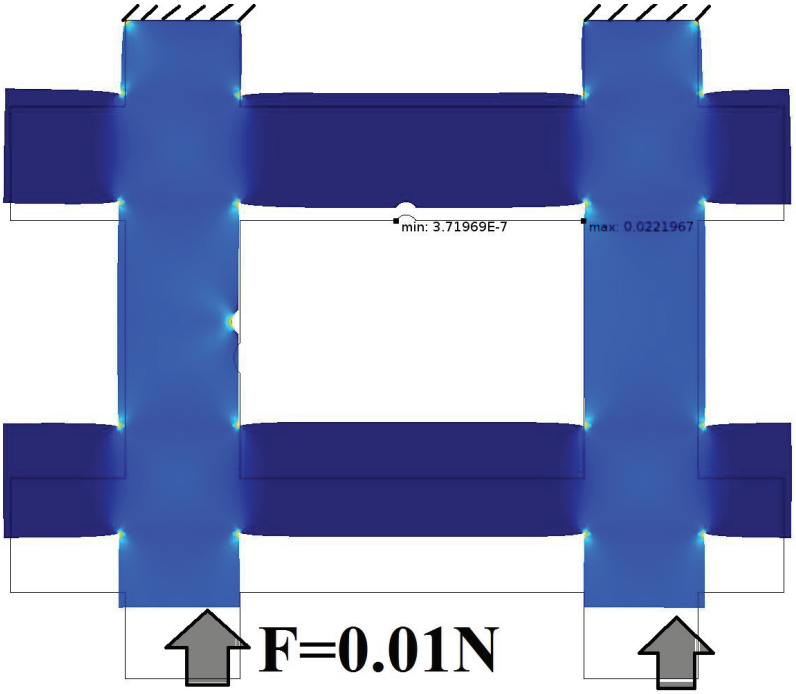

Figure 104 von Mises stress of Case A after smoothing

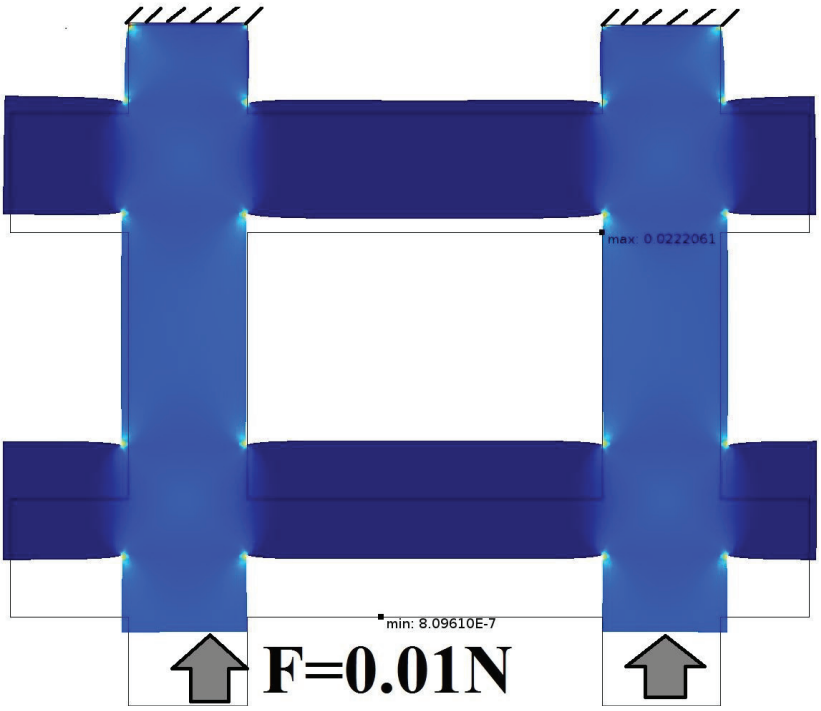

Figure 105 von Mises stress of Case B before smoothing

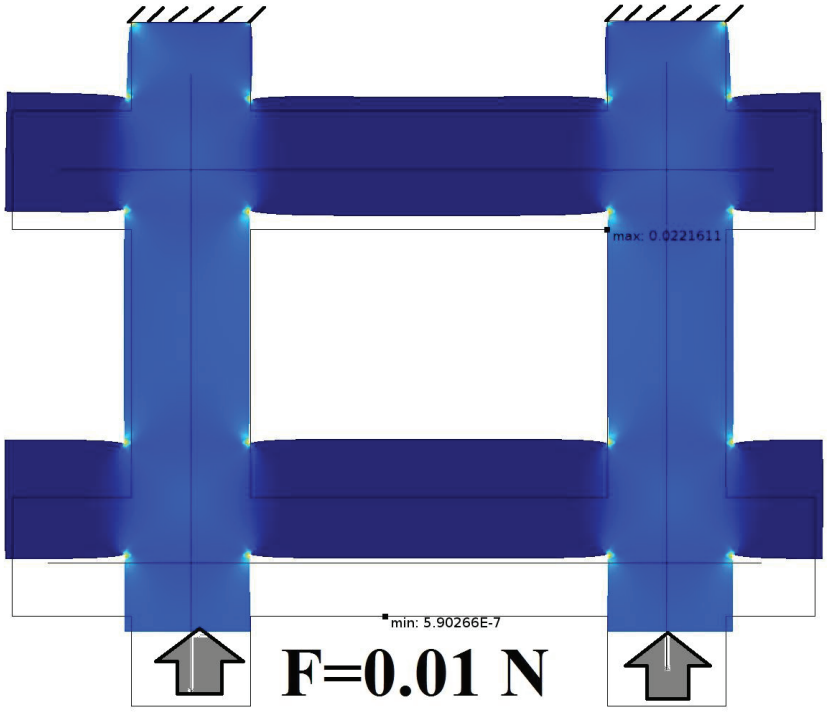

Figure 106 von Mises stress of Case B After smoothing

Chapter 5: Conclusion, and recommendations

5.1. The following remarks are summarizing the research experience

1- Osseointegration failure in long term perspective is the main issue of the orthopedic problem. This problem is translating in terms of Wolfs law as Stress shielding problem.
2- Stress shielding approached by the two approaches, first one is by matching the stiffens of the bone and the designer orthopedic. Second approach is by minimizing the strain energy inside the bone that is induced by the orthopedic for the loading condition.
3- Topology optimization is more suitable as a methodology for designing prosthesis as Shape optimization.
4- Normative function of a verging stress showed stability, and good results in term of shape and fatigue life expectation
5- Topology optimization gives the ability to produce complicated design that satisfy both the aesthetic aspect of the design, as well as stress shielding minimization.
6- Conformal lattice structure gave less stress shielding compatibility (the second stress shielding approach) than pnorm function.
7- Fatigue life is being anticipated to increase with using electropolishing, especially for scaffold and small parts with inclusions.
8- Surface matching possibility of the orthopedic can be achieved using electropolishing.

5.2. Toward fully custom orthopedic design algorithm

It has been noted that in case of disasters, the triage is adopted. Triage is the process of classification of the patient degree of attention and consumes medical resources in order to increase the survivability rate. The advancement in civil engineering, transportation engineering, and warfare technology have maximized the rate of potential patients and the severity of the expected injuries. In many cases, the medical advancement

and resources have proven to be a no match for the number of casualties that it should be saved. The technology or rapid prototyping associated with advanced CAD-CAM are completely enveloped and segregated from the biological experience due to the claim of specialty. The work intended to fill that gap by envisaging the two minds, i.e. the doctor mind and the engineers mined to produces a nucleation of the practical solution to be used. Osseointegration is vital for the bone implant. For short term, it needs the surface roughness associated with aesthetic constraints. For long-term, it needs the minimization of stress shielding problem. Figure.107 is an algorithm to satisfy the two targets for the fully customized orthopedic solution.

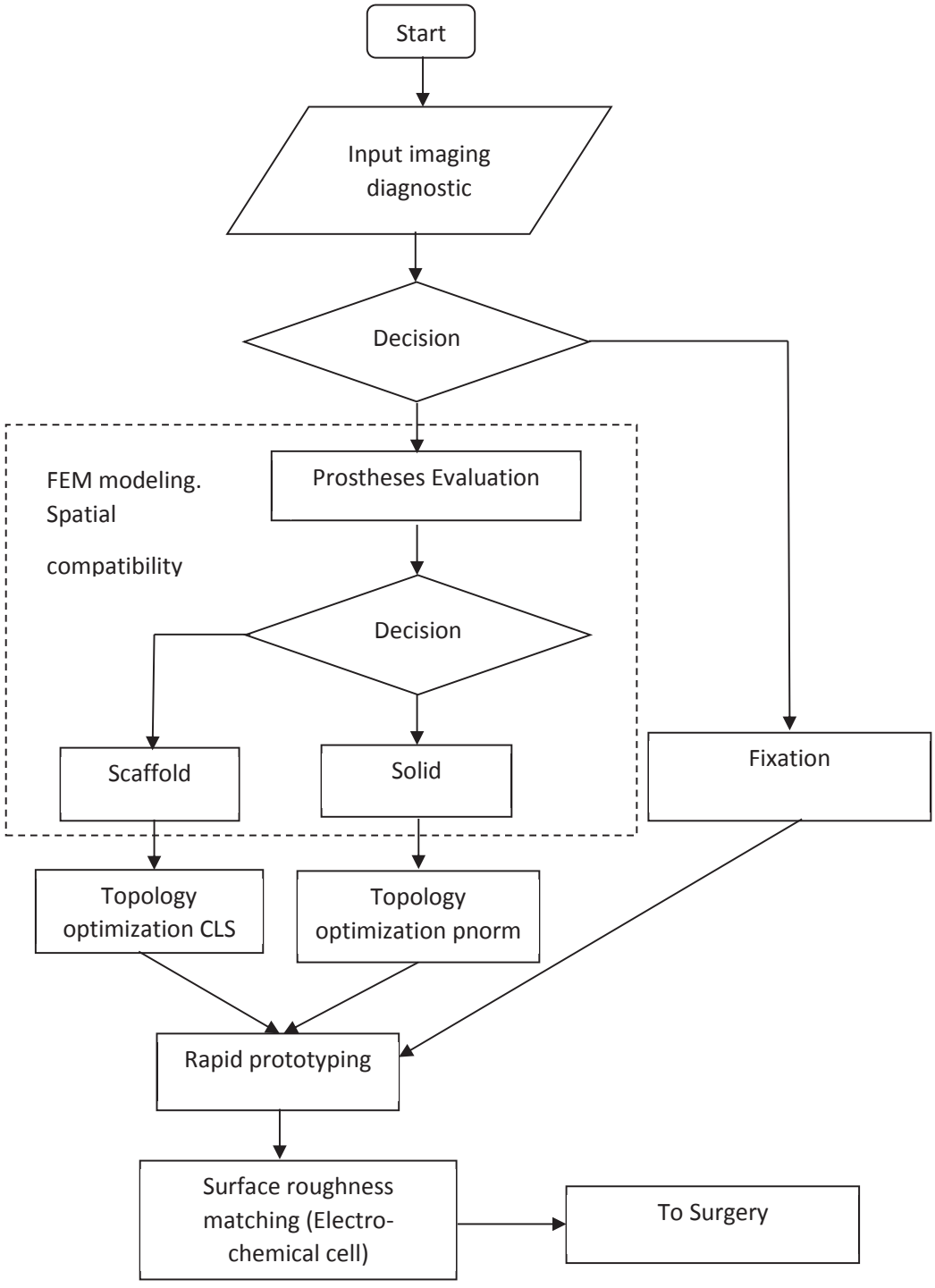

Figure 107 The algorithm of Fully custom rapid orthopedic part design and manufacturing for the best osseointegration

5.3. Recommendations for future work

1- Triobological loading associated with shape optimization.
2- Robust topology optimization of the orthopedic with no design domain stiffness uncertainty.
3- Robust topology optimization of the orthopedic under loading uncertainty.
4- Tribo-fatigue investigation and modeling orthopedic materials.
5- Investigate the significance of surface roughness measurements indices with Osseointegration for various orthopedic material systems.
6- Multiobjective function Topology optimization.

References:

[1] J. M. Lane and H. Sandhu, "Current approaches to experimental bone grafting," *The Orthopedic clinics of North America,* vol. 18, pp. 213-225, 1987.

[2] M. Atinga, R. Gregor, K. M. Selvaraj, and T. F. Hong, "Os acromiale open reduction and internal fixation: a review of iliac crest autogenous bone grafting and local bone grafting," *Journal of shoulder and elbow surgery,* 2018.

[3] E. E. Zaidenberg, E. Martinez, and C. R. Zaidenberg, "Vascularized Distal Radius Bone Graft for Treatment of Ulnar Nonunion," *The Journal of Hand Surgery,* 2018/04/09/ 2018.

[4] P. F. Horstmann, W. H. Hettwer, and M. M. Petersen, "Natural Course of Local Bone Mineralization After Treatment of Benign or Borderline Bone Tumors and Cysts With a Composite Ceramic Bone Graft Substitute," *Journal of Clinical Densitometry,* 2018/03/23/ 2018.

[5] D. C. Ackland, D. Robinson, M. Redhead, P. V. S. Lee, A. Moskaljuk, and G. Dimitroulis, "A personalized 3D-printed prosthetic joint replacement for the human temporomandibular joint: From implant design to implantation," *Journal of the Mechanical Behavior of Biomedical Materials,* vol. 69, pp. 404-411, 2017.

[6] A. Bertram and R. Glüge, "Introduction to tensor calculus," in *Solid Mechanics*, ed: Springer, 2015, pp. 43-120.

[7] E. J. Hearn, *Mechanics Of Materials, vol. 2: An Introduction to the Mechanics Of Elastic and Plastic Deformation Of Solids and Structural Components*: Pergamon, 1985.

[8] E. C. Bingham, *An investigation of the laws of plastic flow* vol. 13: Govt. Print. Off., 1917.

[9] R. A. Higgins, *Engineering metallurgy*: E. Arnold, 1993.

[10] L. R. Alejano and A. Bobet, "Drucker–Prager Criterion," *Rock Mechanics and Rock Engineering,* vol. 45, pp. 995-999, 2012.

[11] S. Kocanda, "Fatigue failure of metals," 1978.

[12] A. Head, "XCVIII. The growth of fatigue cracks," *The London, Edinburgh, and Dublin Philosophical Magazine and Journal of Science,* vol. 44, pp. 925-938, 1953.

[13] M. P. Bendsoe and O. Sigmund, *Topology optimization: theory, methods, and applications*: Springer Science & Business Media, 2013.

[14] J. Bannantine, "Fundamentals of metal fatigue analysis," *Prentice Hall, 1990,* p. 273, 1990.

[15] K. Walker, "The effect of stress ratio during crack propagation and fatigue for 2024-T3 and 7075-T6 aluminum," in *Effects of environment and complex load history on fatigue life*, ed: ASTM International, 1970.

[16] J. Collipriest Jr, "An experimentalist's view of the surface flaw problem," *Paper from" The Surface Crack- Physical Problems and Computational Solutions", ASME, New York. 1972, 43-61.,* 1972.

[17] R. C. Juvinall, *Engineering considerations of stress, strain, and strength* vol. 66: McGraw-Hill New York, 1967.

[18] K.-T. Cheng and N. Olhoff, "An investigation concerning optimal design of solid elastic plates," *International Journal of Solids and Structures,* vol. 17, pp. 305-323, 1981.

[19] G. I. Rozvany, *Topology optimization in structural mechanics* vol. 374: Springer, 2014.

[20] G. Bohm, *Pressure vessels and piping: design and analysis; a decade of progress* vol. 1: American Society of Mechanical Engineers, 1972.

[21] E. Hearn, "Mechanics of Materials. Vols. 1-2," *Pergamon Press, Headington Hill Hall, Oxford OX 3 0 BW, UK, 1985.,* 1985.

[22] J. E. Shigley, *Shigley's mechanical engineering design*: Tata McGraw-Hill Education, 2011.

[23] N. Saintier, G. Cailletaud, and R. Piques, "Multiaxial fatigue life prediction for a natural rubber," *International Journal of Fatigue,* vol. 28, pp. 530-539, 2006.

[24] W. Mars and A. Fatemi, "A literature survey on fatigue analysis approaches for rubber," *International Journal of fatigue,* vol. 24, pp. 949-961, 2002.

[25] A. Fatemi and L. Yang, "Cumulative fatigue damage and life prediction theories: a survey of the state of the art for homogeneous materials," *International journal of fatigue,* vol. 20, pp. 9-34, 1998.

[26] R. P. Janssen, L. E. Govaert, and H. E. Meijer, "An analytical method to predict fatigue life of thermoplastics in uniaxial loading: sensitivity to wave type, frequency, and stress amplitude," *Macromolecules,* vol. 41, pp. 2531-2540, 2008.

[27] R. P. Janssen, D. de Kanter, L. E. Govaert, and H. E. Meijer, "Fatigue life predictions for glassy polymers: a constitutive approach," *Macromolecules,* vol. 41, pp. 2520-2530, 2008.

[28] J. Snyman, *Practical mathematical optimization: an introduction to basic optimization theory and classical and new gradient-based algorithms* vol. 97: Springer Science & Business Media, 2005.

[29] L. Meirovitch, *Fundamentals of vibrations*: Waveland Press, 2010.

[30] C. M. Harris and A. G. Piersol, *Harris' shock and vibration handbook* vol. 5: McGraw-Hill New York, 2002.

[31] C. T. Kelley, *Iterative methods for optimization*: SIAM, 1999.

[32] A. P. Boresi, R. J. Schmidt, and O. M. Sidebottom, *Advanced mechanics of materials* vol. 6: Wiley New York, 1993.

[33] R. Courant, "Variational methods for the solution of problems of equilibrium and vibrations," *Bulletin of the American mathematical Society,* vol. 49, pp. 1-23, 1943.

[34] J. N. Reddy, *An Introduction to Nonlinear Finite Element Analysis: with applications to heat transfer, fluid mechanics, and solid mechanics*: OUP Oxford, 2014.

[35] A. Bermúdez, R. Durán, M. Muschietti, R. Rodríguez, and J. Solomin, "Finite element vibration analysis of fluid–solid systems without spurious modes," *SIAM Journal on Numerical Analysis,* vol. 32, pp. 1280-1295, 1995.

[36] G. Mur, "Edge elements, their advantages and their disadvantages," *IEEE transactions on magnetics,* vol. 30, pp. 3552-3557, 1994.

[37] J. Webber, "An Introduction to the Finite Element Method. Reddy JN. McGraw-Hill Book Company, London. 1984. 495 pp. Diagrams.£ 27.25," *The Aeronautical Journal,* vol. 88, pp. 147-147, 1984.

[38] B. Ramaswamy, M. Kawahara, and T. Nakayama, "Lagrangian finite element method for the analysis of two-dimensional sloshing problems," *International Journal for Numerical Methods in Fluids,* vol. 6, pp. 659-670, 1986.

[39] A. Laadhari and G. Székely, "Eulerian finite element method for the numerical modeling of fluid dynamics of natural and pathological aortic valves," *Journal of Computational and Applied Mathematics,* vol. 319, pp. 236-261, 2017.

[40] J. Donea, A. Huerta, J.-P. Ponthot, and A. Rodriguez-Ferran, "Encyclopedia of Computational Mechanics Vol. 1: Fundamentals., Chapter 14: Arbitrary Lagrangian-Eulerian Methods," ed: Wiley & Sons, 2004.

[41] G. Rozvany, "Topology optimization in structural mechanics," *Structural and Multidisciplinary Optimization,* vol. 21, pp. 89-89, 2001.

[42] H. L. Cox, *The Design of Structures of Least Weight: International Series of Monographs in Aeronautics and Astronautics: Solid and Structural Mechanics* vol. 8: Elsevier, 2014.

[43] J. C. Maxwell, *The Scientific Papers of James Clerk Maxwell* vol. 2: University Press, 1890.

[44] A. G. M. Michell, "LVIII. The limits of economy of material in frame-structures," *The London, Edinburgh, and Dublin Philosophical Magazine and Journal of Science,* vol. 8, pp. 589-597, 1904.

[45] G. Hegemier and W. Prager, "On michell trusses," *International Journal of Mechanical Sciences,* vol. 11, pp. 209-215, 1969.

[46] D. C. Drucker and R. Shield, "Design for Minimum Weight," BROWN UNIV PROVIDENCE RI1956.

[47] A. Chan, "The design of Michell optimum structures," College of Aeronautics Cranfield1960.

[48] D. L. Bartel, "Optimum design of spatial structures," IOWA UNIV IOWA CITY DEPT OF MECHANICS AND HYDRAULICS1969.

[49] D. Charrett and G. Rozvany, "Extensions of the Prager-Shield theory of optimal plastic design," *International Journal of Non-Linear Mechanics,* vol. 7, pp. 51-64, 1972.

[50] G. Rozvany and W. Prager, "Optimal design of partially discretized grillages," *Journal of the Mechanics and Physics of Solids,* vol. 24, pp. 125-136, 1976.

[51] M. Rossow and J. Taylor, "A finite element method for the optimal design of variable thickness sheets," *Aiaa Journal,* vol. 11, pp. 1566-1569, 1973.

[52] M. P. Bendsøe and N. Kikuchi, "Generating optimal topologies in structural design using a homogenization method," *Computer methods in applied mechanics and engineering,* vol. 71, pp. 197-224, 1988.

[53] M. P. Bendsøe, "Optimal shape design as a material distribution problem," *Structural and multidisciplinary optimization,* vol. 1, pp. 193-202, 1989.

[54] M. P. Bendsøe, "Optimal shape design as a material distribution problem," *Structural optimization,* vol. 1, pp. 193-202, 1989.

[55] M. P. Bendsøe and O. Sigmund, "Material interpolation schemes in topology optimization," *Archive of applied mechanics,* vol. 69, pp. 635-654, 1999.

[56] O. Sigmund and J. Petersson, "Numerical instabilities in topology optimization: a survey on procedures dealing with checkerboards, mesh-dependencies and local minima," *Structural and Multidisciplinary Optimization,* vol. 16, pp. 68-75, 1998.

[57] O. Sigmund, "A 99 line topology optimization code written in Matlab," *Structural and multidisciplinary optimization,* vol. 21, pp. 120-127, 2001.

[58] Q. Li, G. Steven, and Y. Xie, "A simple checkerboard suppression algorithm for evolutionary structural optimization," *Structural and Multidisciplinary Optimization,* vol. 22, pp. 230-239, 2001.

[59] C. S. Jog and R. B. Haber, "Stability of finite element models for distributed-parameter optimization and topology design," *Computer methods in applied mechanics and engineering,* vol. 130, pp. 203-226, 1996.

[60] S. Yan, F. Wang, and O. Sigmund, "On the non-optimality of tree structures for heat conduction," *International Journal of Heat and Mass Transfer,* vol. 122, pp. 660-680, 2018.

[61] J. Lee, E. M. Dede, D. Banerjee, and H. Iizuka, "Magnetic force enhancement in a linear actuator by air-gap magnetic field distribution optimization and design," *Finite elements in analysis and design,* vol. 58, pp. 44-52, 2012.

[62] N. Olhoff, M. P. Bendsøe, and J. Rasmussen, "On CAD-integrated structural topology and design optimization," *Computer Methods in Applied Mechanics and Engineering,* vol. 89, pp. 259-279, 1991.

[63] J. Martínez, J. Dumas, S. Lefebvre, and L.-Y. Wei, "Structure and appearance optimization for controllable shape design," *ACM Transactions on Graphics (TOG),* vol. 34, p. 229, 2015.

[64] M. Y. Wang, X. Wang, and D. Guo, "A level set method for structural topology optimization," *Computer methods in applied mechanics and engineering,* vol. 192, pp. 227-246, 2003.

[65] G. Allaire, F. Jouve, and A.-M. Toader, "Structural optimization using sensitivity analysis and a level-set method," *Journal of computational physics,* vol. 194, pp. 363-393, 2004.

[66] C. Groth, A. Chiappa, and M. Biancolini, "Shape optimization using structural adjoint and RBF mesh morphing," *Procedia Structural Integrity,* vol. 8, pp. 379-389, 2018.

[67] P. Penzler, M. Rumpf, and B. Wirth, "A phase-field model for compliance shape optimization in nonlinear elasticity," *ESAIM: Control, Optimisation and Calculus of Variations,* vol. 18, pp. 229-258, 2012.

[68] H. Garcke, C. Hecht, M. Hinze, and C. Kahle, "Numerical approximation of phase field based shape and topology optimization for fluids," *SIAM Journal on Scientific Computing,* vol. 37, pp. A1846-A1871, 2015.

[69] A. Takezawa and M. Kitamura, "Phase field method to optimize dielectric devices for electromagnetic wave propagation," *Journal of Computational Physics,* vol. 257, pp. 216-240, 2014.

[70] T. H. Nguyen, G. H. Paulino, J. Song, and C. H. Le, "Improving multiresolution topology optimization via multiple discretizations," *International Journal for Numerical Methods in Engineering,* vol. 92, pp. 507-530, 2012.

[71] A. Takezawa, S. Nishiwaki, and M. Kitamura, "Shape and topology optimization based on the phase field method and sensitivity analysis," *Journal of Computational Physics,* vol. 229, pp. 2697-2718, 2010.

[72] C. H. Villanueva and K. Maute, "Density and level set-XFEM schemes for topology optimization of 3-D structures," *Computational Mechanics,* vol. 54, pp. 133-150, 2014.

[73] M. Biancolini, C. Groth, E. Costa, and F. Lagasco, "A mesh morphing based technique to efficiently perform FSI analyses for aeroelastic design applications," in *AIDAA Italian Association of Aeronautics and Astronautics XXII Conference*, pp. 9-12.

[74] I. A. Sigal, M. R. Hardisty, and C. M. Whyne, "Mesh-morphing algorithms for specimen-specific finite element modeling," *Journal of biomechanics,* vol. 41, pp. 1381-1389, 2008.

[75] D. Szczerba, E. Neufeld, M. Zefferer, B. Bühlmann, and N. Kuster, "FEM based morphing of whole body human models," in *General Assembly and Scientific Symposium, 2011 XXXth URSI*, 2011, pp. 1-3.

[76] V. E. Foe and B. M. Alberts, "Studies of nuclear and cytoplasmic behaviour during the five mitotic cycles that precede gastrulation in Drosophila embryogenesis," *Journal of cell science,* vol. 61, pp. 31-70, 1983.

[77] J. W. Ager, G. Balooch, and R. Ritchie, "Fracture, aging, and disease in bone," *Journal of Materials Research,* vol. 21, pp. 1878-1892, 2006.

[78] L. Andersson, K.-E. Kahnberg, and M. A. Pogrel, *Oral and maxillofacial surgery*: John Wiley & Sons, 2012.

[79] R. E. Marx, "Mandibular reconstruction," *Journal of oral and maxillofacial surgery,* vol. 51, pp. 466-479, 1993.

[80] M. Miloro, G. Ghali, P. Larsen, and P. Waite, *Peterson's principles of oral and maxillofacial surgery* vol. 1: PMPH-USA, 2004.

[81] L. J. Peterson, E. Ellis, J. R. Hupp, and M. R. Tucker, *Contemporary oral and maxillofacial surgery*: Mosby St. Louis, MO, 1988.

[82] J. Kolahi and Y. S. Shayesteh, "A textbook of advanced oral and maxillofacial surgery," *Dental Hypotheses,* vol. 4, pp. 151-152, 2013.

[83] R. Bolourian, S. Lazow, and J. Berger, "Transoral 2.0-mm miniplate fixation of mandibular fractures plus 2 weeks' maxillomandibular fixation: a prospective study," *Journal of oral and maxillofacial surgery,* vol. 60, pp. 167-170, 2002.

[84] S. Anil, A. P. Krishnan, and R. Rajendran, "Osteosarcoma of the mandible masquerading as a dental abscess: report of a case," *Case reports in dentistry,* vol. 2012, 2012.

[85] P. Infante-Cossio, V. Prats-Golczer, L.-M. Gonzalez-Perez, R. Belmonte-Caro, R. Martinez-De-Fuentes, E. Torres-Carranza*, et al.*, "Treatment of recurrent mandibular ameloblastoma," *Experimental and therapeutic medicine,* vol. 6, pp. 579-583, 2013.

[86] G. P. Pastore, I. S. Martins, D. R. Goulart, A. J. Prati, M. de Moraes, P. R. Pastore*, et al.*, "Tratamiento Quirúrgico de Ameloblastoma Mandibular y la Reconstrucción Inmediata con Injerto Oseo Libre y Terapia con Oxígeno Hiperbárico," *International journal of odontostomatology,* vol. 10, pp. 409-417, 2016.

[87] T. Albrektsson, G. Zarb, P. Worthington, and A. Eriksson, "The long-term efficacy of currently used dental implants: a review and proposed criteria of success," *Int J Oral Maxillofac Implants,* vol. 1, pp. 11-25, 1986.

[88] C. E. Misch, M. L. Perel, H.-L. Wang, G. Sammartino, P. Galindo-Moreno, P. Trisi*, et al.*, "Implant success, survival, and failure: the International Congress of Oral Implantologists (ICOI) pisa consensus conference," *Implant dentistry,* vol. 17, pp. 5-15, 2008.

[89] H. Spiekermann, V. K. Jansen, and E.-J. Richter, "A 10-year follow-up study of IMZ and TPS implants in the edentulous mandible using bar-retained overdentures," *International Journal of Oral & Maxillofacial Implants,* vol. 10, 1995.

[90] T. Karachalios, C. Tsatsaronis, G. Efraimis, P. Papadelis, G. Lyritis, and G. Diakoumopoulos, "The long-term clinical relevance of calcar atrophy caused by stress shielding in total hip arthroplasty: A 10-year, prospective, randomized study1 1No benefits or funds were received in support of this study," *The Journal of arthroplasty,* vol. 19, pp. 469-475, 2004.

[91] L. Jones and B. A. LIEBERMAN, "Interaction of bone and various metals: vanadium steel and rustless steels," *Archives of Surgery,* vol. 32, pp. 990-1006, 1936.

[92] W. Hueper, "Experimental studies in metal cancerigenesis. I. Nickel cancers in rats," *Texas reports on biology and medicine,* vol. 10, pp. 167-86, 1952.

[93] J. Ager, G. Balooch, and R. Ritchie, "Fracture, aging, and disease in bone," *Journal of Materials Research,* vol. 21, pp. 1878-1892, 2006.

[94] V. E. Dube and D. E. Fisher, "Hemangioendothelioma of the leg following metallic fixation of the tibia," *Cancer,* vol. 30, pp. 1260-1266, 1972.

[95] W. Krupp, J. Ryder, D. Pettit, and D. Hoeppner, "Corrosion Fatigue Properties of Ti-6Al-6V-2Sn (STOA)," in *Flaw Growth and Fracture*, ed: ASTM International, 1977.

[96] H. Katoozian, D. T. Davy, A. Arshi, and U. Saadati, "Material optimization of femoral component of total hip prosthesis using fiber reinforced polymeric composites," *Medical Engineering and Physics,* vol. 23, pp. 505-511, 2001.

[97] T. Lu, X. Liu, S. Qian, H. Cao, Y. Qiao, Y. Mei*, et al.*, "Multilevel surface engineering of nanostructured TiO2 on carbon-fiber-reinforced polyetheretherketone," *Biomaterials,* vol. 35, pp. 5731-5740, 2014.

[98] A. H. Poulsson, D. Eglin, S. Zeiter, K. Camenisch, C. Sprecher, Y. Agarwal*, et al.*, "Osseointegration of machined, injection moulded and oxygen plasma modified PEEK implants in a sheep model," *Biomaterials,* vol. 35, pp. 3717-3728, 2014.

[99] B. Tihanyi, Z. Bereczki, E. Molnár, W. Berthon, L. Révész, O. Dutour*, et al.*, "Investigation of Hungarian Conquest Period (10th c. AD) archery on the basis of activity-induced stress markers on the skeleton-preliminary results," *Acta Biologica Szegediensis,* vol. 59, pp. 65-77, 2015.

[100] D. R. Sumner and J. O. Galante, "Determinants of stress shielding: design versus materials versus interface," *Clinical orthopaedics and related research,* vol. 274, pp. 202-212, 1992.

[101] Y. Abdelaziz and A. Hamouine, "A survey of the extended finite element," *Computers & structures,* vol. 86, pp. 1141-1151, 2008.

[102] E. W. H. Groves, "An experimental study of the operative treatment of fractures," *British Journal of Surgery,* vol. 1, pp. 438-501, 1913.

[103] P. Avouris, "Manipulation of matter at the atomic and molecular levels," *Accounts of chemical research,* vol. 28, pp. 95-102, 1995.

[104] E. Biyikli and A. C. To, "Proportional Topology Optimization: A New Non-Sensitivity Method for Solving Stress Constrained and Minimum Compliance Problems and Its Implementation in MATLAB," *PloS one,* vol. 10, p. e0145041, 2015.

[105] A. Blanco, M. Delgado, and M. C. Pegalajar, "A real-coded genetic algorithm for training recurrent neural networks," *Neural networks,* vol. 14, pp. 93-105, 2001.

[106] L. Blankevoort, J. Kuiper, R. Huiskes, and H. Grootenboer, "Articular contact in a three-dimensional model of the knee," *Journal of biomechanics,* vol. 24, pp. 1019-1031, 1991.

[107] M. Bruggi and P. Venini, "A mixed FEM approach to stress-constrained topology optimization," *International Journal for Numerical Methods in Engineering,* vol. 73, pp. 1693-1714, 2008.

[108] P. Bujtár, G. K. Sándor, A. Bojtos, A. Szűcs, and J. Barabás, "Finite element analysis of the human mandible at 3 different stages of life," *Oral Surgery, Oral Medicine, Oral Pathology, Oral Radiology, and Endodontology,* vol. 110, pp. 301-309, 2010.

[109] V. J. Challis, A. P. Roberts, J. F. Grotowski, L. C. Zhang, and T. B. Sercombe, "Prototypes for bone implant scaffolds designed via topology optimization and manufactured by solid freeform fabrication," *Advanced Engineering Materials,* vol. 12, pp. 1106-1110, 2010.

[110] J. S. Chana, Y.-M. Chang, F.-C. Wei, Y.-F. Shen, C.-P. Chan, H.-N. Lin*, et al.*, "Segmental mandibulectomy and immediate free fibula osteoseptocutaneous flap reconstruction with endosteal implants: an ideal treatment method for

mandibular ameloblastoma," *Plastic and reconstructive surgery,* vol. 113, pp. 80-87, 2004.

[111] P. J. Henry, W. R. Laney, T. Jemt, D. Harris, P. H. Krogh, G. Polizzi*, et al.*, "Osseointegrated implants for single-tooth replacement: a prospective 5-year multicenter study," *International Journal of Oral & Maxillofacial Implants,* vol. 11, 1996.

[112] D. Buser, L. Sennerby, and H. De Bruyn, "Modern implant dentistry based on osseointegration: 50 years of progress, current trends and open questions," *Periodontology 2000,* vol. 73, pp. 7-21, 2017.

[113] M. Alzahrani, S.-K. Choi, and D. W. Rosen, "Design of truss-like cellular structures using relative density mapping method," *Materials & Design,* vol. 85, pp. 349-360, 2015.

[114] C. Bathias, *Fatigue of materials and structures*: John Wiley & Sons, 2013.

[115] Y. Zeng, Y. Yan, H. Yan, C. Liu, P. Li, P. Dong*, et al.*, "3D printing of hydroxyapatite scaffolds with good mechanical and biocompatible properties by digital light processing," *Journal of Materials Science,* vol. 53, pp. 6291-6301, 2018.

[116] C.-C. Chang, Y. Chen, S. Zhou, Y.-W. Mai, and Q. Li, "Computational design for scaffold tissue engineering," in *Biomaterials for Implants and Scaffolds*, ed: Springer, 2017, pp. 349-369.

[117] D. Luo, Q. Rong, and Q. Chen, "Finite-element design and optimization of a three-dimensional tetrahedral porous titanium scaffold for the reconstruction of mandibular defects," *Medical Engineering and Physics,* vol. 47, pp. 176-183, 2017.

[118] G. Grigalevičiūtė, D. Baltriukienė, E. Balčiūnas, L. Jonušauskas, and M. Malinauskas, "Fabrication of flexible microporous 3D scaffolds via stereolithography and optimization of their biocompatibility," in *Advanced Fabrication Technologies for Micro/Nano Optics and Photonics XI*, 2018, p. 105441E.

[119] Z. Xiao, Y. Yang, R. Xiao, Y. Bai, C. Song, and D. Wang, "Evaluation of topology-optimized lattice structures manufactured via selective laser melting," *Materials & Design,* 2018.

[120] S. Arabnejad, B. Johnston, M. Tanzer, and D. Pasini, "Fully porous 3d printed titanium femoral stem to reduce stress-shielding following total hip arthroplasty," *Journal of Orthopaedic Research,* vol. 35, pp. 1774-1783, 2017.

[121] G. Campoli, M. Borleffs, S. A. Yavari, R. Wauthle, H. Weinans, and A. A. Zadpoor, "Mechanical properties of open-cell metallic biomaterials manufactured using additive manufacturing," *Materials & Design,* vol. 49, pp. 957-965, 2013.

[122] S. Cowin and D. Hegedus, "Bone remodeling I: theory of adaptive elasticity," *Journal of Elasticity,* vol. 6, pp. 313-326, 1976.

[123] R. Huiskes, H. Weinans, and B. Van Rietbergen, "The relationship between stress shielding and bone resorption around total hip stems and the effects of flexible materials," *Clinical orthopaedics and related research,* pp. 124-134, 1992.

[124] M. G. Joshi, S. G. Advani, F. Miller, and M. H. Santare, "Analysis of a femoral hip prosthesis designed to reduce stress shielding," *Journal of biomechanics,* vol. 33, pp. 1655-1662, 2000.

[125] D. Carter, T. Orr, and D. Fyhrie, "Relationships between loading history and femoral cancellous bone architecture," *Journal of Biomechanics,* vol. 22, pp. 231-244, 1989.

[126] B. Van Rietbergen, R. Huiskes, H. Weinans, D. Sumner, T. Turner, and J. Galante, "The mechanism of bone remodeling and resorption around press-fitted THA stems," *Journal of biomechanics,* vol. 26, pp. 369-382, 1993.

[127] A. Ait Moussa, J. Fischer, R. Yadav, and M. Khandaker, "Minimizing stress shielding and cement damage in cemented femoral component of a hip prosthesis through computational design optimization," *Advances in orthopedics,* vol. 2017, 2017.

[128] J. McFadden and J. Al-Khalili, *Life on the edge: the coming of age of quantum biology*: Broadway Books, 2016.

[129] J. J. Craig, *Introduction to robotics: mechanics and control* vol. 3: Pearson/Prentice Hall Upper Saddle River, NJ, USA:, 2005.

[130] H. S. Alghamdi, "Methods to Improve Osseointegration of Dental Implants in Low Quality (Type-IV) Bone: An Overview," *Journal of functional biomaterials,* vol. 9, p. 7, 2018.

[131] C. N. Elias and L. Meirelles, "Improving osseointegration of dental implants," *Expert review of medical devices,* vol. 7, pp. 241-256, 2010.

[132] M. Geetha, A. Singh, R. Asokamani, and A. Gogia, "Ti based biomaterials, the ultimate choice for orthopaedic implants–a review," *Progress in materials science,* vol. 54, pp. 397-425, 2009.

[133] R. D. Cook, "Finite element modeling for stress analysis/Robert D. Cook," 1994.

[134] P. Duysinx and M. P. Bendsøe, "Topology optimization of continuum structures with local stress constraints," *International journal for numerical methods in engineering,* vol. 43, pp. 1453-1478, 1998.

[135] C. Le, J. Norato, T. Bruns, C. Ha, and D. Tortorelli, "Stress-based topology optimization for continua," *Structural and Multidisciplinary Optimization,* vol. 41, pp. 605-620, 2010.

[136] E. Holmberg, B. Torstenfelt, and A. Klarbring, "Stress constrained topology optimization," *Structural and Multidisciplinary Optimization,* vol. 48, pp. 33-47, 2013.

[137] W. P. Ziemer, *Weakly differentiable functions: Sobolev spaces and functions of bounded variation* vol. 120: Springer Science & Business Media, 2012.

[138] A. Verbart, "Topology Optimization with Stress Constraints," TU Delft, Delft University of Technology, 2015.

[139] F. Dirksen, M. Anselmann, T. I. Zohdi, and R. Lammering, "Incorporation of flexural hinge fatigue-life cycle criteria into the topological design of compliant small-scale devices," *Precision Engineering,* vol. 37, pp. 531-541, 2013.

[140] S. H. Jeong, D.-H. Choi, and G. H. Yoon, "Fatigue and static failure considerations using a topology optimization method," *Applied Mathematical Modelling,* vol. 39, pp. 1137-1162, 2015.

[141] Y. Murakami, *The Rainflow Method in Fatigue: The Tatsuo Endo Memorial Volume*: Butterworth-Heinemann, 2013.

[142] S. H. Jeong, G. H. Yoon, A. Takezawa, and D.-H. Choi, "Development of a novel phase-field method for local stress-based shape and topology optimization," *Computers & Structures,* vol. 132, pp. 84-98, 2014.

[143] O. Amir and B. S. Lazarov, "Achieving stress-constrained topological design via length scale control," *Structural and Multidisciplinary Optimization,* pp. 1-19, 2018.

[144] G. Cheng and X. Guo, "ε-relaxed approach in structural topology optimization," *Structural optimization,* vol. 13, pp. 258-266, 1997.

[145] R. Yang and C. Chen, "Stress-based topology optimization," *Structural optimization,* vol. 12, pp. 98-105, 1996.

[146] Z.-q. Fu, B.-h. Ji, S.-h. Xie, and T.-j. Liu, "Crack stop holes in steel bridge decks: Drilling method and effects," *Journal of Central South University,* vol. 24, pp. 2372-2381, 2017.

[147] M. Ayatollahi, S. Razavi, and H. Chamani, "Fatigue life extension by crack repair using stop-hole technique under pure mode-I and pure mode-II loading conditions," *Procedia Engineering,* vol. 74, pp. 18-21, 2014.

[148] K. Sieradzki and R. Newman, "Stress-corrosion cracking," *Journal of physics and chemistry of solids,* vol. 48, pp. 1101-1113, 1987.

[149] J. Scully, "Kinetic features of stress-corrosion cracking," *Corrosion Science,* vol. 7, pp. 197-207, 1967.

[150] G. S. Was, D. Farkas, and I. M. Robertson, "Micromechanics of dislocation channeling in intergranular stress corrosion crack nucleation," *Current Opinion in Solid State and Materials Science,* vol. 16, pp. 134-142, 2012.

[151] V. Dakshnamoorthy, "Automated Lattice Optimization of Hinge Fitting with Displacement Constraint," 2016.

[152] N. S. Sripada, "A Methodology for Topology and Lattice Structure Optimization of a Cargo Drone Motor Mount," 2018.

[153] S. Daynes, S. Feih, W. F. Lu, and J. Wei, "sandwich structures with 3D printed Functionally graded lattice cores."

[154] M. Fraldi, L. Esposito, G. Perrella, A. Cutolo, and S. Cowin, "Topological optimization in hip prosthesis design," *Biomechanics and modeling in mechanobiology,* vol. 9, pp. 389-402, 2010.

[155] A. Sutradhar, G. H. Paulino, M. J. Miller, and T. H. Nguyen, "Topological optimization for designing patient-specific large craniofacial segmental bone replacements," *Proceedings of the National Academy of Sciences,* vol. 107, pp. 13222-13227, 2010.

[156] A. Sutradhar, J. Park, D. Carrau, T. H. Nguyen, M. J. Miller, and G. H. Paulino, "Designing patient-specific 3D printed craniofacial implants using a novel topology optimization method," *Medical & biological engineering & computing,* vol. 54, pp. 1123-1135, 2016.

[157] X. Wang, S. Xu, S. Zhou, W. Xu, M. Leary, P. Choong*, et al.*, "Topological design and additive manufacturing of porous metals for bone scaffolds and orthopaedic implants: a review," *Biomaterials,* vol. 83, pp. 127-141, 2016.

[158] P. Babaniamansour, M. Ebrahimian-Hosseinabadi, and A. Zargar-Kharazi, "Designing an optimized novel femoral stem," *Journal of medical signals and sensors,* vol. 7, p. 170, 2017.

[159] F. X. Michelet, J. Deymes, and B. Dessus, "Osteosynthesis with miniaturized screwed plates in maxillo-facial surgery," *Journal of Cranio-Maxillo-Facial Surgery,* vol. 1, pp. 79-84, 1973.

[160] J. K. Jones and J. E. Van Sickels, "Rigid fixation: a review of concepts and treatment of fractures," *Oral surgery, oral medicine, oral pathology,* vol. 65, pp. 13-18, 1988.

[161] T. Lee, R. Sawhney, and Y. Ducic, "Miniplate fixation of fractures of the symphyseal and parasymphyseal regions of the mandible: a review of 218 patients," *JAMA facial plastic surgery,* vol. 15, pp. 121-125, 2013.

[162] B. R. Chrcanovic, "Fixation of mandibular angle fractures: clinical studies," *Oral and maxillofacial surgery,* vol. 18, pp. 123-152, 2014.

[163] S. Choudhari, A. Sulabha, N. Warad, A. Krishna, and S. Mujawar, "Bio-degradable osteosynthesis system in treatment of mandibular parasymphysis fractures," *J Med Sci,* vol. 5, pp. 371-5, 2012.

[164] B. R. Chrcanovic, "Fixation of mandibular angle fractures: in vitro biomechanical assessments and computer-based studies," *Oral and Maxillofacial Surgery,* vol. 17, pp. 251-268, December 01 2013.

[165] H.-S. Kim, J.-Y. Park, N.-E. Kim, Y.-S. Shin, J.-M. Park, and Y.-S. Chun, "Finite element modeling technique for predicting mechanical behaviors on mandible bone during mastication," *The journal of advanced prosthodontics,* vol. 4, pp. 218-226, 2012.

[166] J.-P. Geng, K. B. Tan, and G.-R. Liu, "Application of finite element analysis in implant dentistry: a review of the literature," *The Journal of prosthetic dentistry,* vol. 85, pp. 585-598, 2001.

[167] E. Tanaka, K. Tanne, and M. Sakuda, "A three-dimensional finite element model of the mandible including the TMJ and its application to stress analysis in the TMJ during clenching," *Medical engineering & physics,* vol. 16, pp. 316-322, 1994.

[168] W. Parr, U. Chamoli, A. Jones, W. Walsh, and S. Wroe, "Finite element micro-modelling of a human ankle bone reveals the importance of the trabecular network to mechanical performance: new methods for the generation and

comparison of 3D models," *Journal of biomechanics,* vol. 46, pp. 200-205, 2013.

[169] W. Sun and P. Lal, "Recent development on computer aided tissue engineering—a review," *Computer methods and programs in biomedicine,* vol. 67, pp. 85-103, 2002.

[170] R. P. Crawford, C. E. Cann, and T. M. Keaveny, "Finite element models predict in vitro vertebral body compressive strength better than quantitative computed tomography," *Bone,* vol. 33, pp. 744-750, 2003.

[171] D. Ulrich, B. van Rietbergen, H. Weinans, and P. Rüegsegger, "Finite element analysis of trabecular bone structure: a comparison of image-based meshing techniques," *Journal of biomechanics,* vol. 31, pp. 1187-1192, 1998.

[172] O. Lubovsky, M. Liebergall, Y. Mattan, Y. Weil, and R. Mosheiff, "Early diagnosis of occult hip fractures: MRI versus CT scan," *Injury,* vol. 36, pp. 788-792, 2005.

[173] P. Magne, "Efficient 3D finite element analysis of dental restorative procedures using micro-CT data," *Dental materials,* vol. 23, pp. 539-548, 2007.

[174] E. G. Deliverska and H. D. Stoyanov, "SURGICAL TREATMENT AND RECONSTRUCTION FOR CENTRAL GIANT CELL GRANULOMA OF MANDIBLE-case report and literature review," *Journal of IMAB-Annual Proceeding Scientific Papers,* vol. 19, pp. 407-410, 2013.

[175] P. Bujtár, G. K. Sándor, A. Bojtos, A. Szűcs, and J. Barabás, "Finite element analysis of the human mandible at 3 different stages of life," *Oral Surgery, Oral Medicine, Oral Pathology, Oral Radiology and Endodontics,* vol. 110, pp. 301-309, 2010.

[176] R. T. Hart, V. V. Hennebel, N. Thongpreda, W. C. Van Buskirk, and R. C. Anderson, "Modeling the biomechanics of the mandible: a three-dimensional finite element study," *Journal of Biomechanics,* vol. 25, pp. 261-286, 1992.

[177] J. Chen, X. Lu, N. Paydar, H. Akay, and W. Roberts, "Mechanical simulation of the human mandible with and without an endosseous implant," *Medical engineering & physics,* vol. 16, pp. 53-61, 1994.

[178] A. B. Novaes Jr, S. L. S. d. Souza, R. R. M. d. Barros, K. K. Y. Pereira, G. Iezzi, and A. Piattelli, "Influence of implant surfaces on osseointegration," *Brazilian dental journal,* vol. 21, pp. 471-481, 2010.

[179] C. Stanford, "Surface modifications of dental implants," *Australian dental journal,* vol. 53, 2008.

[180] S. J. Ferguson, J. D. Langhoff, K. Voelter, B. v. Rechenberg, D. Scharnweber, S. Bierbaum*, et al.*, "Biomechanical comparison of different surface modifications for dental implants," *The International journal of oral & maxillofacial implants,* vol. 23, p. 1037, 2008.

[181] L. Sennerby, A. Dasmah, B. Larsson, and M. Iverhed, "Bone Tissue Responses to Surface-Modified Zirconia Implants: A Histomorphometric and Removal Torque Study in the Rabbit," *Clinical implant dentistry and related research,* vol. 7, 2005.

[182] F. Schwarz, M. Wieland, Z. Schwartz, G. Zhao, F. Rupp, J. Geis-Gerstorfer*, et al.*, "Potential of chemically modified hydrophilic surface characteristics to support tissue integration of titanium dental implants," *Journal of Biomedical Materials Research Part B: Applied Biomaterials,* vol. 88, pp. 544-557, 2009.

[183] B. H. Lee, J. K. Kim, Y. D. Kim, K. Choi, and K. H. Lee, "In vivo behavior and mechanical stability of surface-modified titanium implants by plasma spray coating and chemical treatments," *Journal of Biomedical Materials Research Part A,* vol. 69, pp. 279-285, 2004.

[184] W. Sun, B. Starly, J. Nam, and A. Darling, "Bio-CAD modeling and its applications in computer-aided tissue engineering," *Computer-aided design,* vol. 37, pp. 1097-1114, 2005.

[185] J. Parthasarathy, B. Starly, S. Raman, and A. Christensen, "Mechanical evaluation of porous titanium (Ti6Al4V) structures with electron beam melting

(EBM)," *Journal of the mechanical behavior of biomedical materials,* vol. 3, pp. 249-259, 2010.

[186] S. Van Bael, G. Kerckhofs, M. Moesen, G. Pyka, J. Schrooten, and J.-P. Kruth, "Micro-CT-based improvement of geometrical and mechanical controllability of selective laser melted Ti6Al4V porous structures," *Materials Science and Engineering: A,* vol. 528, pp. 7423-7431, 2011.

[187] L. Murr, S. Gaytan, F. Medina, H. Lopez, E. Martinez, B. Machado*, et al.*, "Next-generation biomedical implants using additive manufacturing of complex, cellular and functional mesh arrays," *Philosophical Transactions of the Royal Society of London A: Mathematical, Physical and Engineering Sciences,* vol. 368, pp. 1999-2032, 2010.

[188] C. Boller and T. Seeger, *Materials data for cyclic loading: Low-alloy steels* vol. 42: Elsevier, 2013.

[189] B. Yilbas, A. Coban, R. Kahraman, and M. Khaled, "Hydrogen embrittlement of Ti-6Al-4V alloy with surface modification by TiN coating," *International journal of hydrogen energy,* vol. 23, pp. 483-489, 1998.

[190] H. R. Gray, "Hydrogen environment embrittlement," 1972.

[191] G. Wille and J. Davis, "Hydrogen in titanium alloys," McDonnell Douglas Astronautics Co.1981.

[192] B. Yuan, C. Li, H. Yu, and D. Sun, "Influence of hydrogen content on tensile and compressive properties of Ti–6Al–4V alloy at room temperature," *Materials Science and Engineering: A,* vol. 527, pp. 4185-4190, 2010.

[193] Y. Ding, L. Tsay, and C. Chen, "The effects of hydrogen on fatigue crack growth behaviour of Ti–6Al–4V and Ti–4.5 Al–3V–2Mo–2Fe alloys," *Corrosion Science,* vol. 51, pp. 1413-1419, 2009.

[194] T. Van Eijden, "Biomechanics of the mandible," *Critical reviews in oral biology & medicine,* vol. 11, pp. 123-136, 2000.

[195] R. Wong, H. Tideman, M. Merkx, J. Jansen, S. Goh, and K. Liao, "Review of biomechanical models used in studying the biomechanics of reconstructed mandibles," *International journal of oral and maxillofacial surgery,* vol. 40, pp. 393-400, 2011.

[196] Y. Kim, T. J. Oh, C. E. Misch, and H. L. Wang, "Occlusal considerations in implant therapy: clinical guidelines with biomechanical rationale," *Clinical oral implants research,* vol. 16, pp. 26-35, 2005.

[197] J. Mu Jung and C. Sang Kim, "Analysis of stress distribution around total hip stems custom-designed for the standardized Asian femur configuration," *Biotechnology & Biotechnological Equipment,* vol. 28, pp. 525-532, 2014.

[198] B. van Rietbergen and R. Huiskes, "Load transfer and stress shielding of the hydroxyapatite-ABG hip: a study of stem length and proximal fixation," *The Journal of arthroplasty,* vol. 16, pp. 55-63, 2001.

[199] M. Reimeringer, N. Nuño, C. Desmarais-Trépanier, M. Lavigne, and P. Vendittoli, "The influence of uncemented femoral stem length and design on its primary stability: a finite element analysis," *Computer methods in biomechanics and biomedical engineering,* vol. 16, pp. 1221-1231, 2013.

[200] Y. Shishani and R. Gobezie, "Does a short stemmed humeral implant really make a difference?," in *Seminars in Arthroplasty*, 2017.

[201] F. Schmidutz, M. Woiczinski, M. Kistler, C. Schröder, V. Jansson, and A. Fottner, "Influence of different sizes of composite femora on the biomechanical behavior of cementless hip prosthesis," *Clinical Biomechanics,* vol. 41, pp. 60-65, 2017.

[202] J. F. Crowe, V. Mani, and C. S. Ranawat, "Total hip replacement in congenital dislocation and dysplasia of the hip," *JBJS,* vol. 61, pp. 15-23, 1979.

[203] J. Wedge and M. Wasylenko, "The natural history of congenital disease of the hip," *Bone & Joint Journal,* vol. 61, pp. 334-338, 1979.

[204] A. J. Pinkerton, L. Li, and W. Lau, "Effects of powder geometry and composition in coaxial laser deposition of 316L steel for rapid prototyping," *CIRP annals-Manufacturing technology,* vol. 52, pp. 181-184, 2003.

[205] L. E. Murr, S. M. Gaytan, D. A. Ramirez, E. Martinez, J. Hernandez, K. N. Amato*, et al.*, "Metal fabrication by additive manufacturing using laser and electron beam melting technologies," *Journal of Materials Science & Technology,* vol. 28, pp. 1-14, 2012.

[206] B. Baufeld, E. Brandl, and O. Van der Biest, "Wire based additive layer manufacturing: Comparison of microstructure and mechanical properties of Ti–6Al–4V components fabricated by laser-beam deposition and shaped metal deposition," *Journal of Materials Processing Technology,* vol. 211, pp. 1146-1158, 2011.

[207] B. Mueller, "Additive manufacturing technologies–Rapid prototyping to direct digital manufacturing," *Assembly Automation,* vol. 32, 2012.

[208] C. Raub, "The history of electroplating," in *Metal Plating and Patination*, ed: Elsevier, 1993, pp. 284-290.

[209] D. O. Meredith, L. Eschbach, M. A. Wood, M. O. Riehle, A. S. Curtis, and R. G. Richards, "Human fibroblast reactions to standard and electropolished titanium and Ti–6Al–7Nb, and electropolished stainless steel," *Journal of Biomedical Materials Research Part A,* vol. 75, pp. 541-555, 2005.

[210] D. Padhi, J. Yahalom, S. Gandikota, and G. Dixit, "Planarization of copper thin films by electropolishing in phosphoric acid for ULSI applications," *Journal of the Electrochemical Society,* vol. 150, pp. G10-G14, 2003.

[211] C. Hirt, A. A. Amsden, and J. Cook, "An arbitrary Lagrangian-Eulerian computing method for all flow speeds," *Journal of computational physics,* vol. 14, pp. 227-253, 1974.

[212] D. J. Benson, "An efficient, accurate, simple ALE method for nonlinear finite element programs," *Computer methods in applied mechanics and engineering,* vol. 72, pp. 305-350, 1989.

Publications

- Musaddiq Al Ali, Muazez Al Ali, Akihiro Takezawa, Mitsuru Kitamura, "*Topology Optimization and fatigue Analysis of Temporomandibular Joint Prosthesis*". World Journal of Mechanics, Vol.7, No.12, pp 323-339, 2017.

- Musaddiq Al Ali, Akihiro Takezawa, Mitsuru Kitamura, "*Comparative Study of Stress Minimization Using Topology Optimization and Morphing Based Shape Optimization*," *The Asian Congress of Structural and Multidisciplinary Optimization, Dalian, China. 2018.*

Acknowledgment

I would like to express my thanks to the esquire supervisor, Dr. Akihiro Takeaway for his supervision. I would like to express my thanks to the head of the laboratory of structural innovation, Dr. Mitsuko Kimura for his valuable advice regarding finite element, optimization, and homogenization theory. Special thanks to Dr. Yoshikazu Tanaka for his valuable advices regarding fatigue. Special thanks to D. Ole Sigmund for sending his Ph.D. thesis and advice regarding topology optimization. Special thanks to Dr. Anndres Tovar, for his advice regarding 3d topology optimization. I would like to thank also the Japanese ministry of education, culture, sports, science, and technology, for their grant and support. Special thanks to my father, Dr. Abdil Khaliq Maleh, for his highly valuable medical advice. Special thanks to Dr. Muazez Al Ali, Dr. Amjad Y. Sahib, Dr. Rajaa S. Abass, for their financial aid and scientific platforms. Special thanks to Miss T. Sherstobitova, for her aid in the calculations of electrochemical proportionality coefficient of titanium alloy. Thanks to Hiroshima university for the scientific atmosphere. Special thanks to Mr. Yohe Nakano and Dr. Tafukami Nishizu for their advice regarding shape and SIMP topology optimization